

Characterization of Proteins Homologous to Nucleotide Sugar Transporters in  
*Arabidopsis thaliana*

I n a u g u r a l – D i s s e r t a t i o n

zur

Erlangung des Doktorgrades  
der Mathematisch-Naturwissenschaftlichen Fakultät  
der Universität zu Köln

vorgelegt von

Marcela Santaella-Tenorio  
aus Bogotá, Kolumbien

2006

Die dieser Dissertation zugrundeliegenden experimentellen Arbeiten wurden in der Zeit von Oktober 2002 bis Mai 2006 am Botanischen Institut der Universität zu Köln anfertigt.

Berichtersteller:                      Prof. Dr. Ulf-Ingo Flügge  
   Prof. Dr. Reinhard Krämer

Tag der mündlichen Prüfung:      11. Juli 2006

“¿Dices que nada se crea?  
No te importe. Con el barro  
de la tierra haz una copa  
para dar de beber a tu hermano.

¿Dices que nada se crea?  
Alfarero a tus cacharros.  
Haz tu copa y no te importe  
que no puedas hacer barro.”

Antonio Machado.

## Index

	Page
<b>1. Introduction</b>	1
<b>2.1 Materials</b>	8
2.1.1 Vectors	8
2.1.2 Bacteria and Yeast strains	8
2.1.3 Plant Material	9
2.1.4 Plant Procedures	9
2.1.4.1 <i>Arabidopsis</i> seed sterilization	9
2.1.4.2 Pollen staining	10
<b>2.2 Molecular Biology Techniques</b>	10
2.2.1 Gateway™ cloning	10
2.2.2 <i>E. coli</i> transformation	11
2.2.2.1 Preparation of <i>E. coli</i> competent cells for heat-shock transformation	11
2.2.2.2 <i>E. coli</i> heat-shock transformation	12
2.2.3 <i>A. tumefaciens</i> transformation	12
2.2.3.1 Preparation of <i>A. tumefaciens</i> competent cells for electro-transformation	12
2.2.3.2 Electrotransformation of <i>A. tumefaciens</i>	13
2.2.4 <i>S. cerevisiae</i> transformation	13
2.2.5 Isolation and transformation of tobacco protoplasts	14
2.2.6 <i>N. benthamiana</i> leaf epidermal cell transformation	17
2.2.7 <i>Arabidopsis</i> stable transformation	18
2.2.8 Reporter protein detection <i>in planta</i>	18
2.2.8.1 GUS staining	18
2.2.8.2 GFP visualization	19
2.2.9 DNA extraction	19
2.2.9.1 <i>E. coli</i> plasmid DNA isolation	19
2.2.9.2 <i>Arabidopsis</i> DNA isolation	21
2.2.10 Genomic DNA Southern blotting	23

2.2.11 Plant RNA extraction	25
2.2.11.1 Analysis of RNA quality	26
2.2.11.2 Synthesis of first strand cDNA	26
2.2.12 Polymerase Chain Reaction (PCR)	27
2.2.12.1 High-fidelity PCR for cloning	27
2.2.12.2 Colony PCR	28
2.2.12.3 Plant touch-and-go PCR	28
2.2.13 Sequencing	29
<b>2.3 Protein Techniques</b>	<b>29</b>
2.3.1 Protein expression in the yeast heterologous system	29
2.3.1.1 Yeast membrane extraction	29
2.3.1.2 SDS-Polyacrylamide protein gels (SDS-PAGE)	30
2.3.1.3 Protein visualization using Coomassie-brilliant blue stain	31
2.3.1.4 Protein visualization using silver staining	32
2.3.1.5 Transfer of proteins to PVDF membranes (western blot)	33
2.3.1.6 Immune-visualization of recombinant proteins	33
2.3.2 Transport activity measurements	35
2.3.2.1 Purification of phosphatidylcholine for liposome preparation	35
2.3.2.2 Preparation of liposomes	35
2.3.2.3 Membrane proteins solubilization and preparation of proteo- liposomes	35
2.3.2.4 Purification of proteoliposomes through PD-10 gel filtration columns	36
2.3.2.5 Protein transport activity measurements in proteoliposomes	37
2.3.2.5.1 Assembly of the anion exchange columns	37
2.3.2.5.2 Reconstitution of anion exchange resin	37
2.3.2.6 Isolation of proteins using Ni <sup>2+</sup> -nitrilotriacetic acid (Ni-NTA) agarose beads	38
2.3.2.6.1 Ni-NTA agarose beads equilibration	38
2.3.2.6.2 Membrane pellets solubilization and protein-Ni-NTA binding	38
2.3.2.6.3 Isolation of His-tag-bound proteins from the Ni-NTA resin	39
2.3.2.7 Isolation of Golgi-enriched microsomes from yeast cells	39

<b>3. Results</b>	41
3.1 Description of the KV/A/G subfamily	41
3.1.1 Molecular and protein characterization of the KV/A/G subfamily using <i>in silico</i> approaches	41
3.1.2 <i>in silico</i> expression of KVAG genes	45
3.2 Expression of KVAG genes <i>in planta</i>	46
3.2.1 Expression analysis of KVAG genes by semi-quantitative RT-PCR	47
3.2.2 Promoter analysis of KVAG1 and KVAG2 genes	48
3.3 Analysis of KVAG T-DNA insertion lines	51
3.3.1 Identification of homozygous T-DNA insertion plants	51
3.3.2 Verification of the gene knock-out by RT-PCR	54
3.3.3 Determination of the number of T-DNA insertions by Southern blots	56
3.3.4 Generation and verification of <i>kvag1-1 x kvag2-1</i> double knock-out plants	57
3.3.5 Phenotypical characterization of KVAG knock-out lines	59
3.3.5.1 Analysis of lipid composition of <i>kvag1-1</i> and <i>kvag2-1</i> plants	60
3.3.5.2 Analysis of <i>kvag1-1</i> and <i>kvag2-1</i> plants on a phosphate deficient background: crosses with <i>pho1.2</i>	62
3.3.5.3 Analysis of growth properties of single <i>kvag1-1</i> and <i>kvag2-1</i> mutants under phosphate limiting conditions	65
3.3.5.4 Analysis of KVAG1 and KVAG2 gene expression under phos- phate limiting conditions by RT-PCR	66
3.4 Intracellular localization of KVAG proteins: expression of KVAG::GFP fusions <i>in planta</i>	69
3.5 Expression of KVAG proteins in a heterologous system and measure- ments of transport activity	75
3.5.1 Analysis of KVAG heterologous protein expression	76
3.5.2 Measurements of transport activity of the heterologously expressed KVAG proteins	78
3.5.2.1 Protein solubilization from the yeast membrane fraction	78
3.5.2.2 Measurements of transport activity using whole yeast membrane proteins reconstituted into liposomes	79
3.5.2.3 Measurements of transport activity using purified KVAG2 protein reconstituted into liposomes	84

3.5.2.4 Measurements of transport activity using yeast Golgi vesicles enriched with KVAG proteins	85
<b>4. Discussion</b>	89
<b>5. Conclusion</b>	97
<b>6. Abbreviations</b>	99
<b>7. References</b>	102
<b>8. Appendix</b>	114
8.1 Antibiotics	114
8.2 Bacterial growth media	114
8.3 Yeast growth media	115
8.4 Plant growth media	116
8.5 List of primers	118

## 1. Introduction

Many secondary active transporter proteins belong to the Drug and Metabolite transporters superfamily. This diverse cluster that includes prokaryotic and eukaryotic proteins known to mediate efflux of drugs, export of nutrients and metabolites, nutrient uptake, and exchange of metabolites across intraorganellar membranes (Jack *et al.*, 2001). Fourteen families of transporters are differentiated within this superfamily. Six families contain prokaryotic proteins and just a few of them are fully characterized as transporters of cationic drugs, metabolites and nutrients. The other eight families contain exclusively eukaryotic members, some of them known as noduline-like proteins, purine/pyrimidine permeases, phosphate transporters of the inner membrane of plastids (pPT), and nucleotide sugars transporters (NST) (reviewed in Jack *et al.*, 2001).

The eukaryotic proteins of the Drug and Metabolite transporter superfamily generally contain 8-10 transmembrane domains (TMDs). These proteins supposedly originated from gene duplication of bacterial proteins with 4 or 5 TMDs (Jack *et al.*, 2001). In addition, the members of the NST and the pPT families share remarkable sequence and structural similarities and were therefore recently classified as a single family, the NST/pPT family (Ward, 2001; Knappe *et al.*, 2003a). The size of the NST/pPT proteins ranges from 320-340 amino acids and they are thought to assemble in homodimers for proper function. Transport occurs in an antiport manner, exchanging substrates in a strict 1:1 ratio (Capasso and Hirschberg, 1984; Wagner *et al.*, 1989; Gao and Dean, 2000). Despite their similitude, the NST and pPT proteins are specific in their localization and the substrates they transport.

The well characterized pPTs are located in the inner-membrane of plastids and subdivided into four groups based on their function and substrate affinity. The triose phosphate/phosphate transporter (TPT), the first pPT characterized at the molecular level (Flügge *et al.*, 1989), mediates the excretion of photoassimilates like triose phosphate and 3-phosphoglycerate from chloroplasts (Fliege *et al.*, 1978). This protein exports the carbon fixed in chloroplasts during the day to the cytosol, where it is used for the synthesis of sucrose and other metabolites



(Flügge, 1999; Flügge *et al.*, 2003). The second group of phosphoenolpyruvate/phosphate transporters (PPT) imports C3 compounds phosphorylated at the second carbon, i.e. phosphoenolpyruvate and 2-phosphoglycerate, from the cytosol into plastids. In plastids the phosphoenolpyruvate is needed for the synthesis of fatty acids and secondary metabolites of the shikimic acid pathway (Fischer *et al.*, 1997). This was confirmed in *Arabidopsis ppt1* knock-out plants that are unable to produce anthocyanins (Streatfield *et al.*, 1999). Uptake of C3, C5 or C6-phosphorylated compounds, used by plastids upon high demand of substrates and in heterotrophic tissues (e.g. for the synthesis of starch, fatty acids and the oxidative pentose phosphate pathway), is mediated by the third and fourth group of pPT, the glucose 6-phosphate/phosphate transporters (GPT, Kammerer *et al.*, 1998; Niewiadowsky *et al.*, 2005) and the xylulose 5-phosphate/phosphate transporter (XPT, Eicks *et al.*, 2002). Complete absence of GPT1, the predominant functional GPT in *Arabidopsis*, generates unviable plants due to its critical role in embryo sac development and pollen maturation (Niewiadowsky *et al.*, 2005).

NSTs, however, are localized in the membranes of the endoplasmic reticulum (ER) or the Golgi apparatus. They mediate the transport of nucleotide sugars into the luminal side of the ER and Golgi, supplying glycosyltransferases with sugar donors for the subsequent modification of proteins and lipids (Hirschberg *et al.*, 1998; Kawakita *et al.*, 1998; Abeijon *et al.*, 1989) (Figure 1). Several NSTs have been characterized from yeasts, animals and plants (Abeijon, *et al.*, 1996; Eckhardt *et al.*, 1996; Miura *et al.*, 1996; Baldwin *et al.*, 2001). The NSTs have been recently classified into three subfamilies based on sequence similarity, intracellular localization and substrate affinity (Martinez-Duncker *et al.*, 2003) (Figure 1). NST subfamily 1 comprises transporters of UDP-coupled sugars (UDP-Galactose (UDP-Gal) and UDP-N-acetyl glucosamine (UDP-GlcNAc)) and CMP-Sialic acid (CMP-Sia). NST subfamily 2 includes transporters of UDP-sugars; some of them located in the ER membrane (Norambuena *et al.*, 2002; Reyes *et al.*, 2006). The NST subfamily 3 shows the broadest substrate specificity. This family includes transporters of UDP-coupled sugars (e.g. UDP-glucose (UDP-Glc), UDP-Gal, UDP-GlcNAc and UDP-Xylose (UDP-Xyl)) and GDP-coupled sugars (GDP-Mannose (GDP-Man), GDP-Fucose (GDP-Fuc) and GDP-Arabinose

(GDP-Ara)). These proteins are thought to be an evolutionary intermediate between NST subfamilies 1 and 2 (Martinez-Duncker *et al.*, 2003).

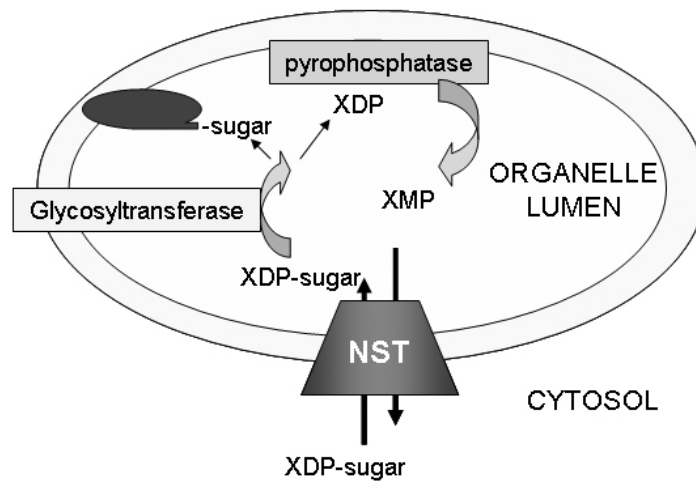


**Figure 1.** General transport mechanism of NSTs.

The NST mediates the transport of XDP-sugars in exchange for the monophosphate nucleoside XMP, which is formed by the action of pyrophosphatases over the diphosphate nucleotide XDP. This XDP is generated as a byproduct of the transfer reaction of the sugar group to an acceptor molecule (oval structure) by glycosyltransferases in the lumen of the organelle. Adapted from Martinez-Duncker *et al.* (2003).

Generally, each NST displays high substrate specificity, which is preferentially defined by the base coupled to the sugar nucleotide (guanidine, G, citidine, C or uridine, U) (Martinez-Duncker *et al.*, 2003; Capasso and Hirschberg, 1984; Chiaramonte *et al.*, 2001). However, in which way the transporters recognize a specific sugar group among compounds coupled to the same nucleotide diphosphate is still unknown. Moreover, similarities between protein sequences do not necessarily reflect substrate specificity or function. For example, mammalian UDP-GlcNAc transporters share a higher sequence identity with mammalian UDP-Gal and CMP-Sia transporters than with the yeast UDP-GlcNAc transporter. On the other hand, the sequence similarity among GDP-activated sugar transporters seems to be more significant for function and specificity (Baldwin *et al.*, 2001; Lühn *et al.*, 2001).

Recently, numerous novel proteins have been identified based on sequence similarity searches with pPT and NST protein sequences (Knappe *et al.*, 2003a; Handford *et al.*, 2004, Bakker *et al.*, 2005). The homologous NST/pPT protein family includes the products of 16 genes of *Caenorhabditis elegans* (Gerardy-Schahn and Eckhardt, 2004), 15 of humans (Ashikov *et al.*, 2005), 2 of yeast and more than 40 genes of *Arabidopsis* (Knappe *et al.*, 2003a; Bakker *et al.*, 2005). The role of the majority of the newly identified NST/pPT proteins is still to be determined and the reason for the existence of this large number of homologous proteins, especially in plants, is still unclear.

The NST/pPT homologous proteins share no more than 20-25% amino acid identity with known NST and pPT proteins, but the common structural characteristics are conserved among them. The NST/pPT like proteins contain 7 to 10 predicted TMDs, positioned in similar regions as the TMDs of known NSTs and pPTs. In addition, several residues are preserved among these proteins, including two conserved lysines (K41 and K273, numbered according to the sequence of the spinach triose phosphate/phosphate transporter), that are presumably required for substrate binding (Knappe *et al.*, 2003a; Handford *et al.*, 2004; Bakker *et al.*, 2005). Lysine<sup>273</sup> belongs to the conserved GALNK motif that is required for GDP-Man binding and seems to be specific for GDP-sugar transporters (Gao *et al.*, 2001). The NST/pPT homologous proteins do not contain the whole conserved motif, except for the lysine.

Sequence comparisons between the NST, pPT and NST/pPT homologous proteins revealed discrete subfamilies (Knappe *et al.*, 2003a; Bakker *et al.*, 2005). Protein sequence alignments (shown as a phylogenetic tree) of 30 of the *Arabidopsis* NST/pPT homologous proteins and representative members from the NST and pPT families are presented in Figure 2. These closely related *Arabidopsis* NST/pPT homologous proteins clearly split in three subfamilies: the KV/A/G, KT and KD families. The names of these subfamilies refer to the presence of the conserved lysine<sup>273</sup> residue, followed by a valine, an alanine or a glycine (V/A/G) in the KV/A/G subfamily, a threonine (T) in the KT subfamily, or an asparagine (D) in the KD subfamily. Because the residue at position 274 is

characteristic of each subfamily, it supposedly has a role in the determination of the substrate specificity of these transporters (Knappe *et al.*, 2003a).

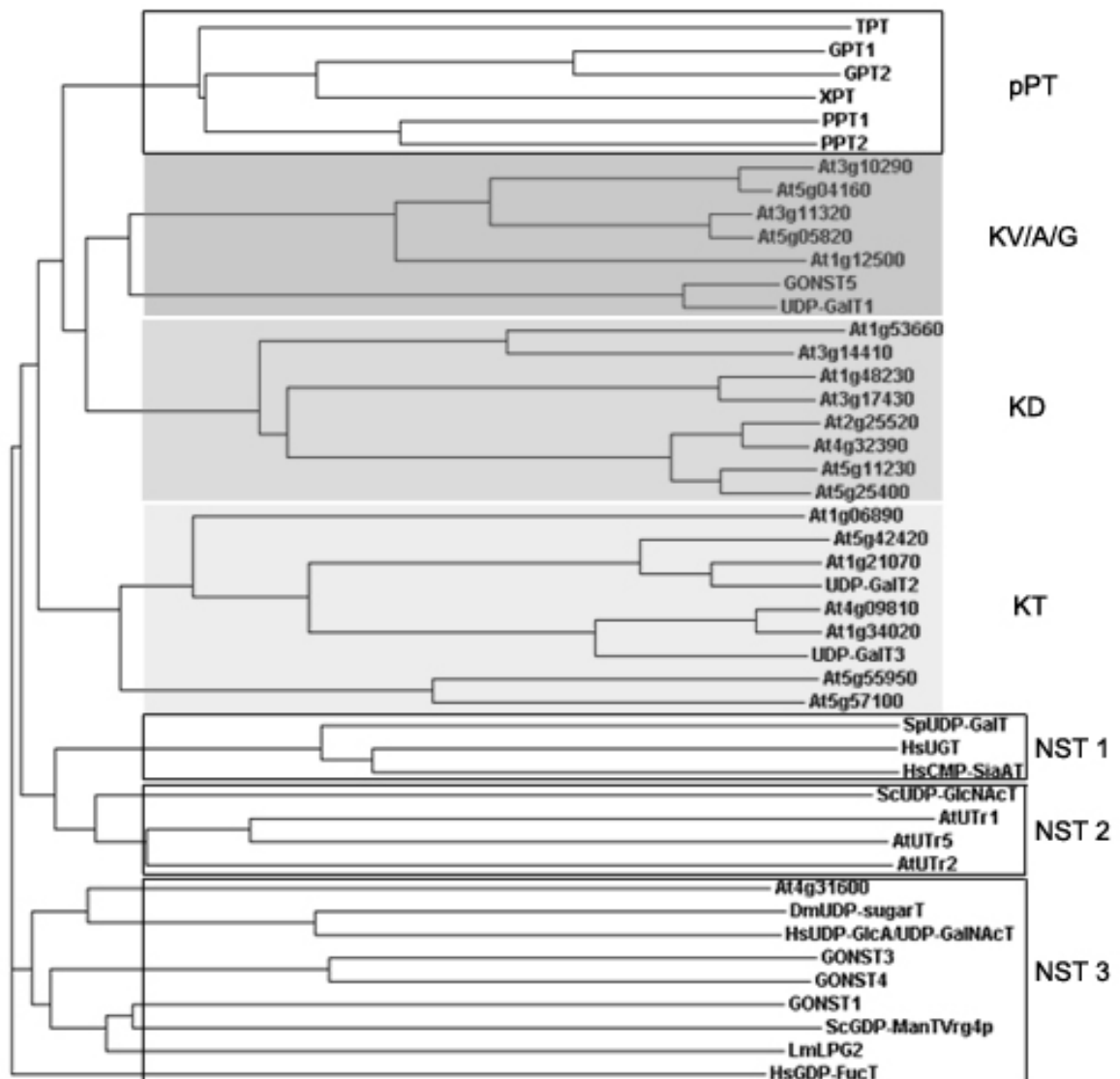


**Figure 2.** Phylogenetic tree of NST/pPT proteins.

Novel *Arabidopsis* proteins homologous to NST and pPT (presented in gray boxes) were aligned with *Arabidopsis* pPTs and with NSTs from yeast (Sp, *Saccharomyces pombe*, Sc, *Saccharomyces cerevisiae*), *Homo sapiens* (Hs), *Drosophila melanogaster* (Dm), *Leishmania mexicana* (Lm) and *Arabidopsis thaliana* (At). The homologous proteins cluster in three differentiated subfamilies, named KV/A/G, KD and KT (Knappe *et al.*, 2003a).

Only recently, studies on plant NST/pPT homologous proteins have led to the characterization of novel UDP-Gal and GDP-Man transporters (Bakker *et al.*, 2005; Handford *et al.*, 2004; Norambuena *et al.*, 2005) that are presumably involved in the synthesis of cell wall components. The *Arabidopsis* UDP-Gal transporter 1 (UDP-GalT1) and UDP-Gal transporter 2 (UDP-GalT2) were identified by expression cloning in a Chinese hamster ovary cell line lacking UDP-Gal transport activity (CHO-Lec8, Bakker *et al.*, 2005). These proteins were heterologously expressed in yeast and showed high affinity for UDP-Gal but almost no affinity for other nucleotide sugars. A third *Arabidopsis* UDP-Gal transporter, AtUTr2, was identified by sequence similarity with AtUTr1, and was found to be specific for UDP-Gal transport *in vitro* and *in vivo* (Norambuena *et al.*, 2005). A group of *Arabidopsis* Golgi nucleotide sugar transporters (GONST2-5) were identified due to similarities with GONST1, and all were shown to transport GDP-Man by complementation of the manosylation defects present in the *vrg4* yeast mutant (i.e. hypersensitivity to hygromycin and reduced manosylation of matrix glycoproteins) (Handford *et al.*, 2004). Interestingly, GONST5 shares high similarity (91% amino acid identity) with UDP-GalT1, although they transport different base-coupled nucleotide substrates (GDP-Man for GONST5 and UDP-Gal for UDP-GalT1). This is unusual compared to other GDP-sugar transporters, which appear to be more conserved in sequence and function than the UDP-sugar transporters (Martinez-Duncker *et al.*, 2003, Bakker *et al.*, 2005).

The identification of more than 20 putative NST/pPT proteins in the genome of *Arabidopsis* raises questions regarding their role in plant metabolism (i.e. supply of precursors for protein, lipid and polysaccharide glycosylation). Most of the NSTs characterized so far are likely located in the Golgi apparatus, including two members of the KV/A/G subfamily and one of the KT subfamily (UDP-GalT1, UDP-GalT2; Bakker *et al.*, 2005, and GONST5, Handford *et al.*, 2004). However, two of the KVAG proteins (KVAG1 and KVAG2) present putative plastid targeting sequences (Aramemnon database, Schwacke *et al.*, 2003). The remaining homologous proteins contain signals for the secretory pathway, ambiguous targeting peptides or no signals detected by computer prediction programs (Knappe *et al.*, 2003a). The main goal of the work presented here was to analyze the physiological role of KVAG1 and KVAG2 in plants.

In animals and yeast, deleterious defects in NSTs have tremendous negative consequences on the metabolism of these organisms, in many cases resulting in lethality (Dean *et al.*, 1997; Freeze, 2001; Lübke *et al.*, 2001; Hirschberg, 2001). However, there are no NST mutants identified in plants that display such drastic characteristics. Therefore, the role of KVAG1 and KVAG2 was investigated by analyzing T-DNA insertion mutants which presented a reduction in leaf phospholipids. Transport measurements were performed using heterologously expressed proteins and a panel of potentially activated substrates was tested.

## 2.1 Materials

### 2.1.1 Vectors

The vectors used for the different processes of cloning, listed in Table 1, were Gateway™ compatible plasmids (see 2.2.1). The construct used for labelling the Golgi apparatus contained the mouse sialyltransferase (ST) cDNA coupled to the cDNA for the green fluorescent protein (GFP), driven by the CaMV 35S promoter (35S-ST::GFP, Lee *et al.*, 2002). This and the construct employed for labelling the ER (35S-mGFP fused to an ER retention signal), were kindly provided by Dr. Martin Hülskamp.

**Table 1.** Vectors employed in cloning and organelle labeling.

Vector	Source	Cloning purpose
pENTR D-TOPO	Invitrogen	Entry cloning of PCR fragments for further delivery into an expression vector.
pGWB3	Dr. T. Nakagawa, Shimane University	Expression of GUS <i>in planta</i> driven by the cloned promoter.
pGWB5	Dr. T. Nakagawa, Shimane University	Expression of GFP <i>in planta</i> fused to the cloned cDNA, driven by 35S CaMV promoter.
pYES-DEST52	Invitrogen	Protein expression in <i>Saccharomyces cerevisiae</i> containing a 6X histidine fusion tag.
35S-ST::GFP	Lee <i>et al.</i> , 2002; Dr. M. Hülskamp	Expression of ST fused to GFP as a marker for Golgi protein localization.
35S-mGFP-ER	Dr. M. Hülskamp	Expression of GFP tagged to the ER as a marker for ER protein localization.

### 2.1.2 Bacteria and Yeast Strains

*Escherichia coli* (*E. coli*) DH5 $\alpha$ , for plasmid DNA amplification  
*supE44 lacU169 ( $\Phi$ 80, lacZ M15) hsdR17 recA1 endA1 gyrA96 thi-1 relA1*

*Agrobacterium tumefaciens* (*A. tumefaciens*)

strain GV3101, Rif<sup>R</sup> Gm<sup>R</sup>, for *Arabidopsis* transformation  
 strain GV2260, Rif<sup>R</sup> Carb<sup>R</sup>, for tobacco transformation.

*Saccharomyces cerevisiae* (*S. cerevisiae*) InvSC1, for protein expression.  
*his3 $\Delta$ 1 leu2 trp1-287 ura3-52*

### 2.1.3 Plant Material

#### *Arabidopsis thaliana* (L.) Heynh. (*Arabidopsis*)

Ecotype Columbia (Col-0), as source of wild type (WT) DNA, mRNA and for control when compared to mutant lines.

Col-0 T-DNA insertion lines, for studies on plant development in the absence of a single protein. Salk and GabiKat Lines were obtained from the Nottingham *Arabidopsis* Stock Center (NASC, Alonso *et al.*, 2003).

*pho1.2* mutant line, phosphate deficient shoot, for crossings with *KVAG* mutant lines (Hamburger *et al.*, 2002)

#### Tobacco

*Nicotiana benthamiana* (*N. benthamiana*)

Bright Yellow 2 culture cells (BY2)

Variety Samsun

For subcellular localization of proteins fused to GFP. BY2 and Samsun cells were employed as protoplasts. The leaves of *N. benthamiana* were directly infiltrated with *Agrobacteria*.

### 2.1.4 Plant Procedures

#### 2.1.4.1 *Arabidopsis* Seed Sterilization

##### Sterilization Solution

Na-hypochlorite 15% (v/v)

Tween 20 0.5% (v/v)

Seeds were distributed in eppendorf tubes (200-300 seeds) and rinsed shortly with 70% ethanol, following incubation in 1 ml of sterilization solution for 20 min with agitation. The solution was removed and the seeds were rinsed 4-5 times with double distilled (dd) sterile water. Alternatively, for sterilization of several sets of seeds chlorine-gas was employed. For this, eppendorf tubes containing the seeds were placed into a glass desiccator along with a beaker containing 100 ml of Na-hypochlorite. Three ml of HCl were carefully added to the Na-hypochlorite and the



chamber was closed tightly. The seeds were incubated 4-6 hours with the chloride-gas. Before sowing, the remnant chloride-gas was allowed to evaporate from the seeds under sterile conditions (15-20 min).

#### 2.1.4.2 Pollen Staining

##### Alexander Stain

Ethanol 95%	10% (v/v)
Malachite green	100 mg/l
Glycerol	25% (v/v)
Phenol	50 g/l
Chloral hydrate	50 g/l
Acid fuchsine	500 mg/l
Orange G	50 g/l
Acetic acid (glacial)	1% (v/v)

The procedure was as described by Alexander (1969), preparing the stain by mixing the reagents in the order given (with addition of  $\frac{1}{2}$  total volume of water after malachite green). The solution was stored at room temperature (RT) in a light-protected bottle. Pollen was placed over a microscope glass slide and covered with a few drops of stain. The slide was briefly heated on the flame of a burner, preventing the stain from boiling. The coloured pollen grains were observed under the light microscope.

## 2.2 Molecular Biology Techniques

### 2.2.1 Gateway™ Cloning

This cloning system uses the specific recombination properties of the bacteriophage lambda to facilitate transfer of a DNA fragment of interest into multiple expression vectors conserving its orientation and open-reading-frame (ORF). The vectors used in Gateway cloning contain recombination sites framing the insertion region (*att* sites, in entry vectors, 100 bp; in expression vectors, 25 bp) which allow specific recombination among them, exchanging the inserts between the entry and destination vectors. The results include an expression clone containing the DNA of interest and a byproduct clone having the entry clone

backbone and the *ccdB* gene, previously enclosed within the destination vector *att* sites, for strong negative selection.

#### Cloning into pENTR/D-TOPO Vector

The directional cloning of DNA fragments into the pENTR/D-TOPO vector (Invitrogen) was achieved by designing the forward primer with a 5' extension (CACC) that anneals to an overhang sequence present in the vector (GTGG), and promotes the directional joining of the fragment by the action of topoisomerases. The cloning reaction contained 10-20 ng of insert DNA (fresh PCR product), 0.3  $\mu$ l salt solution and 0.3  $\mu$ l of TOPO vector (final volume 2-5  $\mu$ l), and was incubated at RT for 1 hour. *E. coli* competent cells were transformed with 2  $\mu$ l of the reaction.

#### Recombination of Entry and Destination Vectors

Site specific recombination of entry and destination vectors was accomplished by incubation with a mixture of integrase and excisionase enzymes (LR Clonase Mix<sup>TM</sup>, Invitrogen) that catalyzed the reaction. Equal amounts (30-50 ng) of both plasmid DNAs were incubated overnight (O/N) at RT with 1X LR reaction buffer and 0.4  $\mu$ l of LR clonase mix (final volume 3-4  $\mu$ l). The enzymes were inactivated by addition of 1  $\mu$ g proteinase K and incubation at 37°C for 10 min. Two  $\mu$ l of the recombination reaction were used for transforming *E. coli* competent cells.

### 2.2.2 *E. coli* Transformation

#### 2.2.2.1 Preparation of *E. coli* Competent Cells for Heat-shock Transformation

##### TSS Solution

PEG 8000	10% (w/v)
MgCl <sub>2</sub>	40 mM
Dimethyl-sulfoxide (DMSO)	5% (v/v)

The TSS procedure described by Chung and Miller (1993) was initiated with an O/N culture of *E. coli* DH5 $\alpha$  grown at 37°C. A 600  $\mu$ l aliquot was diluted in 100 ml of LB medium (Appendix 8.2) and cultured until reaching an optical density (OD)<sub>600</sub> of 0.3-0.4. The bacteria were transferred to sterile 50 ml Falcon tubes and pelleted at 2500 xg, 4°C for 5 min. The cell pellet was resuspended softly in 4 ml

of cold TSS solution. The cells were aliquoted in 100 µl fractions and quick frozen in an ice/ethanol bath. The cells were stored at -80°C.

### 2.2.2.2 *E. coli* Heat-shock Transformation

For one transformation 50-100 µl of competent cells were thawed on ice and gently mixed with 200 ng of plasmid DNA. After 10 min incubation on ice the cells were heat-shocked by incubation at 42°C for 30-60 sec, and immediately brought back to ice. The cells were recovered in the presence of 900 µl SOC medium (Appendix 8.2) for one hour at 37°C. For selection of recombinant clones the transformed cells were pelleted at 2000 rpm for 2 min, resuspended in 200 µl of SOC and an aliquot plated on solid medium with suitable antibiotics.

### 2.2.3 *A. tumefaciens* Transformation

#### 2.2.3.1 Preparation of *A. tumefaciens* Competent Cells for Electrotransformation

##### MGL Medium

Bacto-Trypton	0.5% (w/v)
Yeast extract	0.25% (w/v)
NaCl	0.5% (w/v)
Mannitol	0.5% (w/v)
Na-Glutamate	0.12% (w/v)
KH <sub>2</sub> PO <sub>4</sub>	0.02% (w/v)
MgSO <sub>4</sub>	0.01% (w/v)
Biotin	1 µg/ml

One colony of *A. tumefaciens* was pre-cultured for 1-2 days in 5 ml of MGL medium with the corresponding antibiotics under vigorous shaking at 28°C. The culture was diluted in 100 ml of MGL medium and grown until reaching an OD<sub>600</sub> of 0.5 (4-6 hours). The bacteria were transferred to cold and sterile 50 ml Falcon tubes and centrifuged at 3000 rpm, 4°C for 10 min. All further steps were performed on ice. The cells were resuspended in 40 ml cold 1 mM HEPES pH 7.0 and centrifuged again. The cell pellet was resuspended in 40 ml of cold storing solution (1 mM HEPES pH 7.0 / 10% glycerin) and centrifuged again. The cells were resuspended in subsequently reduced volumes of cold storing solution (2 ml

and 200  $\mu$ l), and finally 50  $\mu$ l aliquots were frozen in liquid nitrogen and kept at -80°C.

#### **2.2.3.2 Electrotransformation of *A. tumefaciens***

Competent *A. tumefaciens* cells were thawed on ice and mixed with 200-500 ng of plasmid DNA (preferably desalted). After 5 min incubation on ice the bacteria-DNA mixture was transferred to a cold electroporation chamber and subjected to an electroshock (conditions: 25  $\mu$ F; 400  $\Omega$ ; 2.5 kV pulse for 2 sec). One ml of YEB medium (Appendix 8.2) at RT was immediately added and the cells were incubated 2 hours at 28°C. The transformed cells were shortly centrifuged at 2000 rpm and resuspended in 200  $\mu$ l of YEB medium. An aliquot was plated on solid YEB medium, containing suitable antibiotics, and incubated at 28°C for 2 days.

#### **2.2.4 *S. cerevisiae* Transformation**

The transformation of yeast strain InvSC1 was performed following the recommendations of Invitrogen™ Instruction Manual for pYES-DEST52 Gateway™ Vector. Briefly, an O/N culture was diluted to an OD<sub>600</sub> of 0.4 in 50 ml of YPD medium (Appendix 8.3) and grown for additional 2-4 hours at 30°C. The cells were centrifuged at 2500 rpm and washed in 40 ml 1X TE (100 mM Tris-HCl, pH 7.5; 10 mM EDTA, pH 8.0). The cell pellet was resuspended in 2 ml 1X LiAc/0.5X TE (pH 7.5) and incubated at RT for 10 min. For each transformation 100  $\mu$ l of the yeast suspension was mixed with 0.5-1  $\mu$ g of plasmid DNA and 100  $\mu$ g of denatured sheared salmon sperm DNA. This was mixed with 700  $\mu$ l of 1X LiAc/40% PEG-3350/1X TE (pH 7.5, prepared fresh and filter-sterilized) and incubated at 30°C for 30 min. Finally, 88  $\mu$ l of DMSO were added and the cells were heat shocked at 42°C for 7 min. After a short centrifugation, the cells were washed with 1 ml 1X TE, re-pelleted and resuspended in 50-100  $\mu$ l of 1x TE and plated on selective medium (SC without uracil, Appendix 8.3). The positive transformed colonies were distinguishable after 3-4 days of incubation at 30°C.

### 2.2.5 Isolation and Transformation of Tobacco Protoplasts

#### Washing Solution

BSA Bovine Albumin	0.5% (w/v)
2-Mercaptoethanol	0.01% (v/v)
CaCl <sub>2</sub>	50 mM
Na-Acetate, pH 5.8	10 mM
Mannitol	0.25 M

The solution was filter-sterilized and kept at 4°C.

#### Digestion Solution

Cellulase Onozuka RS	1% (w/v)
Macerozyme Onozuka RS	0.5% (w/v)
Pectinase	0.1% (w/v)

The enzymes were dissolved in 50 ml of washing solution and mixed with a stirrer for 20-30 min. Prepared fresh every time and filter-sterilized prior to use.

#### W5 Solution

NaCl	154 mM
CaCl <sub>2</sub>	125 mM
KCl	5 mM
Glucose	5 mM

The pH was adjusted to 5.8-6.0 with KOH. It was filter-sterilized and kept at 4°C.

#### MMM Solution

MgCl <sub>2</sub>	15 mM
MES-KOH, pH 5.8	0.1% (w/v)
Mannitol	0.5 M

The solution was filter-sterilized and kept protected from light at 4°C.

#### PEG Solution

PEG 4000 or 6000	40% (w/v)
Mannitol	0.4 M
Ca(NO <sub>3</sub> )	20.1 M

The pH was adjusted to 8.0-9.0 with KOH and autoclaved. It was stored at -20°C and thawed at 37°C, 2-3 hours prior to use.

**K3- Medium 0.4 M**

The medium was prepared by diluting all component stocks to 1X following addition of 12.6 mg/ml Ca-phosphate, 1 mg/ml myo-Inositol, 2.5 mg/ml D(+)-Xylose, 1.37 g/ml of sucrose and adjusting the pH to 5.6. Finally, 0.01 mg/ml of NAA and Kinetin were added and the medium was filter-sterilized.

## Macroelements 10X Stock

NaH <sub>2</sub> PO <sub>4</sub>	1.5 mg/ml
CaCl <sub>2</sub>	9 mg/ml
KNO <sub>3</sub>	25 mg/ml
NH <sub>4</sub> NO <sub>3</sub>	2.5 mg/ml
(NH <sub>4</sub> ) <sub>2</sub> SO <sub>4</sub>	1.34 mg/ml
MgSO <sub>4</sub>	2.5 mg/ml

## Microelements 100X Stock

KI	0.7 mg/ml
H <sub>3</sub> BO <sub>3</sub>	3 mg/ml
MnSO <sub>4</sub>	0.01 mg/ml
ZnSO <sub>4</sub>	2 mg/ml
Na <sub>2</sub> -MoO <sub>2</sub>	0.25 mg/ml
CuSO <sub>4</sub>	0.025 mg/ml

## Vitamins 100X Stock

Nicotinacid	1 mg/ml
Pyridoxin-HCl	1 mg/ml
Thiamin-HCl	0.01 mg/ml

## EDTA/Fe 500X Stock:

EDTA	7.5 mg/ml
Fe(II)SO <sub>4</sub>	5.5 mg/ml

The EDTA and Fe(II)SO were dissolved by heating separately in dd water. The two components were subsequently mixed and autoclaved.

Ca-phosphate:

CaHPO<sub>4</sub> 1.26 mg/ml

Dissolved in dd water, pH adjusted to 3.0 with 25% HCl and autoclaved.

Naphtyl-acetic acid (NAA) 1 mg/ml

Dissolved in dd water adding a few drops of NaOH, and filter-sterilized.

Kinetin 0.5 mg/ml

Dissolved in 0.1 M HCl and filter sterilized.

### Cell wall digestion

The procedure followed the indications of Ros and Kunze (2001) with some modifications. All steps were performed under maximum sterile conditions. A pre-culture of BY2 cells 3-4 days old or leaves from 3-4 weeks old tobacco Samsun var. sterile plants were used for protoplasts preparation. The BY2 cell suspension (25 ml) was centrifuged at 100 xg at RT for 5 min, and the supernatant was carefully discarded afterwards. The cell pellet was gently resuspended in 25 ml of washing solution and centrifuged again. The supernatant was removed and 10-13 ml of digestion solution was slowly added. The suspension was incubated O/N inside a Petri dish at RT in the dark. To obtain "green protoplasts" the Samsun leaves (4 g) were finely sliced with a scalpel inside a Petri dish, covered with digestion solution (20 ml) and incubated O/N in the darkness.

### Cell wall debris removal and PEG mediated transformation

The Petri dish was gently shaken (3-4 times) to improve cell wall removal from the protoplasts. The cell suspension was transferred to a sterile 50 ml Falcon tube and centrifuged without brake at 50 xg at RT for 5 min. The supernatant from BY2 protoplasts was removed and 25 ml of washing solution was slowly added. The cells were centrifuged as mentioned before; the supernatant removed and 10 ml W5 solution was gently added. In the case of Samsun cells, after the first centrifugation the middle phase was transferred to a new Falcon tube (the upper phase contained floating cells while the bottom phase cell debris) and 8 ml of W5 was slowly added.

Both cells suspensions, BY2 and Samsun protoplasts, were pelleted again and after supernatant removal 5-10 ml of W5 solution was softly added. An aliquot was observed under the microscope to check the quantity and quality of the protoplasts (total approximately expected:  $10^6$  viable protoplasts). The protoplast suspension was incubated 1 hour at 4°C. The supernatant was completely removed and 10 ml of MMM solution was added very slowly until complete resuspension. The cells were centrifuged (without brake at 50 xg, RT for 5 min), and the supernatant was exchanged by 1 ml of MMM solution (in order to obtain  $1 \times 10^6$  viable protoplasts/ml). For one transformation, 300  $\mu$ l of protoplast suspension was mixed with 30  $\mu$ g of plasmid DNA (maximum 30  $\mu$ l in volume), and 300  $\mu$ l of PEG solution was added drop-by-drop. The protoplasts-DNA-PEG suspension was incubated 20 min at RT, prior gently addition of 10 ml of W5 solution. The protoplasts were centrifuged (without brake at 50 xg at RT for 5 min) and the supernatant removed. Gently, 4 ml of K3 medium was added in 1 ml aliquots, and the cell suspension was transferred to a small Petri dish. The cells were incubated in the dark at 24-26°C O/N, and the expression of the reporter protein was followed 18, 24, 38, and 44 hours after transformation.

### 2.2.6 *N. benthamiana* Leaf Epidermal Cell Transformation

#### Agro-mix Solution 10X

MgCl <sub>2</sub>	100 mM
MES, pH 5.6	100 mM

The pH was adjusted to 5.6 with KOH and autoclaved.

#### Acetosyringone (3',5'-Dimethoxy-4'-hydroxyacetophenone, 97%)

Acetosyringone	15 mM
----------------	-------

Dissolved in 100% ethanol (3 mg/ml) and stored at 4°C.

*N. benthamiana* plants were 1-2 month old (before flowering). A fresh colony or liquid culture of *A. tumefaciens* strain 2260, containing the binary vector of interest, was grown O/N at 28°C in 50 ml of YEB (Appendix 8.2) with antibiotics. In parallel, the helper agrobacteria strain 19K (Rif<sup>R</sup>, Kan<sup>R</sup>) was also grown. The cells were centrifuged at 3000 rpm for 15 min, the supernatant discarded and the cell pellet was resuspended in 1.5 ml of 1X Agro-mix solution (with 0.15 mM Acetosyringone). The cells were incubated at RT for 2-6 hours. The recombinant



Agrobacteria were mixed with the helper strain (1:1 volume) and using a syringe (without needle) were infiltrated into the abaxial surface of the leaf. The expression of the reporter protein was monitored 2-4 days after inoculation.

### 2.2.7 *Arabidopsis* Stable Transformation

#### Infiltration Medium

Sucrose	5% (w/v)
Silwete	0.03% (v/v)

The sucrose was dissolved in water and the pH was adjusted to 5.7. The bacteria were resuspended in the sucrose solution and silwete was added just before plant inflorescence transformation.

The floral dip method for *Arabidopsis* transformation was performed as described by Clough and Bent (1998), employing *Arabidopsis* plants on the onset of flowering (6-8 weeks old). A preculture of transformed agrobacteria (2 ml) was diluted in 200 ml of YEB medium (in the presence of suitable antibiotics, Appendix 8.2) and grown O/N at 28°C. The culture was centrifuged at 3000 rpm for 10 min and the cell pellet was resuspended in infiltration medium to an OD<sub>600</sub> of 0.8. Flowers of *Arabidopsis* were dipped in the bacterial solution for 20 sec and the plants were laid horizontally for 2 days avoiding direct light at 22-25°C. The plants were transferred to the greenhouse and the transformed seeds were collected a few weeks later.

### 2.2.8 Reporter Protein Detection *in planta*

#### 2.2.8.1 GUS Staining

##### Staining Solution

NaPO <sub>4</sub> , pH 7.2	100 mM
EDTA	10 mM
K-Ferricyanide	0.5 mM
K-Ferrocyanide	0.5 mM
Triton X-100	0.1% (v/v)
D-Glucuronic acid (X-Gluc)	1 mM

The procedure was as described by Gallager Ed. (1992). The substrate X-Gluc was prepared as a stock at 20 mM in N'-N'-Dimethylformamide (DMF), and added to the staining solution just prior tissue immersion. For protein fixation in the tissue it was first imbedded in 2% para-formaldehyde, 100 mM Na-phosphate pH7.0, and 1 mM EDTA and incubated on ice for 30 min. The material was rinsed in 100 mM of Na-phosphate buffer, covered with sufficient staining solution and vacuum infiltrated for 15-20 min. The tissue was incubated at 37°C for some hours (or O/N). The staining solution was discarded and replaced by 50% ethanol, 5% acetic acid and 3.7% formaldehyde, to fix the stained tissues. It was incubated at 60°C for 30 min, following several washes with 80% ethanol, necessary for chlorophyll removal. To prevent browning of tissues like flowers or fruits, 10 mM of ascorbic acid was added to the staining solution.

### 2.2.8.2 GFP Visualization

Transforming cells or tissues expressing a protein of interest fused to the Green Fluorescent Protein (GFP) were observed under an epi-fluorescence microscope (Nikon, Eclipse E800) with a filter GFP (R) – BP (EX 460-500, DM 505, BA 420). The image data were acquired by a digital camera (Nikon Coolpix 995) coupled to the microscope and analyzed using the DISKUS v.4.30.20 (2002) program.

### 2.2.9 DNA Extraction

#### 2.2.9.1 *E. coli* Plasmid DNA Isolation

##### Solution I

Tris-HCl, pH 8.0	25 mM
Glucose	50 mM
EDTA	10 mM

##### Solution II

NaOH	0.2 M
SDS	1% (w/v)

##### Solution III

Potassium acetate, pH 4.5	3 M
---------------------------	-----

This protocol was performed after Birnboim and Doly (1979). An O/N culture of recombinant bacteria (3-5 ml in LB with antibiotic, Appendix 8.2) was centrifuged

at 3000 rpm at 4°C for 10 min, following resuspension of the cell pellet in 750 µl of 50 mM Tris-HCl pH 8.0. The cells were pelleted again and resuspended in 100 µl of solution I, following incubation for 5 min at RT. 200 µl of solution II were added and mixed strongly, and the cell lysate was incubated at RT for 10 min. For neutralization 150 µl of solution III were added, mixed gently by inversion and incubated 10 min on ice. Plasmid DNA was separated from cell debris and genomic DNA by centrifugation (14000 rpm at 4°C for 15 min), transferring the supernatant to a new eppendorf tube. One volume of phenol and one of chloroform:isoamyl alcohol (24:1) were added to remove protein contaminants, shaking vigorously until an emulsion was formed. After centrifugation at 12000 rpm for 10 min, the upper phase was transferred to a new tube where the DNA was precipitated by adding 1 ml of 100% ethanol and centrifugation at 14000 rpm for 20 min. The nucleic acid pellet was rinsed with 70% ethanol and air dried before resuspending in 50 µl of TE containing 10 µg/ml of RNase.

An alternative protocol for *E. coli* plasmid isolation employing diatomaceous earth as binding matrix was also used (BioRad):

**Cell Resuspension Buffer (Solution 1)**

Glucose	50 mM
Tris-HCl, pH 8.0	25 mM
EDTA, pH 8.0	10 mM
RNase A	20 µg/ml

**Alkaline Lysis Solution (Solution 2)**

NaOH	0.2 N
SDS	1% (w/v)

**Neutralization Solution (Solution 3)**

Guanidine-HCl	5.3 M
Potassium acetate, pH 5.0	0.7 M

**Binding Matrix**

Guanidine-HCl	5.3 M
Tris-HCl, pH 8.0	20 mM
Diatomaceous earth	0.15 g/ml

**Washing Buffer**

Tris-HCl, pH 8.0	20 mM
EDTA, pH 8.0	2 mM
NaCl	0.2 M
Ethanol	50% (v/v)

From an O/N bacterial culture 1.5 ml were centrifuged at 13000 rpm for 30 sec. The cell pellet was resuspended by vortexing in 200 µl of solution 1 following addition of 200 µl of solution 2 and gently mixed by inversion (10 times). The suspension was incubated at RT for 5 min; solution 3 was added (200 µl) and mixed in by inversion (10 times). The cell debris was precipitated by centrifugation (13000 rpm for 5 min) and the supernatant was transferred to a filter column placed in a 2 ml eppendorf tube. The binding matrix (200 µl) and plasmid DNA containing solution were mixed by pipetting, and the column was centrifuged at 13000 rpm for 30 sec, discarding the flow through afterwards. 500 µl of washing buffer were added to the column, centrifuged (13000 rpm for 30 sec) and the flow through discarded. Additional washing buffer was added (500 µl) and centrifuged for 2 min (13000 rpm) this time, removing all traces of ethanol. For DNA elution the column was placed in a new eppendorf tube and 50-100 µl of 10 mM Tris-HCl pH 8.0 were added, following centrifugation for 1 min (13000 rpm).

**2.2.9.2 Arabidopsis DNA Isolation****2X Buffer**

NaCl	0.6 M
Tris-HCl, pH 7.5	100 mM
EDTA	40 mM
Sarcosyl	4% (w/v)
SDS	1% (w/v)

**Extraction Buffer I**

2X Buffer	1X
Urea	4.8 M
Phenol	5% (v/v)

This protocol was used for obtaining high amounts of good quality DNA from inflorescences. Three to four inflorescences were frozen in liquid nitrogen and grinded with a pestle. 500 µl of extraction solution were added and mixed well with the tissue powder. To remove proteins and carbohydrates, 400 µl of phenol:chloroform:isoamylalcohol (25:24:1) were added and the probe was vigorously shaken forming an emulsion, followed by centrifugation at 3500 rpm for 10 min. The upper phase was transferred to a new eppendorf tube and 0.8 volumes of isopropanol were added to precipitate the nucleic acids. After 10 min incubation at -20°C the samples were centrifuged again (3500 rpm for 10 min) and the pellet was washed twice with 70% ethanol. The DNA precipitate was air dried and resuspended in 50 µl of TE (10 mM Tris-HCl pH 8.0, 1 mM EDTA) containing 10 µg/ml of boiled RNase.

A second and quicker protocol for DNA extraction was employed when DNA was required for regular amplifications. It rendered DNA with lower quality than the previous protocol but was sufficient for PCR.

#### **Extraction Buffer II**

Tris-HCl, pH 7.5	200 mM
NaCl	250 mM
EDTA	25 mM
SDS	0.5% (w/v)

Rosette leaves from *Arabidopsis* (2-3) were collected in an eppendorf tube, frozen into liquid nitrogen and grinded with a pestle. 400 µl of extraction buffer were added and mixed vigorously by vortexing. The proteins were removed by adding 150 µl of potassium acetate (3M, pH 6.0) and centrifugation at 13000 rpm for 2 min. The supernatant was transferred to a new tube and 1 volume of isopropanol was added. The sample was mixed by inversion and incubated at RT for 10 min, following centrifugation at 13000 rpm for 10 min. The nucleic acid pellet was washed twice with 70% ethanol and air dried before resuspension in 50-100 µl of TE.

### 2.2.10 Genomic DNA Southern Blotting

#### Denaturing Solution

NaCl	1.5 M
NaOH	0.5 M

#### Neutralization Solution

Ammonium acetate (NH <sub>4</sub> Ac)	1 M
NaOH	10 mM

The DNA of interest (10-20 µg) was fully digested with suitable restriction enzymes for 6-16 hours and the genomic fragments were slowly separated by electrophoresis on 0.8% agarose gels (25 volts/cm). The DNA containing gel was submerged in denaturing solution for 30 min with gentle agitation, following immersion in neutralization solution for 30 min.

Transfer of separated DNA fragments from the gel to a nylon membrane (Hybond-N<sup>+</sup>, Amersham) was achieved by capillar transfer. A blotting system was arranged placing a tray with sodium saline citrate (SSC, 20X) as the liquid phase, a glass plate covering the tray and a stripe of Whatman paper pre-wet on SSC laid on top of the glass. The paper stripe was long enough to immerse both ends in the SSC and as wide as the gel. Two more pre-wet sheets of Whatman paper, the size of the gel, were stacked on top of the first stripe. The gel was briefly rinsed in dd water and placed on top of the papers with its bottom side facing up. The membrane was damped in SSC and placed on top of the gel, avoiding the formation of air bubbles. Two more sheets of Whatman paper (pre-soaked on SSC) covered the membrane and these were peaked by a thick stack of absorbent paper. A 0.5-1 kg weight on top of the structure enhanced the transfer and after 16 hours the blot was dismantled. The membrane was briefly rinsed on 2X SSC and the DNA was cross linked by ultraviolet light (UV).

#### Hybridization Buffer

Sodium phosphate buffer, pH 7.2	0.5 M
SDS	7% (w/v)
Salmon sperm DNA (denatured)	1 µg/ml

Alternatively Roti-Hybri-Quick Buffer (Roth) was used.

For pre-hybridization the membrane filter was incubated on a rotating flask with hybridization buffer (1 ml/cm<sup>2</sup>) for 2-6 hours at 65°C. The radioactive labeled probe (see below) was denatured for 10 min at 96°C, added to the buffer and incubated O/N at 62-65°C. The filter was washed once with non-radioactive hybridization buffer (30 min at 65°C) and twice with 2X SSC, 0.1% SDS (30 min at 65°C). A last, more stringent wash, was performed with 0.2X SSC, 0.1% SDS (10 min at 65°C), and the filter was briefly allowed to dry before wrapping it in plastic foil. The radioactivity on the blot was detected by a phosphor-image screen (Kodak Storage Phosphor Screen SO230) after several hours of incubation at RT, and the image was acquired using a phosphor-imager scanner device (Storm 860, Molecular Dynamics).

**Probe Labelling Solution A**

Tris-HCl, pH 8.2	1.2 M
MgCl <sub>2</sub>	0.125 M
2-Mercaptoethanol	2% (v/v)
dCTP, dGTP, dTTP	0.5 M (each)

**Probe Labelling Solution B**

HEPES/NaOH, pH 6.6	2 M
--------------------	-----

**Probe Labelling Mix A (5X)**

Solution A	20% (v/v)
Solution B	50% (v/v)
Random hexa-nucleotides	3.6 µg/ml

The radioactive labeled probe was prepared by first denaturing 300 µg template DNA (plasmid DNA or PCR product) with 10 µl of 5X mix A for 5 min at 96°C. BSA (2 µl from 1 mg/ml), 20-30 µCi (α-P<sup>32</sup>)-dATP and 3 U of Klenow fragment were added (final volume 25 µl) and incubated for 1-2 hours at 37°C. The labeled fragments were separated from non-integrated (α-P<sup>32</sup>)-dATP by passing through Sephacryl MicroSpin Columns S-200 (Pharmacia Biotech) and collected in a new eppendorf tube.

### 2.2.11 Plant RNA Extraction

All tools and containers employed were cleaned to remove RNAses (with 2% SDS or sterilized) prior to be in contact with the material and solutions used in the extraction of RNA. The solutions were prepared with Diethylpyrocarbonate (DEPC) treated dd water (autoclaved twice).

#### Extraction Solution

Sodium acetate (NaAc)	100 mM
Na-EDTA	1 mM
SDS	4% (w/v)

Prepared fresh every time, and the pH was adjusted to 5.0 with acetic acid.

This protocol was as described by Eggermont *et al.* (1996). Collected tissue (0.5-1 g) was grinded in liquid nitrogen and 1-2 ml of extraction solution was added to the pulverized material. As the solution started to thaw 1 volume of phenol:chloroform:isoamylalcohol (25:24:1) was added and mixed vigorously until an emulsion was formed, transferring it to a new tube and centrifuged at 10000 xg for 10 min. The supernatant was placed in a new eppendorf tube adding 0.5 volumes of lithium chloride (LiCl, 8M) and incubated on ice for 1 hour. After centrifugation at 10000 xg for 10 min, the RNA pellet was rinsed 3-4 times with 70% ethanol and allowed to air dry for 15 min. It was finally resuspended in 50-100  $\mu$ l of dd DEPC-water.

#### Trizol Protocol

RNA from small quantities of tissue (50-100 mg) was extracted using the Trizol (Invitrogen) protocol. The tissue was collected in an eppendorf tube, frozen in liquid nitrogen and disrupted with a pestle. Trizol reagent was added (0.8-1 ml), mixed vigorously and incubated for 5 min at RT. Chloroform (0.2 ml) was added and shaken until forming an emulsion. After 2-3 min of RT incubation the suspension was centrifuged at 12000 xg, 4°C for 15 min and the upper phase was transferred to a new tube. For RNA precipitation 0.5 ml of isopropanol was added, mixed by inversion and incubated 10 min on ice, following centrifugation (12000 xg, 4°C for 10 min). The nucleic acid pellet was washed twice with 75% ethanol and centrifuged at 7500 xg, 4°C for 5 min. After the pellet was air dried it was dissolved in 30  $\mu$ l of dd DEPC-water by incubating at 55°C for 10 min.



### 2.2.11.1 Analysis of RNA Quality

The quality of the extracted RNA was assayed by electrophoresis on agarose/formaldehyde gels, while quantification of the RNA was performed by spectrophotometric analyzes.

#### 10X Running Buffer

MOPS, pH 7.0	200 mM
Sodium acetate (NaAc)	50 mM
EDTA	5 mM

#### Agarose/Formaldehyde Gel

Agarose	1% (w/v)
Running buffer	1X
Formaldehyde	2% (v/v)

#### RNA Sample Preparation

RNA	1-2 $\mu$ l
Running buffer	1X
Formaldehyde	4.4% (v/v)
Formamide	40% (v/v)

The agarose was dissolved in warm dd DEPC-water and running buffer and formaldehyde were added under a gas extraction chamber, following pouring on the gel cast and allowing it to solidify. The RNA sample was denatured at 65°C for 10 min and immediately incubated on ice. Ethidium bromide was added to the sample (final concentration of 0.04 mg/ml) before loading the gel, and the electrophoresis was run with 1X running buffer at 150 volts for 2-3 hours. The RNA was monitored by observation under UV.

### 2.2.11.2 Synthesis of First Strand cDNA

Messenger RNA (mRNA) present in the total RNA extraction was reverse transcribed by Superscript<sup>TM</sup> II RNase H<sup>-</sup> Reverse Transcriptase (Invitrogen) using oligos poly-dT that anneal to the poly-A region of mRNA and prime the reaction. Total RNA (2  $\mu$ g) was treated with DNase (10 U, Roche) at 37°C for 15 min, to remove contaminating DNA, following DNase inactivation by adding EDTA (2.27 mM final concentration) and heating at 65°C for 10 min. The reverse transcription reaction contained 1X reaction buffer, 20 ng/ $\mu$ l oligo poly-dT, 0.5 mM dNTPs, 10

mM Di-thiotreitol (DTT) and 200 U of reverse transcriptase. The reaction was incubated at 42°C for 1 hour followed by enzyme inactivation by heating at 70°C for 15 min. This first strand cDNA product was stored at -20°C and used as template for PCR (reverse transcribed-PCR, RT-PCR).

### 2.2.12 Polymerase Chain Reaction (PCR)

The Polymerase Chain Reaction or PCR is a method for the enzymatic amplification of specific sequences of DNA (Mullis *et al.*, 1986), consisting in the repetition of a cycle of 1<sup>st</sup> . DNA heat-denaturation, 2<sup>nd</sup> . primer annealing and 3<sup>rd</sup> . copy of the template DNA chain or extension. The steps within the cycle are determined by changes in temperature: 94°C for double strand DNA denaturation, 50-60°C for primer annealing, and 72°C for extension. The synthesis of new DNA strands is generated by the activity of *Taq* DNA polymerase, with optimal performance at 72°C and high tolerance to elevated temperatures. During every cycle the number of DNA strands duplicates, resulting in an exponential production of the sequences defined by the primers. In general, a PCR involved 1-10 ng of template DNA, 0.2 µM of each primer, 0.5 mM dNTPs, 1X of reaction buffer and 2-5 U of *Taq* polymerase, and the cycles were controlled using a thermocycler machine (Perkin Elmer).

Identification of homozygous T-DNA insertion mutants was accomplished by PCR. The DNA of each individual was assayed in two parallel PCR reactions per plant: (i) the wild type reaction amplified a fragment of the gene using primers flanking the region of the T-DNA insertion; (ii) and the mutant reaction amplified one border of the T-DNA together with the gene flanking fragment. The combination of PCR products indicated the genotype of individual plants for the T-DNA insertion and the gene of interest. The primers used for genotyping the T-DNA insertion lines are listed on Appendix 8.5.

#### 2.2.12.1 High-fidelity PCR for Cloning

With the purpose of cloning functional genes or promoters, a polymerase with high copy fidelity and a 3' exonuclease proofreading activity (Platinum *Pfx* DNA polymerase, Invitrogen, or *Pfu* Turbo DNA polymerase, Promega) was used for generating the PCR products. The reactions contained 10 ng of genomic DNA, 1X of reaction buffer, 1 mM MgCl<sub>2</sub> or MgSO<sub>4</sub>, 0.5 mM dNTPs, 0.3 µM primers and 1-2

U high fidelity DNA polymerases. The extension step for *Pfx* polymerase was at 68°C.

The generation of cDNA and promoter inserts for *in vivo* analysis was achieved by PCR using proofreading polymerases and specific primers (Appendix 8.5). The cDNA inserts were obtained from reversed transcribed mRNA from seedlings, flowers and roots (see 2.2.11). The exception were *KVAG1* and *UDP-GaIT1* full-length cDNAs that were amplified from the cDNA clones pda10276 and pda01968 (RAFL clones), obtained from the Riken Tsukuba Institute, Japan.

### 2.2.12.2 Colony PCR

A fast method to identify positive clones containing the desired insert was to perform a colony PCR. A regular PCR mixture was prepared (see 2.2.12, lacking template DNA) including one primer laying in the insert and another one in the vector backbone, aliquoted in 0.2 ml PCR tubes (or plates) and kept on ice. Using a sterile toothpick one transformed bacterial colony was picked from a selective plate and placed into one tube containing the PCR mix. The same was done with all selected colonies, followed by 30-35 cycles of PCR. The products were analyzed by agarose electrophoresis and clones presenting bands of the expected size were inoculated for subsequent plasmid DNA isolation, sequence analysis or cell transformation.

### 2.2.12.3 Plant Touch-and-Go PCR

This protocol for fast PCR analysis of plants (Berendzen *et al.*, 2005) was used to determine the zygotic state of T-DNA insertion lines when several dozens of individuals were analyzed in parallel (i.e. F2 progenies from crosses). The method is comparable to the colony PCR, since the template for *Taq* DNA polymerase was a small piece of plant leaf instead of genomic DNA solution. A PCR mix was prepared (2.5 µM each gene specific primers, 2.5 mM dNTPs, 5-10 U *Taq* polymerase, 1X reaction buffer, 1 mM MgCl<sub>2</sub>) and 50 µl aliquots were distributed in 0.2 ml PCR tubes or plates and kept on ice. Using a yellow pipette tip, a leaf was punctured against a firm surface (e.g. a finger covered with glove) and the tissue was transferred to the PCR mix by pipetting up and down. The samples were subjected to 40 cycles of PCR with extended annealing time (45 sec). The products were analyzed by agarose electrophoresis and putative homozygous

plants identified. The gene dose of the selected individuals was confirmed by PCR using as template genomic DNA isolated through the procedures described above (see 2.2.9.2).

### **2.2.13 Sequencing**

Sequencing reactions were performed using a mixture of sequenase and fluorochrome-labeled terminators contained in the BigDye® Terminator v1.1 & v3.1 Cycle Sequencing Kit (Applied Biosystems). The reaction, similar to a PCR, included 100-200 ng of plasmid DNA, 10  $\mu$ M of primer (one primer per reaction), 1X sequencing buffer and 2  $\mu$ l sequencing PreMix, in a final volume of 10  $\mu$ l. The sequencing reaction was subjected to 30-35 cycles of 10 sec denaturation (94°C), 12 sec of annealing (50°C) and 4 min extension (60°C). The products were analyzed in an automated sequencer ABI PRISM™ 310 Genetic Analyzer, and the results were edited using the EditView and AutoAssembler programs (Perkin Elmer Corp.).

## **2.3. Protein Techniques**

### **2.3.1 Protein Expression in the Yeast Heterologous System**

The native expression of NST and related proteins *in planta* is relatively low which represents a constraint for functional studies. To overcome this bottleneck, over expression of the protein in an organism with simpler cultivation methods is usually helpful, and can also minimize the background activity or interference from similar endogenous proteins.

#### **2.3.1.1 Yeast Membrane Extraction**

An O/N culture (20 ml) of transformed yeast cells was pelleted by centrifugation (2500 rpm) and resuspended in 50 ml of induction medium (SC-galactose lacking uracil, Appendix 8.3). The culture was further incubated 3 to 8 hours, depending on the optimal time for protein expression (individually studied for each protein). The induced cells were centrifuged and the pellet was resuspended in 200  $\mu$ l of pre-chilled 1x TE containing 100 mM of protease inhibitor Phenyl-methyl-sulfonyl-fluoride (PMSF).

The entire procedure from here on was performed at 4°C. The cells were broken using 0.4 mm glass beads (400 mg) and strong shaking for 10 min. The cell debris was separated from the membranes by adding 700 µl of 1x TE+PMSF and centrifuging at 8000 rpm. The milky supernatant was transferred to a new eppendorf tube. Three rounds of low speed centrifugation (8000-10000 rpm) were performed, to remove contaminants from the membrane suspension. The supernatant from the last cleaning step was subjected to ultra-centrifugation at 42000 rpm for 20 min, and the pellet was immediately frozen in liquid nitrogen. The membrane pellets were stored at -80°C until needed.

### 2.3.1.2 SDS-Polyacrylamide Protein Gels (SDS-PAGE)

#### Concentrating gel (upper part)

Concentrating buffer	1X
Acrylamide/Bisacrylamide solution	4.5/ 0.1%
N,N,N',N'-Tetramethylethyldiamine (Temed)	0.13% (v/v)
Ammoniumpersulfate (APS)	0.03%(w/v)

#### 4X Concentrating buffer

Tris-HCl, pH 6.8	0.5 M
SDS	0.4% (w/v)

#### Separating gel (lower part)

Separating buffer	1X
Acrylamide / Bisacrylamide solution	12.5/0.33%
Temed	0.05% (v/v)
APS	0.05% (w/v)

#### 4X Separating buffer

Tris-HCl, pH 8.8	1.5 M
SDS	0.4% (w/v)

#### 10X Electrophoresis Laemmli buffer

Tris	250 mM
Glycine	192 mM
SDS	0.5% (w/v)

**2X Sample buffer**

Tris-HCl, pH 6.8	0.125 M
SDS	4% (w/v)
Glycerin	20% (v/v)
2-Mercaptoethanol	10% (v/v)
Bromo-phenol blue	0.01% (w/v)

**Gel preparation and electrophoresis**

The protein gels were prepared in a Mini-gel device System 2050 Midget (Pharmacia-LKB, Freiburg) and mounted as recommended. The SDS-PAGE preparation was done following the Laemmli (1970) protocol. First, the separating gel was prepared and allowed to polymerize on the bottom of the cast before pouring the concentrating gel (2-3 cm) on top. After complete polymerization the gels were used for electrophoresis. The chamber was assembled and sufficient electrophoresis buffer (1X) was poured in the bottom as well as in the vertical buffer collector, in contact with the gel.

The protein samples were thawed on ice and resuspended in 1X TE or solubilisation buffer (100 mM phosphate buffer, 50 mM NaCl, pH 7.8) and sample buffer (to a final concentration of 1X). After complete resuspension of the samples 5 to 30  $\mu$ l were placed in each slot. In parallel, 5  $\mu$ l of protein marker (Fermentas Prestained Protein Molecular Weight Marker, apparent molecular weights between 20-118 kDa) were also loaded. The first 20 min of electrophoresis, through the concentrating gel, were run at 20 mA. The current was then increased to 30 mA for additional 40-60 min (electrophoresis through the separating gel) until the bromo-phenol blue line reached the bottom.

**2.3.1.3 Protein Visualization Using Coomassie-Brilliant Blue Stain****Staining solution I**

Coomassie-Brilliant blue	0.5% (w/v)
--------------------------	------------

**Staining solution II**

Acetic acid	20% (v/v)
-------------	-----------

**Distaining solution**

Acetic acid	10% (v/v)
Methanol	40% (v/v)

The procedure followed the directions of Weber and Osborn (1969). The staining solutions I and II were mixed in a 1:1 ratio. The gel was incubated in the combined staining solutions for 1 hour (or O/N) with gentle agitation. The staining solution was removed and the gel was incubated in destaining solution until the protein signals were clearly distinguishable from the background (2-4 hours). The gel was then covered by plastic foil or alternatively, vacuum dried and scanned for data compilation.

### 2.3.1.4 Protein Visualization Using Silver Staining

#### Fixing solution I

Methanol	50% (v/v)
Acetic acid	12% (v/v)
Formaldehyde	0.019% (v/v)

#### Washing solution II

Ethanol	50% (v/v)
---------	-----------

#### Solution III

Sodium thiosulfate	615 mM
--------------------	--------

#### Silver staining solution

Silver nitrate	0.2% (w/v)
Formaldehyde	0.075% (v/v)

#### Developing solution

Sodium carbonate	0.57 M
Formaldehyde	0.019% (v/v)
Sodium thiosulfate	17.3 $\mu$ M

#### Stop solution

Methanol	50% (v/v)
Acetic acid	12% (v/v)

The staining of proteins with silver nitrate is more sensitive and therefore is recommended for detection of low amounts of protein in the sample. The method was used as described by Blum *et al.* (1987). The gel was fixed in solution I for 30 min and washed three times with solution II (10 min per wash). Then, it was incubated for 1 min in solution III (65  $\mu$ l in 50 ml of H<sub>2</sub>O) and rinsed three times in

H<sub>2</sub>O. The gel was immersed in silver staining solution (5 ml in 45 ml of H<sub>2</sub>O) and incubated for 20 min. The solution was removed (for disposal in a separate container) and the gel was rinsed twice in H<sub>2</sub>O. Developing solution (10 ml 7x5 in 40 ml H<sub>2</sub>O + 10 µl solution III) was added and the gel was inspected until the bands were clearly visible. Then, it was rinsed twice in H<sub>2</sub>O and incubated for 10-15 min in the stop solution. For later disposal, the staining solution was treated with salt (NaCl) to precipitate the silver nitrate and separate it from the water.

### 2.3.1.5 Transfer of Proteins to PVDF Membranes (Western Blot)

The proteins separated by SDS-PAGE were transferred to PVDF membranes (BioRad) using an electric transfer chamber (Carboglass, Schleicher & Schuell) in a semi-dry-blot manner (Khyse-Andersen, 1984). The blot was built by lying on the anode side 4 sheets of Whatman paper soaked in 1X anode buffer (Roti-Blot, buffer 2A, Roth). The transfer membrane was wetted in methanol and laid on top of the Whatman paper. The SDS-PAGE was laid over the membrane and it was covered by 4 more sheets of Whatman paper imbibed in 1X cathode buffer (Roti-Blot, buffer 2K, Roth). The system was closed with a weight of 1-2 kg placed on top of the system, and current was applied for 2 hours (1 mA / cm<sup>2</sup> of membrane).

### 2.3.1.6 Immune-Visualization of Recombinant Proteins

#### Blocking buffer

Milk powder	4 % (w/v)
10X TBS buffer	1 X
Stored at 4°C.	

#### 10X TBS buffer

Tris-HCl, pH 7.5	100 mM
NaCl	1.5 M

#### TBST-T buffer

10X TBS buffer	3 X
Tween 20	0.05% (v/v)
Triton X-100	0.2% (v/v)



**Staining solution (prepared fresh, light-protected)**

Buffer A	10 ml
NBT-stock (5% (w/v) NBT in 70% DMF)	66 $\mu$ l
BCIP-stock (5% (w/v) BCIP in 70% DMF)	33 $\mu$ l

**Buffer A**

Tris-HCl, pH 9.5	100 mM
NaCl	100 mM
MgCl <sub>2</sub>	5 mM

**NBT-stock** (p-Nitro-blue-tetrazolium-chloride) stored at -20°C.

**BCIP-stock** (5-Bromo-4-chloro-3-indoylphosphate) stored at -20°C.

**CSPD (Roche) Detection buffer**

Tris-HCl, pH 9.5	100 mM
NaCl	100 mM
CSPD	1:100 dilution from stock

Used up to 2 times when kept cold (2-8°C), sterile and in dark conditions.

The western blot membrane was washed twice in TBS solution and incubated 2 hours or O/N in blocking solution (4% (w/v) milk powder in TBS). Then, it was washed twice (10 min each) in TBST-T solution and once in TBS for 10 min, before incubating for 2 hours in the first antibody solution (6x His-antibody, 1:2000 dilution in blocking solution, reused up to 10 times). The membrane was washed twice in TBST-T and TBS as indicated before, prior incubation with the second antibody (goat anti-mouse IgG, Alkaline Phosphatase-coupled, 1:2500 dilution in blocking solution, reused up to 10 times) for 1-2 hours. Then it was washed four times in TBST-T and incubated in staining solution until the signals were visible (BCIP is hydrolyzed and an indigo precipitate is formed after oxidation with NBT). The blot was briefly rinsed in water, incubated for 5 min in 3% trichloroacetic acid, rinsed again in water and finally dried on absorbent paper. The processed membranes were photographed and stored protected from light.

Alternatively, instead of NBT and BCIP for signal detection, the chemiluminescent substrate CSPD (Disodium 3-[4-methoxyspiro {1, 2-dioxetane-3, 2'-(5'-chloro) tricyclo [3.3.1.1<sup>3,7</sup>] decan} -4-yl] phenyl phosphate, Roche) was also used. It allowed more sensitive detection of biomolecules since the dephosphorylation of

the substrate produces visible light that can be recorded by few minutes exposure to an X-ray film.

### **2.3.2 Transport Activity Measurements**

#### **2.3.2.1 Purification of Phosphatidylcholine for Liposome Preparation**

Phosphatidylcholine (30 g, Sigma) was first dissolved in 100 ml chloroform and later on separated by adding 540 ml of ice-cold acetone with continuous mixing for 2 hours at RT. The lipids were precipitated O/N at 4°C. After supernatant removal the precipitate was dissolved in diethyl ether (50-100 ml), which was later extracted under vacuum on a rotting flask. The lipids were dried on filter paper until the ether was completely evaporated. The purified phospholipids (without free fatty acids) were stored at -20°C.

#### **2.3.2.2 Preparation of Liposomes**

For one transport activity measurement (kinetic) 120 mg (or 12% w/v) of purified lipids were used. Additionally, the liposome buffer contained 20 mM potassium-phosphate buffer, pH 7.6 (KH<sub>2</sub>PO<sub>4</sub>), 50 mM of K-gluconate and 0.2 mM of substrate (CDP-choline, CDP-ethanolamine or different nucleotide sugar diphosphates). Using an ultrasonic pulse-echo instrument (Branson Sonifier 250, Branson Ultrasonics, Danbury/USA) the lipids were broken into small spheres (liposomes) by pulsing 3 min at 50% duty cycle on ice. 750 µl of liposomes was transferred to a new 1.5 ml tube, and kept on ice until mixed with the membrane proteins.

The liposomes used for reconstitution of Ni-NTA isolated proteins (see 2.2.6) were prepared in a concentrated manner because of the high volume resulting from the isolated proteins (500 µl). Nevertheless, the proportions of phospholipids, KH<sub>2</sub>PO<sub>4</sub>, K-gluconate and substrate were maintained in the final volume (120 mg, 20 mM, 50 mM and 0.2 mM, respectively in 1 ml), and four rounds of 30 sonication pulses (50% duty cycle) dissolved the lipids.

#### **2.3.2.3 Membrane Proteins Solubilisation and Preparation of Proteoliposomes**

One membrane fraction obtained via expression in a heterologous system (i.e. *S. cerevisiae*) was thawed on ice and resuspended in 50-100  $\mu$ l of H<sub>2</sub>O. When performing several experiments with the same protein, the corresponding number of membrane pellets was thawed and mixed together in order to standardize the amount and quality of proteins in all experiments. The proteins were solubilized from the membranes by adding a detergent (1-2% Triton-X100, n-Dodecyl- $\beta$ -D-maltoside (DM) or any other shown to dissolve the protein properly). Approximately 100  $\mu$ l of the protein suspension were added to the liposomes, mixed gently by inversion and centrifuged shortly. The mixture was frozen in liquid nitrogen and subsequently thawed slowly on ice, which allowed the proteins to reconstitute into the liposome artificial membranes (Kasahara and Hinkle, 1977). A second round of sonication was performed applying 30 pulses at 20% duty cycle on ice, in order to maximize the proportion of intact proteoliposomes.

#### **2.3.2.4 Purification of Proteoliposomes through PD-10 Gel Filtration Columns**

PD-10 columns (Pharmacia Biotech) contain Sephadex G-25 for size exclusion chromatography, which permits the separation of proteoliposomes preloaded with a substrate from the external solution that also contains the substrate. The columns were equilibrated with PD-10 buffer (3 times) before pouring the proteoliposomes. Depending on the characteristics of the proteins (e.g. stability) the PD-10 buffer could contain Tricine-KOH or KH<sub>2</sub>PO<sub>4</sub> (pH 7.6).

##### **PD-10 Buffer**

Na-gluconate	100 mM
K-gluconate	50 mM
KH <sub>2</sub> PO <sub>4</sub> / Tricine-KOH (pH 7.6)	10 mM

The proteoliposomes (850  $\mu$ l) were loaded onto the PD-10 column, and washed with 1.7 ml of PD-10 buffer. When the flow-through drops became milky, 950  $\mu$ l of PD-10 buffer were added and the liposomes were collected in a new tube. The proteoliposomes were directly used for transport activity measurements and the PD-10 columns were washed several times with water, and finally stored in the presence of 0.1% (w/v) sodium azide (NaN<sub>3</sub>).

### 2.3.2.5 Protein Transport Activity Measurements in Proteoliposomes

The proteins reconstituted in liposomes were assayed for its transport activity using a radiolabeled counter substrate (i.e. nucleoside monophosphates, UMP, GMP or CMP). In a new tube 850  $\mu$ l of proteoliposomes were briefly mixed with 45  $\mu$ l of counter substrate (16.6  $\mu$ M final concentration). The transport was evaluated at 25°C and stopped at different time points (10 sec, 30 sec, 60 sec, 120 sec) by passing an aliquot (200  $\mu$ l) through an anion exchange column (Dowex AG 1-X8, mesh size 100-200, BioRad, equilibrated with sodium fluoride (NaF)). The liposomes on each column were recovered by elution with 0.4 M Sorbitol (1100  $\mu$ l) while the radiolabeled counter substrate outside the liposomes remained bound to the resin. The elution was mixed with 4.5 ml of scintillation buffer (Rotiszint eco Plus, Roth) and the radioactivity inside the liposomes was measured using a scintillation counter (LS-6000TA, Beckman).

#### Radiolabeled counter substrate mix

Three commercially available radiolabeled nucleoside monophosphates (UMP, GMP and CMP) were used for testing the transport activity of the KVAG proteins. These substrates were  $^{33}\text{P}$  labeled, with 10  $\mu\text{Ci}/\mu\text{l}$  activity.

Radiolabeled counter substrate	150000-200000 cpm
No radiolabeled counter substrate	0.3 mM

#### 2.3.2.5.1 Assembly of the Anion Exchange Columns

The column material was supported on Pasteur pipettes plugged with cotton. The pipettes were filled to 1/3 of their height with the resin (Dowex AG 1-X8, BioRad) and equilibrated (3-4 runs through) with 0.4 M Sorbitol (when resin equilibrated with fluoride was used). Sorbitol binds weakly to the resin and can be easily exchanged against ions that bind more strongly, such as phosphate (Pi).

#### 2.3.2.5.2 Reconstitution of Anion Exchange Resin

The anion exchange resin (Dowex AG 1-X8, mesh size 100-200, BioRad) was reused several times after complete removal of the radiolabeled substrate. For this purpose, the columns were washed 3-4 times with 1 M HCl (the flow through discarded as radioactive waste). Then, it was saturated with 1 M NaOH and

several washes with NaF (0.6-1 M) were performed in order to exchange the OH<sup>-</sup> ions against the F<sup>-</sup> (until the pH was near to neutral). The resin was stored at 4°C.

### **2.3.2.6 Isolation of Proteins Using Ni<sup>2+</sup>-nitrilotriacetic acid (Ni-NTA) Agarose Beads**

The translational fusion of a protein cDNA with a sequence encoding a poly-histidine tag allowed the isolation and purification of the corresponding protein for further functional studies.

#### **2.3.2.6.1 Ni-NTA Agarose Beads Equilibration**

The Ni-NTA agarose beads mixture (# 30230, QIAGEN) was placed into a 2 ml tube (150 µl for 2 kinetics), and mixed well with 150 µl of equilibration buffer (Buffer II). After 1 min centrifugation at 10000 rpm the supernatant was discarded and the agarose was kept on ice.

##### **Buffer II**

Na-phosphate buffer, pH 7.8	100 mM
NaCl	50 mM

#### **3.2.6.2 Membrane Pellets Solubilization and Protein-Ni-NTA Binding**

For each kinetic (transport activity assay) 3 membrane pellets were used. Each pellet was dissolved in 140 µl of solubilisation buffer (Buffer I) and combined in a 2 ml tube (end volume of 450 µl).

##### **Buffer I**

Na-phosphate buffer, pH 7.8	100 mM
NaCl	50 mM
Imidazol	8 mM

To solubilize the proteins from the membranes 75 µl of 20% (w/v) DM were added, mixed softly and incubated on ice for 2 min. One volume of Buffer I was added, incubated 4 minutes on ice and centrifuged 2 min at 10000 rpm. The supernatant was transferred to the previously equilibrated Ni-NTA agarose, and mixed by gently rotation at 4°C for at least 2 hours.

### 2.3.2.6.3 Isolation of His-tag-bound Proteins from the Ni-NTA Resin

#### Buffer III

Na-phosphate buffer, pH 7.8	100 mM
Imidazol	8 mM
Dodecylmaltoside	0.06% (w/v)

#### Buffer IV

Na-phosphate buffer, pH 7.8	50 mM
Imidazol	150 mM
Dodecylmaltosid	0.06% (w/v)

The procedure was performed at 4°C. The protein-Ni-NTA mixture was poured into a Pasteur pipette stocked with cotton at the shrinkage. The resin remaining in the pipette was rinsed 2-3 times with 500 µl of Buffer III, to remove unbound proteins. The histidine-tag coupled proteins were recovered in a new tube by elution in 500 µl of buffer IV. The isolated proteins are unstable and therefore were immediately mixed with the liposomes, in a 1:1 volume proportion, and frozen in liquid nitrogen. Small aliquots (50 µl) from the cleaning and elution fractions were subjected to electrophoresis to verify the presence of the expected protein.

### 2.3.2.7 Isolation of Golgi-enriched Microsomes from Yeast Cells

#### Spheroplast solution

Sorbitol	1.4 M
K-phosphate, pH 7.5	50 mM
2-mercaptoethanol	40 mM
NaN <sub>3</sub>	10 mM

#### Lysis buffer

HEPES-Tris (KOH), pH 7.4	10 mM
Sorbitol	0.8 M
EDTA	1 mM

Following the procedure described by Aoki *et al.* (2003) the induced yeast cells (500 ml) were centrifuged at 3000-4500 rpm at 4°C for 5 min and washed twice in ice-cold 10 mM NaN<sub>3</sub>. The cell pellet was resuspended in 20 ml spheroplast

solution containing 2 mg of zymolyase 100T per g of packed cells, and incubated at 37°C for 40 min with occasional mixing. The spheroplasts were collected by centrifugation at 1000 xg for 5 min at 4°C, resuspended in 20 ml of cold lysis buffer containing a cocktail of protease inhibitors (Mini tablets, EDTA-free, Boehringer Mannheim), and disrupted by pottering 20 times at 4°C. The homogenate was centrifuged at 3500 rpm at 4°C for 5 min to remove cell debris. The supernatant was centrifuged at high speed, 26000 rpm for 45 min at 4°C, and the pellet was finally resuspended in 200-300 µl of lysis buffer (0.8 ml/g cells). The microsomal fraction was used immediately in transport activity assays.

#### Transport Activity Measurements *in vitro*

The microsomal preparation (50 µl) was added to the reaction mixture (0.8 M sorbitol, 10 mM Tris-HCl pH 7.0, 1 mM MgCl<sub>2</sub>, 20 µmol of the radiolabeled monophosphate counter substrate) and incubated at 30°C. To stop the reaction 1 ml of ice-cold stop buffer was added (0.8 M sorbitol, 10 mM Tris-HCl pH 7.0 and 1mM MgCl<sub>2</sub>) and passed through a Dowex ion-exchange column. The flow-through containing the microsome vesicles was collected in a scintillation vial and the radioactivity incorporated was measured by a scintillation counter.

When preloading the Golgi vesicles they were incubated with 0.2 mM of substrate (i.e. UDP-Gal) and 10-20 sonication pulses (20%) were applied on ice. High speed centrifugation for 10-15 min at 42000 rpm at 4°C was performed in order to remove the non-integrated extra substrate. The microsomal pellet was resuspended in 50 µl of lysis buffer.

### 3. RESULTS

#### 3.1 Description of the KV/A/G Subfamily

##### 3.1.1 Molecular and Protein Characterization of the KV/A/G Subfamily using *in silico* approaches

The KV/A/G subfamily of NST/pPT homologues comprises seven putative proteins: KVAG1 (At1g12500), KVAG2 (At3g10290), KVAG3 (At5g04160), KVAG4 (At5g05820), KVAG5 (At3g11320), GONST5 (At1g21870) and UDP-GalT1 (At1g77610) in *Arabidopsis*. The deduced KVAG protein sequences share between 33-95% of amino acid identity (Table 2). The most similar proteins are KVAG2, KVAG3, KVAG4 and KVAG5 have more than 70% sequence identity, which is reflected in the conserved exon/intron structure of the genes (Figure 3). These four genes contain four exons, as inferred from cDNA sequence analyses. However, the second predicted exon of *KVAG5* was neither observed in plant mRNA nor in ESTs reported in TAIR (see section 3.4). Comparisons between the KVAG and other NST/pPT proteins showed that only KVAG5 contains an insertion of 34 amino acids in the third highly similar region (Figure 4). Moreover, a sequence similar to the predicted second exon of *KVAG5* was found within the first intron of *KVAG2*, *KVAG3* and *KVAG4* indicating that the gene was misannotated.

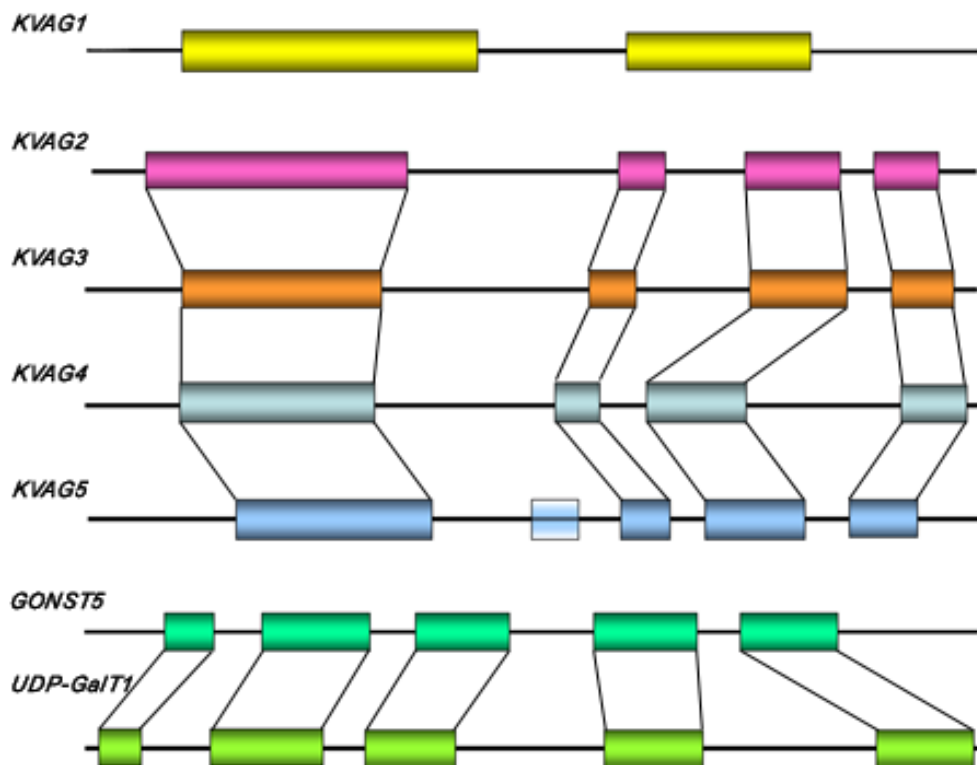
In the *Arabidopsis* genome the *KVAG2* and *KVAG5* genes are located on chromosome III while *KVAG3* and *KVAG4* reside on chromosome V. GONST5 and UDP-GalT1 are very similar in their deduced amino acid sequence (Table 2). Both possess a similar gene structure, with five exons and conserved intron positions. These two genes are present on the *Arabidopsis* chromosome I, as well as *KVAG1*, which is the only gene harbouring a single intron (Figure 3).



**Table 2.** Amino acid identity within the KV/A/G subfamily.

Percentage of identical amino acids shared between the deduced protein sequences of the KVAG proteins (data from the Aramemnon database, Schwacke *et al.*, 2003).

Protein	Amino acid identity (%)					
	KVAG2	KVAG3	KVAG4	KVAG5	GONST5	UDP-GaIT1
<b>KVAG1</b>	56	58	68	65	34	34
<b>KVAG2</b>		94	71	72	34	34
<b>KVAG3</b>			71	73	36	36
<b>KVAG4</b>				95	34	34
<b>KVAG5</b>					35	33
<b>GONST5</b>						91

**Figure 3.** Schematic exon/intron representation of the structure of the KVAG genes.

Exon sequences are represented by filled boxes and introns by the lines connecting the exons. Objects are drawn in a comparable scale. The second lighter box in KVAG5 stands for a predicted exon, not observed in the cDNA (see section 3.4).

Analysis of the results from 16 different transmembrane helix prediction programs suggests that the KVAG proteins contain 8 to 10 TMDs (Figure 4) (Aramemnon database, Schwacke *et al.*, 2003). Therefore, they are thought to be highly hydrophobic and integrated into membranes. This is in accordance with other pPT and NST proteins which also contain a similar number of TMDs (Figure 4). The topology of the mammalian CMP-Sia transporter, the only NST that has been studied in detail so far (Eckhardt *et al.*, 1999), revealed 10 TMDs with the amino and carboxyl terminal ends facing the cytosol. The positions of the TMDs within the KVAG proteins match those of the CMP-Sia transporter and of other NST and pPT members (Figure 4).

The protein sequences of KVAG1 and KVAG2 display amino terminal extensions (~50 amino acids long) that contain 27-28% of serine/threonine residues and a similar percentage of basic amino acids (histidine, lysine and arginine). These sequence stretches are predicted as plastid targeting peptides by the TargetP\_v1, ChloroP\_v1.1 and PCLR\_v0.9 algorithms (Aramemnon database, Schwacke *et al.*, 2003). Therefore, these two proteins might play roles as metabolite transporters in plastids. Uptake of solutes synthesized in the cytosol (like nucleotide sugars) have been recognized to be required in plastids (Capasso and Hirschberg, 1984; Knappe *et al.*, 2003a; Kelly and Dörmann, 2004), but the proteins mediating such transport have not been identified yet.

Several residues are conserved between the KVAG and known pPT and NST proteins (Figure 4). These residues are more frequently found inside the five regions of high similarity previously described in the pPTs (Knappe *et al.*, 2003a), including two lysines proposed to be involved in substrate binding (K41 and K273, Figure 4). However, the identification of sequence similarities with well characterized transporters does not reveal specific information about function or substrate affinity of the KVAG proteins.

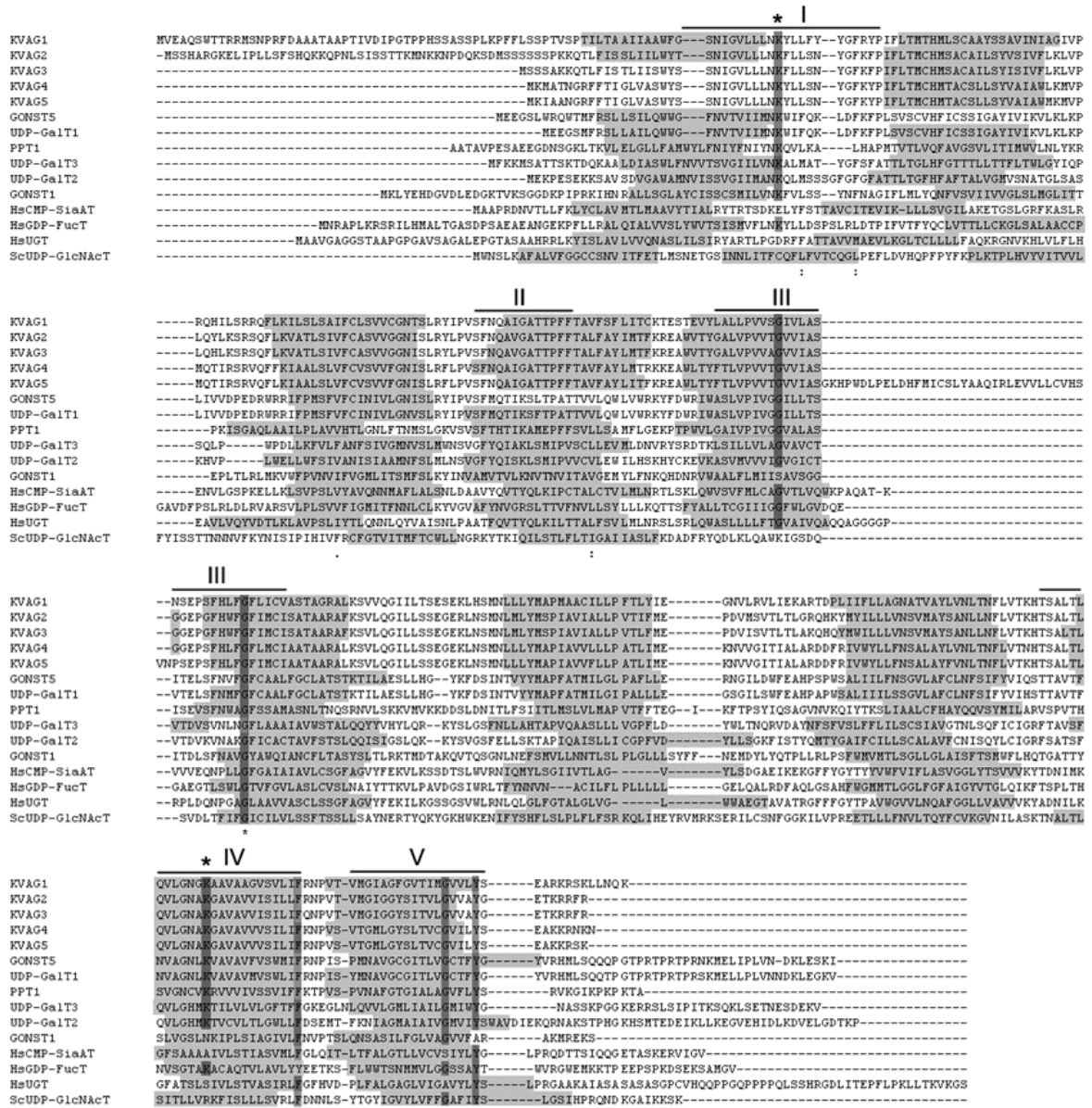


**Figure 4.** Multiple alignment of KVAG proteins and members of the NST/pPT family.

TMDs for each protein are highlighted in gray. The sequence regions labelled I-V indicate the five regions of high similarity between the pPT proteins. Conserved residues are highlighted in dark gray. Two lysines, K41 and K273, depicted with stars (\*), are presumably involved in substrate binding. PPT1 is presented as a mature protein sequence. Sc, *Saccharomyces cerevisiae*; Hs, *Homo sapiens*; Lm, *Leishmania mexicana*.

### 3.1.2 *in silico* Expression of KVAG Genes

Publicly available databases containing microarrays hybridization results are useful tools to obtain information about the expression features of many genes. Genevestigator ([www.genevestigator.org](http://www.genevestigator.org), Zimmermann *et al.*, 2004) comprises gene expression results from experiments performed with a standardized platform as the Affymetrix microarrays. The expression is presented as absolute normalized signal intensities obtained for each gene in all the microarray chips (1330 in total). The data can be visualized in a heat colour code. Dark blue marks the organ(s) with high expression while white represents the organ(s) with low expression of the gene. This facilitates comparisons between expression in different organs for a single gene.

Examination of the expression of the KVAG genes in the Genevestigator database showed nearly ubiquitous expression in all organs and tissues of *Arabidopsis* (Figure 5). However, the KVAG3 and GONST5 genes yielded higher expression in the inflorescence, especially in stamina and pollen, while expression of UDP-GaIT1 is higher in the stigma. High levels of expression in roots were observed for KVAG5 and KVAG4 genes, the latter gene also showing high expression signals in hypocotyls, stamina and stems. High expression in stems was also observed for the KVAG1 gene (Figure 5). The KVAG2 cDNA is not reported in the Affymetrix chips, most likely because of the high similarity with KVAG3 (87% cDNA nucleotide identity). Due to this high identity between the coding regions of the two genes, it is possible that microarray hybridizations cross react with both KVAG3 and KVAG2 cDNAs, detecting the combined expression of both genes (Figure 5).

Analysis of expression of the other members of the NST/pPT homologous genes (from the KT and KD subfamilies) also revealed broad organ and tissue expression (Figure 6). Nevertheless, differences in expression profiles of some genes were also observed. Two main groups of genes could be distinguished based on these expression data: (i) a group of highly expressed genes in the inflorescence, including genes also expressed in stems, roots and cultured cells; and (ii) a group of more ubiquitously expressed genes (Figure 6). Thus, the

presence of some proteins may overlap in certain organs, principally in leaves, roots and stamina.

Gene name	0 callus	1 cell suspension	2 seedling	21 cotyledons	22 hypocotyl	23 radicle	3 inflorescence	31 flower	311 carpel	3111 ovary	3112 stigma	312 petal	313 sepal	314 stamen	3141 pollen	315 pedicel	32 silique	33 seed	34 stem	35 node	36 shoot apex	37 cauline leaf	4 rosette	41 juvenile leaf	42 adult leaf	43 petiole	44 senescent leaf	5 roots	52 lateral root	55 elongation zone	AGI number	
GONST5	6.7	7.2	6.4	5.8	7.4	6.5	6.5	6.8	6.7	5.3	6.5	6.5	6.3	7.6	8.2	6.6	7.0	5.9	6.9	5.4	5.8	7.0	6.4	6.6	6.5	6.2	7.0	6.8	7.1	6.6	AT1G21870	
KVAG3*	8.5	9.5	10.0	9.2	10.5	10.1	10.4	10.6	10.1	9.5	9.1	10.3	8.5	11.1	11.1	10.3	10.5	9.4	10.5	10.3	10.8	8.3	10.0	10.5	10.1	10.3	9.6	10.0	10.3	AT5G04160		
KVAG5	9.4	9.8	9.8	9.0	9.7	10.2	9.2	9.2	8.7	8.8	8.8	8.8	9.1	9.0	9.9	9.7	9.2	9.3	8.8	9.7	9.3	9.0	9.3	9.4	9.6	9.7	9.6	9.1	9.9	10.6	10.6	AT3G11320
UDP-GalT1	10.8	11.1	10.2	9.1	11.1	10.8	11.3	11.4	12.0	11.4	12.2	11.1	10.3	11.1	11.5	10.8	11.4	10.9	10.9	11.0	11.9	10.8	10.3	10.6	10.2	10.0	10.4	10.6	9.9	10.0	AT1G77610	
KVAG1	8.8	9.5	11.0	10.6	11.0	10.6	10.3	10.3	10.1	9.6	10.2	10.8	9.1	9.6	8.2	11.3	10.4	8.8	11.6	11.6	10.2	10.5	10.7	11.0	10.6	11.0	7.6	10.2	10.6	11.0	AT1G12500	
KVAG4	10.0	10.0	10.2	9.9	10.5	10.3	10.1	10.2	9.8	9.5	10.0	10.2	9.6	10.5	9.4	10.3	10.4	9.8	10.5	10.5	10.1	9.7	10.1	10.3	10.1	10.4	9.5	10.1	10.4	10.6	AT5G05820	

**Figure 5.** Organ and tissue expression of the *KVAG* genes evidenced by microarray experiments (Genevestigator).

The numbers inside the cells indicate the intensities data, shown as the log<sub>2</sub>(n). *KVAG3\** = *KVAG3* expression data might be combined with the expression of *KVAG2* due to high similarity between both cDNAs.

Gene name	Protein subfamily	0 callus	1 cell suspension	2 seedling	21 cotyledons	22 hypocotyl	23 radicle	3 inflorescence	31 flower	311 carpel	3111 ovary	3112 stigma	312 petal	313 sepal	314 stamen	3141 pollen	315 pedicel	32 silique	33 seed	34 stem	35 node	36 shoot apex	37 cauline leaf	4 rosette	41 juvenile leaf	42 adult leaf	43 petiole	44 senescent leaf	5 roots	52 lateral root	55 elongation zone	AGI number			
UDP-GalT3	KT	10.4	9.6	9.9	9.1	9.5	10.3	9.9	9.9	9.4	8.9	9.8	10.3	9.6	9.9	9.4	9.3	11.3	9.7	9.8	9.9	9.3	9.1	9.4	9.8	9.6	9.7	8.5	10.4	10.6	11.1	AT4G39390			
	KD	10.7	10.9	9.9	8.5	10.6	10.9	10.4	10.3	10.1	9.4	10.5	10.0	9.8	10.8	8.8	10.2	11.7	10.1	10.2	10.3	9.8	9.0	9.4	9.8	9.7	9.5	8.4	10.7	11.5	11.1	AT5G11230			
	KD	8.6	8.3	8.3	7.5	8.8	8.5	7.9	7.5	7.1	7.0	7.6	7.1	7.0	8.2	7.2	8.1	7.2	7.2	8.2	7.1	7.3	8.0	8.2	8.0	8.4	7.5	8.4	9.0	11.1	11.1	AT1G53660			
	KT	9.8	9.3	9.3	10.4	10.5	9.6	9.3	9.4	8.6	8.3	9.3	9.0	8.7	8.6	9.3	9.6	10.1	9.7	10.1	9.7	8.8	9.1	9.2	9.0	9.1	8.2	10.1	9.8	8.9	11.1	11.1	AT5G57100		
UDP-GalT2	KT	8.0	8.3	9.3	8.5	9.5	9.4	9.6	9.6	8.6	8.3	7.9	9.1	8.4	8.4	8.4	9.2	9.2	10.4	9.1	9.8	9.2	9.3	7.3	8.9	9.3	9.0	9.0	8.9	8.7	8.6	9.0	AT1G021070		
	KT	8.5	8.5	8.8	8.9	9.3	9.1	9.1	9.3	8.3	7.7	7.6	8.7	7.9	8.6	9.2	8.9	9.0	8.8	9.1	9.2	8.4	8.6	8.7	8.5	9.2	8.2	8.4	9.3	8.8	11.1	11.1	AT4G09810		
	KT	11.8	11.4	11.2	10.9	11.5	11.6	11.4	11.8	10.8	10.0	10.4	11.4	10.7	13.2	11.2	11.0	11.1	11.6	11.5	10.9	11.0	10.9	11.1	11.1	11.1	11.1	11.1	11.1	11.1	11.1	11.1	AT1G06890		
	KT	7.7	7.9	7.4	7.2	9.1	7.4	8.3	8.4	6.9	6.5	6.6	7.0	7.2	10.1	10.1	8.0	9.7	7.4	9.1	9.1	5.9	7.4	7.5	7.3	7.5	7.8	7.0	7.5	8.4	8.5	11.1	11.1	AT5G55950	
	KD	7.7	7.1	7.2	6.5	7.2	6.6	8.2	9.0	6.7	7.0	6.8	6.7	6.8	9.6	6.7	7.3	7.1	7.6	6.1	6.2	6.7	7.0	7.2	7.1	7.3	6.5	7.0	7.5	7.8	11.1	11.1	AT5G25400		
	KD	9.8	10.2	10.0	9.7	10.3	10.7	10.1	10.0	10.0	9.1	9.1	9.8	9.3	9.7	9.5	10.2	10.2	9.5	10.2	11.7	10.2	11.7	9.7	9.6	9.9	9.5	10.0	9.4	10.2	10.0	9.6	11.1	11.1	AT1G48230
	KD	11.6	11.3	11.6	11.0	11.8	11.8	11.8	11.1	11.9	11.2	10.4	11.5	7.4	11.7	11.6	11.4	11.6	11.5	11.6	11.5	11.6	11.5	11.6	11.5	11.9	11.7	11.4	10.7	11.6	11.4	11.6	11.1	11.1	AT4G32390
	KT	10.2	10.4	10.2	9.9	10.6	10.3	10.4	9.9	9.4	9.7	10.2	9.7	9.7	9.1	10.3	10.4	10.1	10.5	10.7	10.4	10.0	10.0	10.3	9.9	10.8	9.6	10.4	10.4	10.4	10.4	10.4	10.4	10.4	AT1G34020
	KT	10.0	10.6	10.7	9.9	10.5	10.4	10.4	10.0	9.6	9.6	10.6	9.7	10.3	10.4	10.8	10.4	10.1	10.8	10.5	10.5	10.1	10.5	10.5	10.8	10.6	10.1	10.8	10.3	10.3	10.3	10.3	10.3	AT5G42420	
	KD	10.0	9.9	9.6	10.1	10.1	10.0	10.0	9.9	9.3	9.4	10.1	9.7	10.0	9.3	9.9	10.0	9.7	10.1	10.1	10.2	9.5	9.6	10.0	9.6	9.7	9.1	10.1	10.0	10.0	10.0	10.0	10.0	AT3G17430	
	KD	12.8	12.0	12.6	11.8	12.7	12.5	12.6	12.1	12.1	11.6	12.2	12.5	12.0	11.3	8.9	12.6	12.4	12.3	12.5	12.8	12.6	12.3	12.5	12.7	12.1	12.4	12.7	12.7	12.7	12.7	12.7	12.7	AT2G25520	
	UDP-GalT2	KT	11.4	11.3	12.1	12.0	12.5	12.1	12.2	12.1	11.6	11.1	11.2	11.2	11.5	11.3	12.5	12.2	11.9	12.7	12.7	11.9	12.0	12.3	12.1	12.5	12.5	12.0	11.6	11.9	11.9	11.9	11.9	11.9	AT1G76670
KD		10.8	10.0	10.2	10.6	10.8	10.7	10.1	10.0	9.9	8.9	9.1	10.4	10.0	10.2	8.8	10.4	10.2	9.7	10.6	10.6	10.3	10.8	10.0	9.9	10.0	10.5	10.2	10.6	10.6	11.1	11.1	AT3G14410		

**Figure 6.** Organ and tissue expression of NST/pPT homologous genes evidenced by microarray experiments (Genevestigator).

The numbers inside the cells indicate the intensities data, shown as the log<sub>2</sub>(n). KD and KT indicate the NST/pPT homologous subfamily to which the indicated genes belong to.

### 3.2 Expression of *KVAG* genes *in planta*

### 3.2.1 Expression Analysis of *KVAG* Genes by Semi-quantitative RT-PCR

The expression of *KVAG1* and *KVAG2* genes was evaluated by semi-quantitative RT-PCR using RNA isolated from different wild type (Col-0) plant organs. Reference PCRs were performed with primers for *Arabidopsis Actin2* and the same templates in order to compare the level of *KVAG* expression to a constitutively expressed gene. The results from RT-PCR were reproducible with RNA extracted from several biological replicates.

The expression of *KVAG1* and *KVAG2*, examined by 28 and 30 RT-PCR cycles respectively, rendered transcripts in all *Arabidopsis* tissues with minor variations in the intensities of the bands. Both genes were expressed at relatively high levels compared to *Actin2* (29 RT-PCR cycles) (Figure 7). The major differences in expression were observed in the inflorescence and rosette leaves. The transcript amount of *KVAG1* was reduced in flowers from elderly plants in comparison to the same gene expression in other organs. In contrast, *KVAG2* transcripts were increased in the inflorescence, but diminished in old rosette leaves (Figure 7).

The expression of *KVAG3* and *KVAG5* genes was also inspected following the same approach. Expression of *KVAG5* was relatively high in all evaluated organs except in rosette leaves from young mature plants. Transcripts were detected in the latter but in reduced amounts compared to expression in other organs (Figure 7). An increase in *KVAG3* mRNA was detected in young inflorescences, in contrast to a drastic reduction of expression in the vegetative organs of the mature plants (Figure 7). From these patterns of expression, the *KVAG1*, *KVAG2* and *KVAG5* genes are ubiquitously expressed, while expression of the *KVAG3* gene appears to be differentially regulated in reproductive and vegetative organs. In general, these data confirmed the expression patterns observed in the microarray experiments, including that of the *KVAG3* gene.

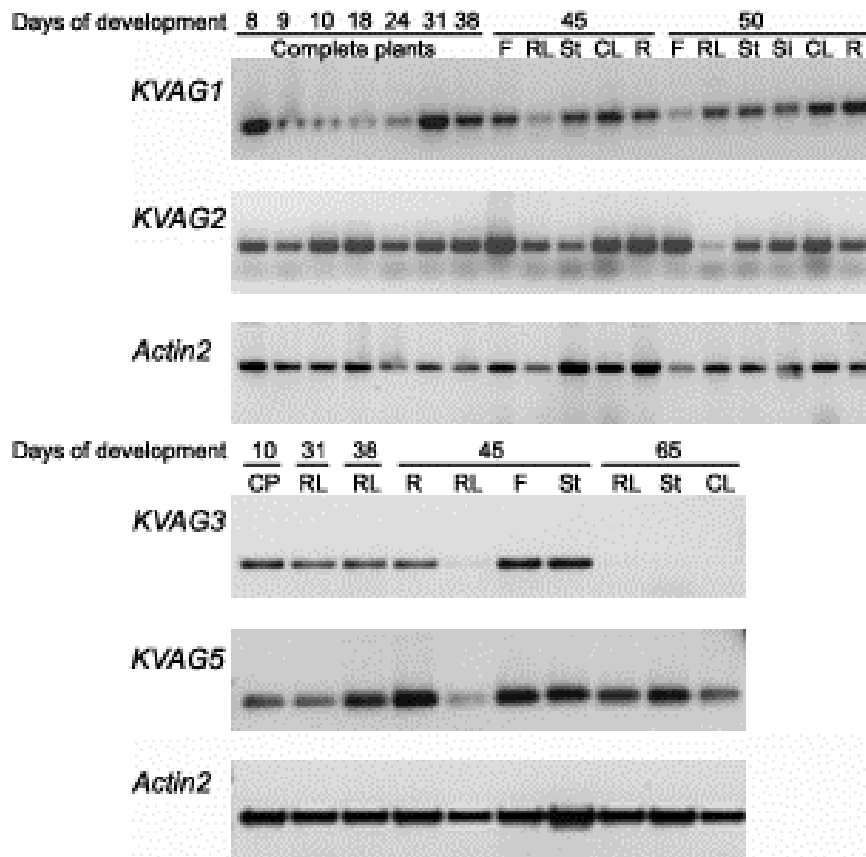


**Figure 7.** Expression analysis of KVAG genes by semiquantitative RT-PCR.

Semiquantitative RT-PCR: KVAG1, 28 cycles; KVAG2, 29 cycles; KVAG3, 32 cycles; KVAG5, 30 cycles; Actin2, 30 cycles. Actin2 as control for constitutive expression. CP = complete plants, RL = rosette leaves, R = roots, F = flowers, Si = siliques, St = stems, CL = cauline leaves.

### 3.2.2 Promoter Analysis of KVAG1 and KVAG2 Genes

To investigate the promoter activity of KVAG1 and KVAG2 genes *in vivo*, translational fusions with the *uidA* gene, encoding the *E. coli*  $\beta$ -glucuronidase protein (GUS, Jefferson, 1987) were performed. The expression of the reporter GUS protein driven by each promoter gave a more refined view of the tissue and cell specific expression of these putative plastidic KVAG proteins.

The promoter regions of KVAG1 (promKVAG1) and KVAG2 (promKVAG2) included 1062 and 1641 bp upstream of the start codon, respectively, and part of the 5' coding region of each gene. Stable *Arabidopsis* transformations were achieved employing *A. tumefaciens*. Transformed plants were selected with

kanamycin. More than 50 antibiotic resistant seedlings were obtained for *promKVAG1::GUS* and 20 for *promKVAG2::GUS*. Preliminary GUS histochemical assays of these T1 plants revealed high *promKVAG1::GUS* activity in cotyledons, young leaves and root tips, while GUS expression was restricted to the stipules of *promKVAG2::GUS* plants. T2 plants derived from several of the GUS T1 lines were studied in more detail.

GUS expression driven by the *promKVAG1* was strongly detected in the aerial parts of young plants, including hypocotyls, cotyledons and developing leaves (Figure 8). Fainter GUS staining was observed in organs that reached maturity, with remains of activity in the vasculature of leaves (Figure 8, E and F). The GUS activity was high in young developing tissues throughout plant development (Figure 8C). In the inflorescences, GUS staining was observed in stems and flowers, the latter particularly in the filaments of stamen, the carpel and the vasculature of petals (Figure 8, G and H). GUS expression was also detected in the procambium zone near the root tip but not in the columella, lateral cap and root epidermis cells (Figure 8D). The expression of GUS was also evident in the transition zone between root and hypocotyl, and furthermore in defined areas along the primary root that represent groups of pericycle cells, later developing secondary roots (Figure 8, A and B).

The *promKVAG2* yielded a different GUS expression pattern *in planta* compared to that of *promKVAG1*. Histochemical GUS staining assays showed activity only in defined aerial organs of *Arabidopsis*. The stipules, at the base of rosette leaves, and the anthers and ovaries in the flowers presented GUS staining (Figure 9). GUS activity was completely absent in roots and leaves. Young anthers presented GUS expression in the epidermis, tapetum cells and pollen sacs, while in dehiscent anthers GUS staining was limited to the cytoplasm of pollen grains (Figure 9, E and F). In the ovaries GUS activity was observed particularly in the embryonic sac, where the ovule, the synergids and the central cell reside (Figure 9, G and H).



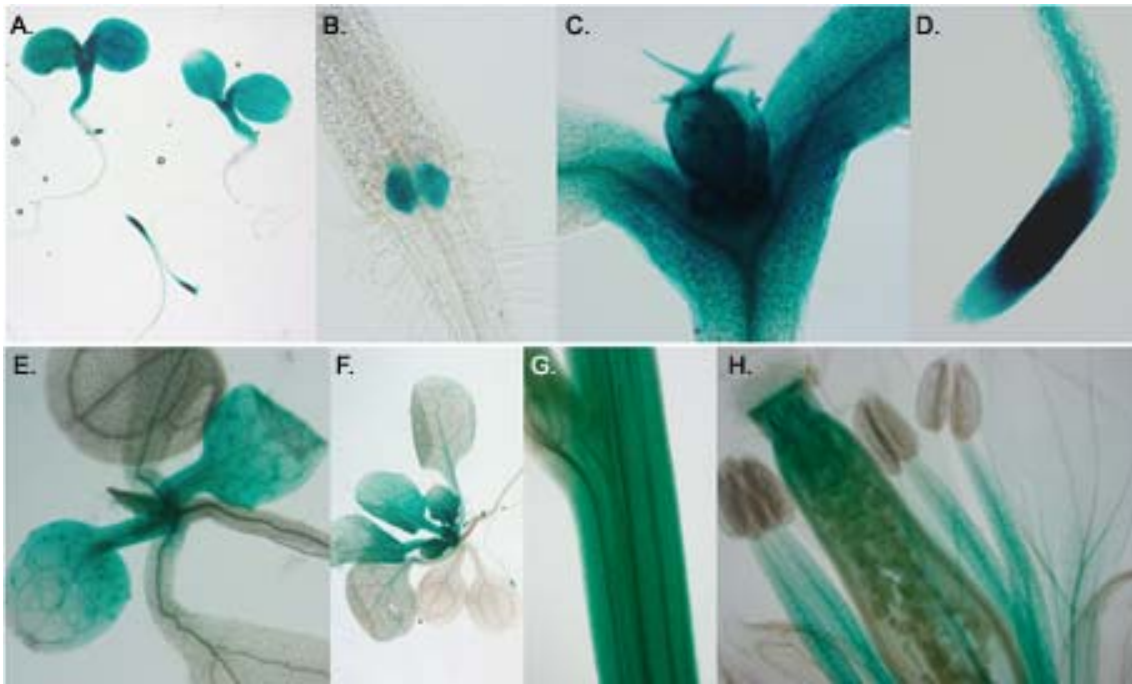


**Figure 8.** Expression analysis of *promKVAG1::GUS* in *Arabidopsis* plants.

Histochemical GUS staining shows the expression of the reporter protein in blue. A, cotyledons and young roots; B, hypocotyl and primary root fusion; C, young developing leaves; D, root tip; E, old cotyledons and young rosette leaves; F, mature and young rosette leaves; G, inflorescence stem; H, mature flower; A to D, 12-day-old seedlings; E, 20-day-old plant; F, 30-day-old plant; G and H, 45-day-old plant.

The observed patterns of GUS expression were reproducible in the progeny (T2) of at least five independent T1 lines for each construct. These results indicate that despite the similarities between the KVAG1 and KVAG2 proteins, their promoter activities appear rather different and contrasting.

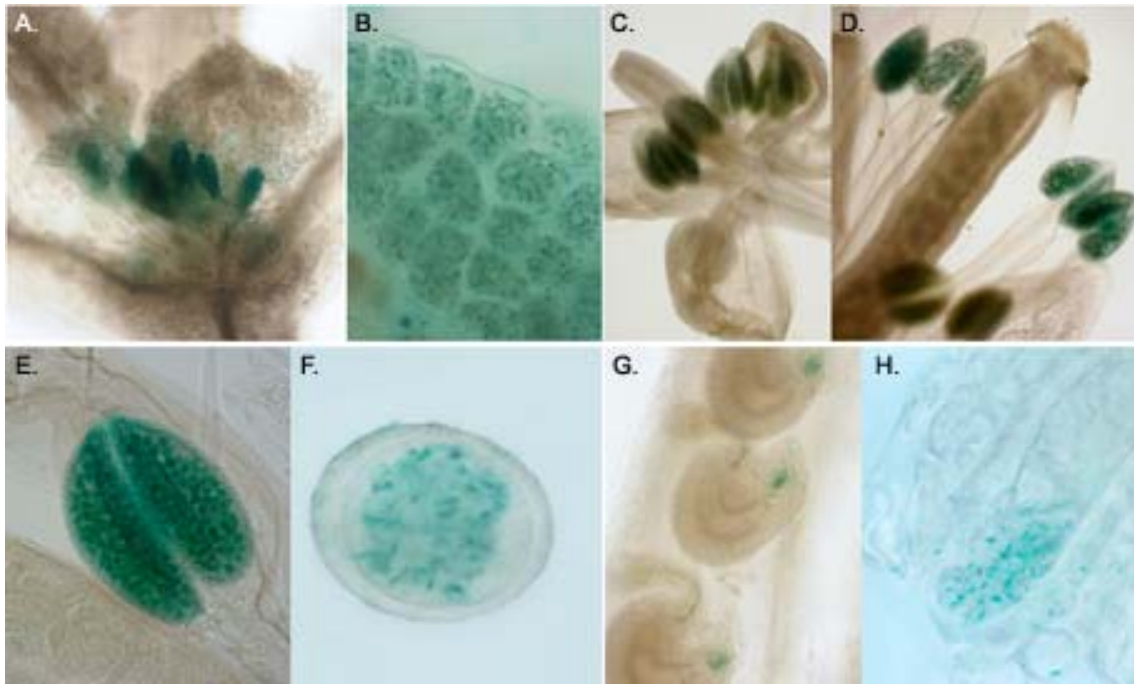


**Figure 9.** Expression analysis of promKVAG2::GUS in *Arabidopsis* plants.

Histochemical GUS staining shows the expression of the reporter protein in blue. A, stipules in young rosette leaves; 15-day-old plant; B, enlargement of one stipule; C, young developing flower; D, mature flower; E, developing anther; F, mature pollen grain ; G, carpel section showing 3 ovaries; H, enlargement of an ovary, GUS expression in the embryonic sac; C to H, 45-day-old plants. The magnification was: E, 20X; B and G, 40X; F and H, 100X.

### 3.3 Analysis of KVAG T-DNA Insertion Lines

#### 3.3.1 Identification of Homozygous T-DNA Insertion Plants

Reverse genetics has proven to be a powerful tool to elucidate the role of a protein in specific metabolic pathways (like synthesis of secondary metabolites) or developmental processes (e.g. Ronen *et al.*, 1999; Schumacher *et al.*, 1999). T-DNA insertion lines for all the KV/A/G subfamily genes, except *GONST5*, were obtained from the *Arabidopsis* Biological Resource Centre, ABRC (Nottingham *Arabidopsis* Stock Centre, NASC, Alonso *et al.*, 2003) (Table 3).

**Table 3.** T-DNA insertion lines of the KVAG genes.

Protein	AGI	T-DNA insertion line	Designation
KVAG1	At1g12500	Salk_034139	<i>kvag1-1</i>
KVAG2	At3g10290	Salk_080551	<i>kvag2-1</i>
		Salk_010795	<i>kvag2-2</i>
KVAG3	At5g04160	Salk_105023	<i>kvag3-1</i>
		E-trap1967	<i>kvag3-2</i>
KVAG4	At5g05820	GabiKat_380D03	<i>kvag4-1</i>
KVAG5	At3g11320	GabiKat_498B04	<i>kvag5-1</i>
UDP-GalT1	At1g77610	GabiKat_229E08	<i>ugt1-1</i>

The transgenic seeds obtained from the stock centre were segregating lines that contained the indicated T-DNA insertion. Therefore, they were screened in order to identify individual plants possessing the predicted insertion in a homozygous state. The screening was made by evaluating two parallel PCR reactions per plant. The first reaction was designed to amplify a fragment of the original gene, using primers flanking the region of the T-DNA insertion (wild type reaction). The second reaction amplifies one border of the T-DNA together with the original gene's flanking region (mutant reaction). There are three possible results according to the genotype of the plant: (i) a PCR fragment only in the wild type reaction and none in the mutant reaction corresponds to a homozygous genotype for the wild type allele of the gene; (ii) a PCR product in the wild type reaction and also in the mutant reaction indicates a heterozygous genotype where the wild type allele of the gene is present in one of the chromatids while a second allele, containing the T-DNA insertion, is present in the second chromatid; (iii) a PCR fragment only in the mutant reaction and not in the wild type reaction corresponds to a homozygous genotype for the mutant allele. These plants are the putative candidates for carrying a gene knock-out.

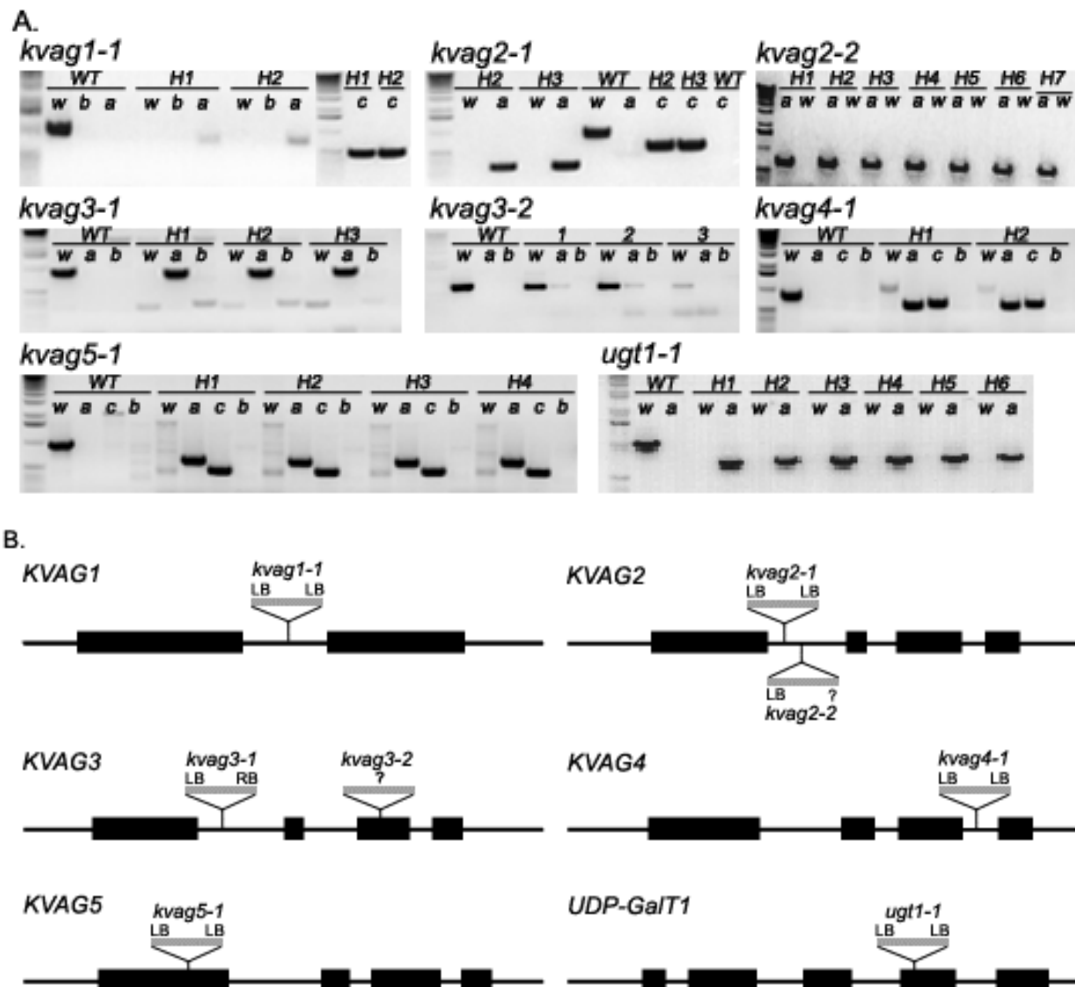


**Figure 10.** Identification of homozygous T-DNA insertion plants by PCR.

A, PCR reactions were performed with primers specific for wild type alleles or T-DNA insertion mutant alleles. WT = Col-0 wild type genomic DNA; H = homozygous individual; w = wild type reaction; a = 1<sup>st</sup> mutant reaction, primers: gene specific forward and T-DNA left border; b = 2<sup>nd</sup> mutant reaction, primers: gene specific forward and T-DNA right border; c = 3<sup>rd</sup> mutant reaction, primers: gene specific reverse and T-DNA left border; B, position of the T-DNA insertions in *KVAG* genes displaying T-DNA border characteristics in each mutant line. The T-DNA insertion of *kvag3-2* was not detected by PCR. ? = not determined.

For each line, plants carrying the T-DNA in a homozygous state could be identified (Figure 10 A). The position of the T-DNA insertion in each line was verified by sequence analysis of the T-DNA PCR product (the mutant reaction used in genotyping, Figure 10 B and Table 4). However, for the *kvag3-2* line the T-DNA insertion was not identified in the predicted region (third exon of *KVAG3*). This specific line is part of an enhancer traps project (S. Poething,

<http://enhancertraps.bio.upenn.edu>) which aims at detecting the expression of individual genes by monitoring a reporter gene (UAS::mGFP5-ER) located within the insertion. Furthermore, no GFP expression could be observed in these plants. However, the putative *kvag3-2* plants are characterized by dwarfish growth and yellowish leaves, with only one shoot and short and frail inflorescences (Figure 11). The failure of identifying the T-DNA insertion in the *KVAG3* gene of these mutant plants, in addition to absence of GFP expression, strongly suggests that the phenotype is caused by a second site mutation. Therefore the work on this line was suspended.

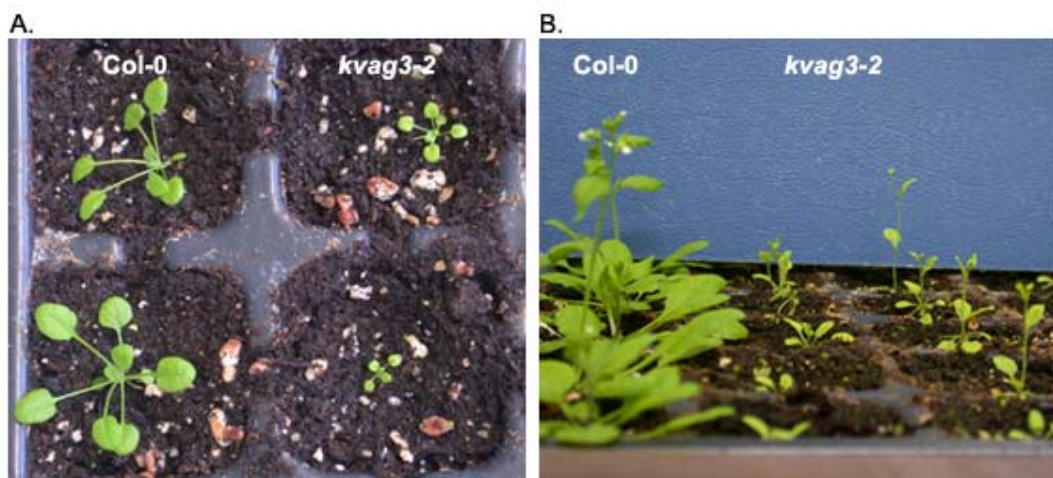


**Figure 11.** Phenotype of *kvag3-2* mutant plants.

Plants grown on soil under greenhouse conditions (16/8 hours light/dark cycle). A, two-week-old plants; B, four-week-old plants.

### 3.3.2 Verification of the Gene Knock-out by RT-PCR

The presence of a long insertion within a gene usually generates its disruption and leads to a loss-of-function mutation. The gene knock-out in the homozygous plants was assayed by RT-PCR with specific primers for each gene that enclosed the site of T-DNA insertion and were located on coding regions. The quality of the template RNA was checked by amplification of the housekeeping gene *Actin2*.

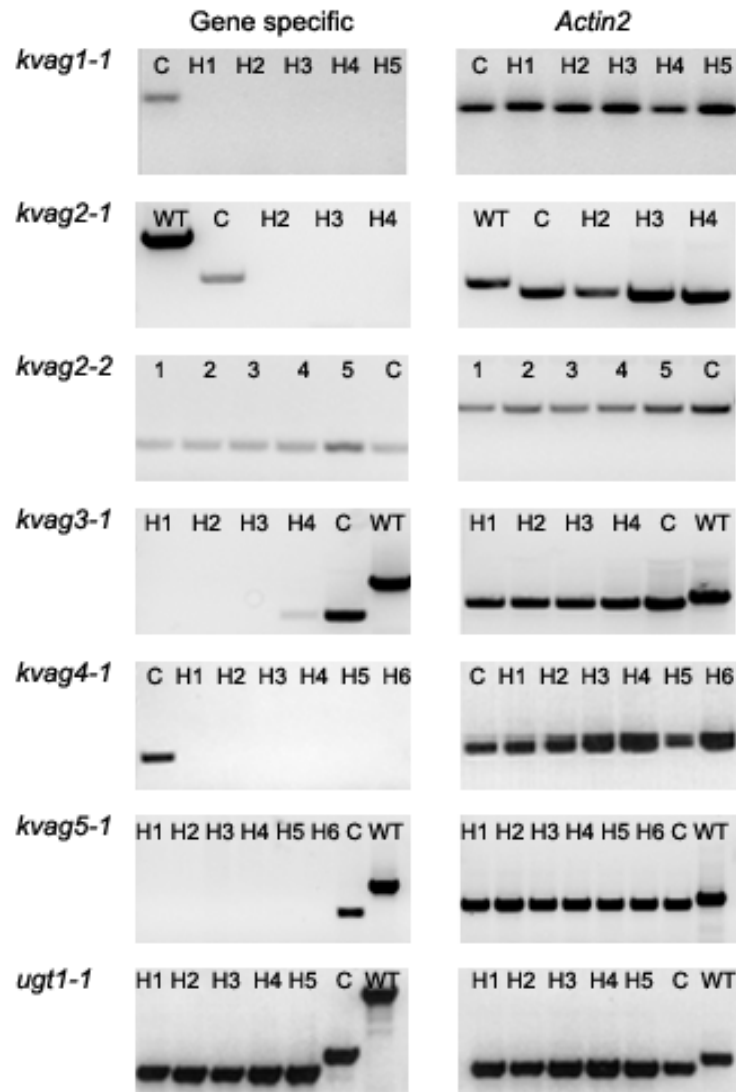


**Figure 12.** Analysis of homozygous *KVAG* T-DNA insertion lines by RT-PCR.

C = Col-0 wild type cDNA; WT = Col-0 wild type genomic DNA; H1-H6 = homozygous individual plants. *Actin2* as control for a housekeeping gene.

The absence of RT-PCR products in the reactions for *kvag1-1*, *kvag2-1*, *kvag3-1*, *kvag4-1* and *kvag5-1* indicated that the corresponding genes in these mutant plants were knocked-out (Figure 12). In contrast, the RT-PCR from the lines *kvag2-2* and *ugt1-1* showed transcript amplification (Figure 12). The transcript from *kvag2-2* had the same length as the original *KVAG2* mRNA. In this case the T-DNA insertion was located within the first intron of this gene (Figure 10 and Table 4). The amplification of an mRNA product from the T-DNA insertion line equally sized to that of the wild type mRNA (Col-0) suggests a normal intron excision and correct arrangement of the exons. This is surprising, as the T-DNA

characteristics of the *kvag2-1* line are similar but no transcript was detected. However, work on the *kvag2-2* line was stopped and the study of a *KVAG2* knock-out was further investigated in the *kvag2-1* mutant line.

The transcript amplified from *ugt1-1* was shorter in size than that expected from the wild type gene (Figure 12). In addition, this transcript contained a short deletion (183 bp) and a 47 bp insertion with similarity to an *Arabidopsis* T-DNA insertion (Forsbach *et al.*, 2003). Analysis of the whole transcript sequence disclosed an early stop codon, which most likely produces a truncated protein. If this is the case, the first half of the protein (184 aa) might still be present *in planta*.

### 3.3.3 Determination of the Number of T-DNA Insertions by Southern-Blots

Mutant plants generated by *A. tumefaciens* T-DNA transformation are likely to integrate more than one copy of the T-DNA (Gelvin, 2003). Therefore, it is recommendable to analyze the number of T-DNA insertions present in the mutant genome to rule out the presence of multiple insertions that can lead to misinterpretations (i.e phenotypes). For this purpose, Southern blot hybridizations with the genomic DNA of the mutants and a probe specific for the left border of the T-DNA were performed.

The mutant lines *kvag4-1* and *ugt1-1* yielded a single T-DNA hybridization band (Figure 13 A) suggesting a single copy T-DNA insertion. Two T-DNA bands were observed in the genome of *kvag2-1* (Figure 13 A). These bands resulted from hybridization of the probe with the two left borders previously detected in the insertion in *KVAG2* (Figure 10). Thus, *kvag2-1* also contains a single but complex T-DNA insertion. The Southern hybridization patterns of *kvag1-1*, *kvag3-1* and *kvag5-1* revealed multiple bands (Figure 13 A). Those bands could be the result of linked T-DNA insertions containing several left borders in one locus or due to second site insertions. Therefore, the *kvag1-1* mutant was backcrossed to the wild type in order to search for plants that have lost second site T-DNA insertions in the segregating population. Several individual plants of the F2 progeny, homozygous for the insertion, showed the same hybridization pattern as the mutant parent (Figure 13 B). This indicated close segregation of the T-DNAs and pointed to a

single, complex T-DNA insertion. Backcrosses for *kvag3-1* and *kvag5-1* were performed and are still under investigation.

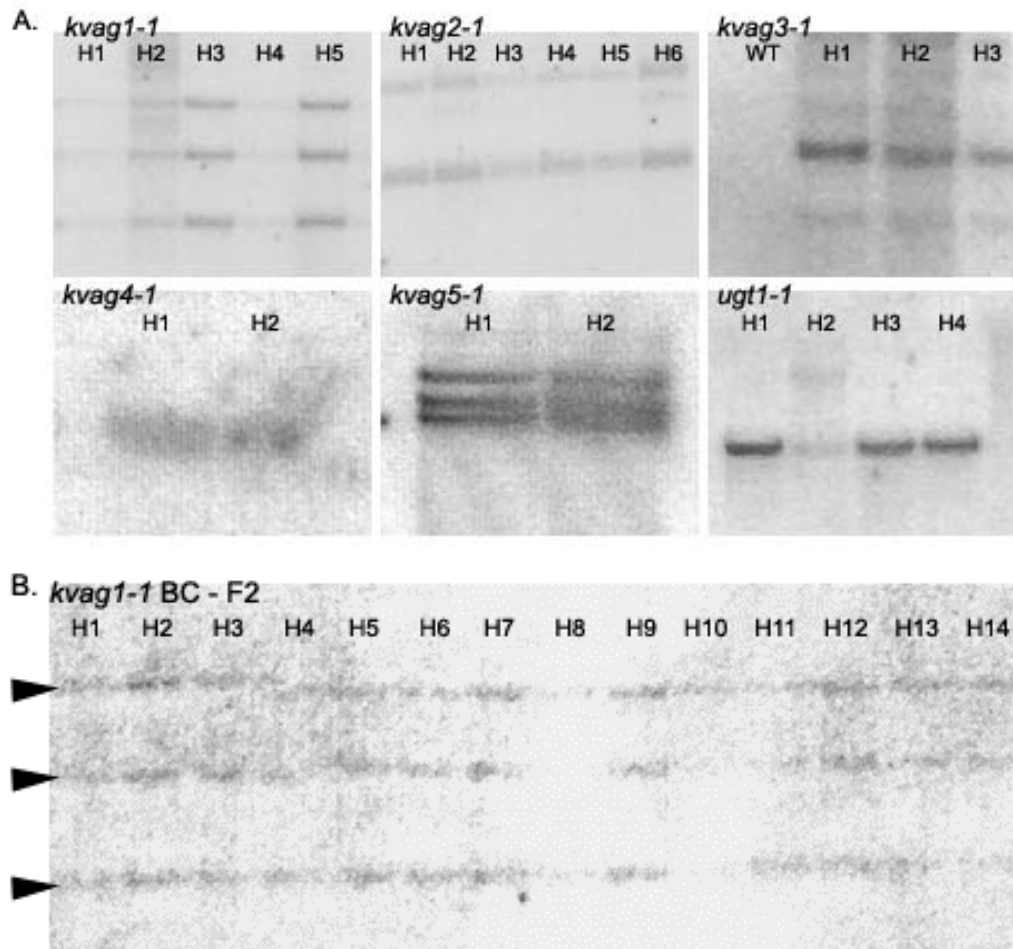


**Figure 13.** Determination of the number of T-DNA insertions in the KVAG mutant lines by Southern blot hybridizations.

A, genomic DNA of the KVAG mutants (*kvag1-1* *Eco* RI digested; *kvag2-1* *Eco* RI digested; *kvag3-1* *Sac* I digested; *kvag4-1* *Hind* III digested; *kvag5-1* *Hind* III digested; *ugt1-1* *Sac* I digested); B, genomic DNA of F2 plants from the *kvag1-1* backcrossed to Col-0 (*Eco* RI digested). Arrowheads indicate the parental bands.

### 3.3.4 Generation and Verification of *kvag1-1* x *kvag2-1* Double Knock-out Plants

Mutant plants with alterations in both putative plastidic proteins (KVAG1 and KVAG2) might encounter greater metabolic and/or developmental limitations than plants mutated in one of these carriers, especially when both proteins are involved



in similar processes. Double *kvag1-1 x kvag2-1* knock-out plants were generated by cross pollination to investigate whether this situation could be evidenced. Double homozygous plants from the F2 generation were identified by PCR analysis (Figure 14 A) and the presence of the corresponding mRNAs was evaluated by RT-PCR (Figure 14 B).

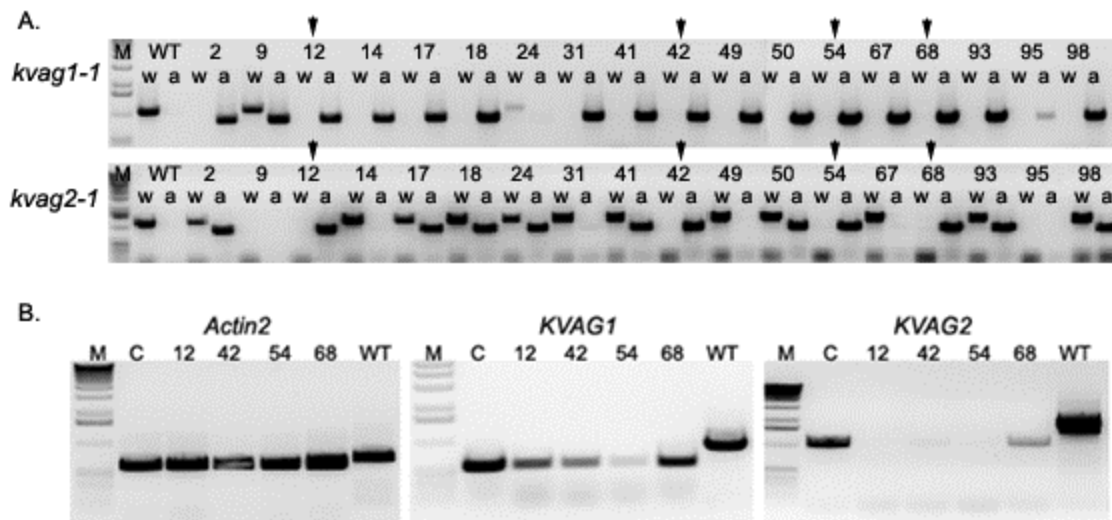


**Figure 14.** Identification of homozygous *kvag1-1 x kvag2-1* mutant plants and verification of double knock-outs.

A, identification of double homozygous plants by PCR (depicted with arrowheads). WT = Col-0 wild type genomic DNA; w = wild type reaction; a = 1<sup>st</sup>. mutant reaction, primers: gene specific forward and T-DNA left border; B, confirmation of *kvag1-1 x kvag2-1* double knock-out plants by RT-PCR. *Actin2*, as control for a housekeeping gene; C = cDNA Col-0 wild type; RT-PCR 40 cycles. M = 1kb DNA molecular weight marker (Fermentas).

The double homozygous plants (in Figure 14 A, samples 12, 42, 54 and 68) did not show transcripts for the *KVAG2* gene. Unexpectedly, a RT-PCR product was detected for the *KVAG1* gene in all selected plants (Figure 14 B). This was an intriguing outcome because all plants appeared homozygous for the T-DNA insertion in both genes. Moreover, the single T-DNA insertion mutants for *KVAG1* were also confirmed as knock-outs (Figure 12). However, the F2 individual plant 54 presented just a faint product after 40 cycles of RT-PCR, indicating highly reduced *KVAG1* transcript level (Figure 14 B). Analysis of the F2 progeny obtained from plant 54, after self-pollination, distinguished three individual plants that

revealed almost no *KVAG1* transcript (Figure 15, F3 plant samples 2, 3 and 7) and were therefore chosen for phenotypic analyses.

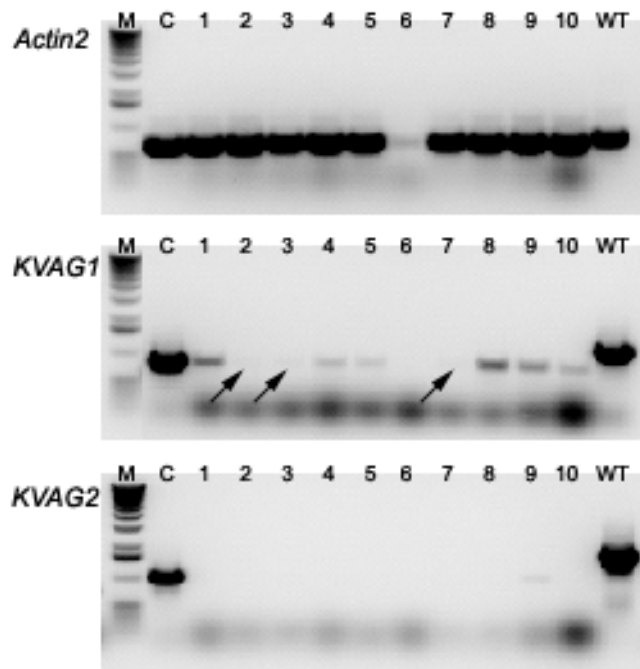


**Figure 15.** Confirmation of *kvag1-1 x kvag2-1* F3 double knock-out plants by RT-PCR.

The arrows mark individual plants with reduced *KVAG1* transcript. RT-PCR 40 cycles; *Actin2* as control for a housekeeping gene; C = cDNA Col-0 wild type; WT = Col-0 wild type genomic DNA. M = 1kb DNA molecular weight marker (Fermentas).

### 3.3.5 Phenotypical Characterization of *KVAG* Knock-out Lines

As only one T-DNA insertion was detected in the *kvag1-1*, *kvag2-1* and *kvag3-1* knock-out lines (Figure 13), possible alterations of the phenotype or fitness of these plants were expected to be directly related to the loss-of-function of the corresponding gene. To evaluate their phenotype and development in comparison to the wild type background (Col-0) the knock-out lines were grown on both,  $\frac{1}{2}$  MS medium and soil, under regular conditions (22-25°C, 16/8 hours light/dark cycle). All individual knock-out plants showed resembled the wild type in performance and morphological characteristics (not shown). The germination, growth and developmental characteristics of the *ugt1-1*, *kvag4-1* and *kvag5-1* lines also resembled that of wild type plants. In the case of *ugt1-1*, the presence of a C-terminally truncated UDP-GaIT1 protein, as indicated by the RT-PCR results, may

partially mask a potential mutant phenotype. The homozygous *kvag4-1* and *kvag5-1* lines may contain second site T-DNA insertions in other genes that could affect the mutants phenotype. However, neither the insertion in the respective *KVAG* gene nor in other loci appeared to alter the morphology or development of these plants significantly.

The *kvag1-1 x kvag2-1* double knock-out plants grown on ½ MS medium and soil under regular conditions, displayed developmental and morphological characteristics similar to the Col-0 wild type control. The germination rate of *kvag1-1 x kvag2-1* double knock-out plants was analyzed and yielded comparable results to the germination rate of the wild type (98% and 95%, respectively, n=120). Both results suggest that the *KVAG1* and *KVAG2* proteins are not essential for plant development under regular conditions.

#### **3.3.5.1 Analysis of Lipid Composition of *kvag1-1* and *kvag2-1* Plants**

There is a vast diversity of distinct lipids that build the membranes of plant cells, and within a single membrane each class of lipids has different fatty acid composition. Current knowledge explaining this is still limited. It is known that important developmental processes and responses to environmental factors are affected by the lipid composition of membranes. Specifically, some membrane proteins are functionally sustained by a certain ratio of characteristic lipids (Buchanan *et al.*, 2000). The *de novo* synthesis of fatty acids in plants occurs inside the plastids. A significant portion of fatty acids is exported to the cytoplasm and further processed in the ER through the so called eukaryotic lipid synthesis pathway. However, a glycerol-3-phosphate lipid biosynthesis pathway also exists in plastids, by which specific plastidial glycolipids are synthesized (Millar *et al.*, 2000; Dowhan, 1997).

The precursors for glycosylation of plastidial glycolipids are imported from the cytosol (Miège *et al.*, 1999; Tietje and Heinz, 1998), and the putative plastidic *KVAG* transporters were proposed to be involved in this task (Knappe *et al.*, 2003a). The lipid composition of leaves from the wild type and the *kvag1-1* and *kvag2-1* mutants was determined in collaboration with Dr. Dörmann (MPI for

Molecular Plant Physiology, Golm) to investigate whether these two mutants synthesize reduced amounts of specific plastid glycolipids, in response to a decreased plastid import of sugar donors caused by alterations in this specific transport machinery.

The results showed that the amount of plastidic or prokaryotic lipids (monogalactosyl-diacylglycerol, MGDG; digalactosyl-diacylglycerol, DGDG; sulfoquinovosyl-diacylglycerol, SQDG) was not reduced with respect to the wild type levels (Figure 16). In contrast, there was a small but significant reduction of the phospholipid levels, i.e. phosphatidyl-choline and phosphatidyl-ethanolamine, in comparison to the wild type (Figure 16). This observation rather indicated a defect in the synthesis of eukaryotic lipids in the lumen of the ER than in the plastid localized prokaryotic pathway. The total amount of fatty acids was also reduced in the *kvag2-1* mutant (Table 4) reflecting this disturbance in phospholipid biosynthesis. Furthermore, the ratio between the C16 and C18 fatty acid chains was slightly increased in the *kvag2-1* plants (0.65) compared to wild type (0.52), sustaining diminished amounts of ER lipids. The C16/C18 fatty acids ratio from *kvag1-1* plants was 0.55, similar to the wild type value.

These results indicate that the process of phospholipid synthesis in leaves is slightly affected in the two putative plastidic *KVAG* knock-out plants. It is still unclear how the phospholipid synthesis in the organs where the genes are highly expressed (pollen in *kvag2-1*, and stems or roots in *kvag1-1*, section 3.2.2) is affected by the mutations. Lipid composition analyses of the *kvag1-1* x *kvag2-1* double mutants are currently in progress. Whether this defect in lipid biosynthesis occurs also in the other gene mutants (*kvag3-1*, *kvag4-1*, *kvag5-1* and *ugt1-1*) is unknown.

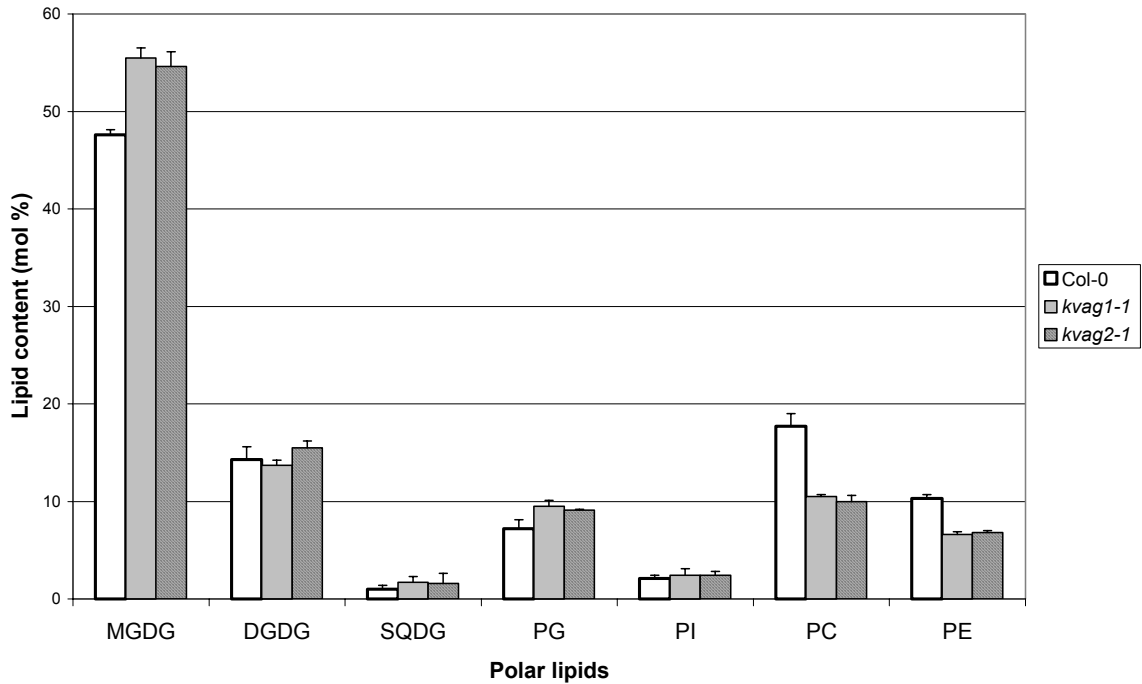


**Figure 16.** Lipid composition of leaves from *kvag1-1* and *kvag2-1*.

Content (in mol %) of individual polar lipids present in leaves from Col-0, *kvag1-1* and *kvag2-1*. n = three independent measurements. MGDG = monogalactosyl-diacylglycerol, DGDG = digalactosyl-diacylglycerol, SQDG = sulfoquinovosyl-diacylglycerol, PG = phosphatidyl-glycerol, PI = phosphatidyl-inositol, PC = phosphatidyl-choline, PE = phosphatidyl-ethanolamine.

**Table 4.** Total fatty acid content of *kvag1-1* and *kvag2-1* leaves.

Total fatty acid content and amount of C16, C18 fatty acids were measured in leaves. n = three independent measurements.

Plant genotype	Total fatty acid content (mg/g <sup>-1</sup> fresh weight)	Total C16 mol%	Total C18 mol%
Wild type Col-0	4.33 +/- 0.21	33.70 ± 0.36	64.80 ± 0.92
<i>kvag1-1</i>	4.45 +/- 0.19	34.93 ± 0.40	63.70 ± 0.34
<i>kvag2-1</i>	3.45 +/- 0.19	38.81 ± 0.89	59.45 ± 0.67

### 3.3.5.2 Analysis of *kvag1-1* and *kvag2-1* Plants on a Phosphate Deficient Background: Crosses with *pho1.2*

Single knock-out plants for *KVAG1* and *KVAG2* showed that these gene products are putatively involved in phospholipid biosynthesis. To study the performance of

mutants lacking these NST/pPT carriers in a phosphate-starved background crosses between the shoot-phosphate deficient mutant *pho1.2*, and the *kvag1-1* and *kvag2-1* single mutants were performed. *pho1.2* plants are unable to mobilize phosphate from the roots to the shoots because of a point mutation leading to a truncated version of the PHO1 protein. PHO1 is crucial for phosphate efflux out the stellar cells of the roots facilitating phosphate transport into the xylem vessels (Hamburger *et al.*, 2002). The phenotype of the *pho1.2* mutant is typical for plants under phosphate starvation displaying dark green leaves, stunted growth and late flowering (Figure 18).

Double knock-out individuals from the crosses were identified by PCR specific for the *kvag1-1* and *kvag2-1* (Figure 17) and by sequence analyses of the *pho1.2* gene (containing a premature stop codon). Approximately 100 F2 individuals were screened in the *pho1.2 x kvag1-1* and *pho1.2 x kvag2-1* populations. Three *pho1.2 x kvag1-1* and seven *pho1.2 x kvag2-1* double homozygous T-DNA insertion plants could be identified.

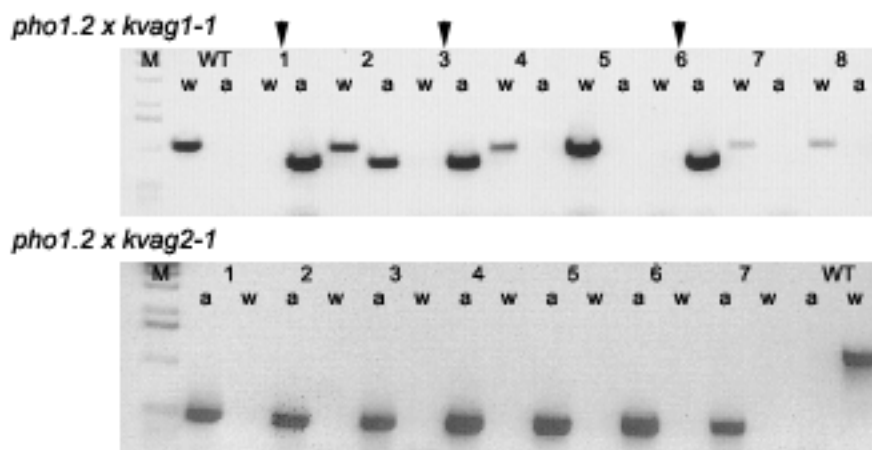


**Figure 17.** Identification of homozygous *pho1.2 x kvag1-1* and *pho1.2 x kvag2-1* plant mutants by PCR.

WT = Col-0 wild type genomic DNA; w = wild type reaction; a = 1<sup>st</sup> mutant reaction, primers: gene specific forward and T-DNA left border. M = 1kb DNA molecular weight marker (Fermentas). The *pho1.2* mutation was confirmed by sequencing the gene in the mutants (arrowheads mark the *pho1.2 x kvag1-1* homozygous plants; all seven *pho1.2 x kvag2-1* plants were homozygous).

The homozygous double knock-out plants *pho1.2 x kvag2-1* developed similarly to the *pho1.2* single mutants whereas the *pho1.2 x kvag1-1* plants revealed more severe developmental defects than the *pho1.2* mutant. Principally, they showed pronounced dwarfism and delayed flowering time (more than twice the time to reach reproductive maturity, Figure 18). Despite this, all plants produced fewer but normal siliques. The seeds from both, *pho1.2 x kvag1-1* and *pho1.2 x kvag2-1* plants, did not display distinguishable morphological anomalies whereas the germination rates changed significantly. Approximately 70% of *pho1.2* seeds germinated on  $\frac{1}{2}$  MS medium, while the double mutants reached levels similar to the wild type (wild type Col-0 98%, *pho1.2 x kvag1-1* 94%, *pho1.2 x kvag2-2* 96%, n=120). The distinguished phenotype of *pho1.2 x kvag1-1* mutants suggests that the KVAG1 protein is involved in processes where phosphate is required for plant development.



**Figure 18.** Phenotype of *pho1.2 x kvag1-1* double knock-out plants.

*kvag1-1* and *pho1.2* plants, 7-week-old; *pho1.2 x kvag1* double knock-out F2 progeny, 14-week-old plants.

### 3.3.5.3 Analysis of Growth Properties of Single *kvag1-1* and *kvag2-1* Mutants under Phosphate Limiting Conditions

The results observed in section 3.2.5.1 indicate that KVAG1 and KVAG2 are putatively involved in phospholipid biosynthesis. In addition, lack of KVAG1 in the *pho1.2* background showed increased dwarfism in comparison to *pho1.2* plants. Therefore, it was interesting to assess the performance of *kvag2-1* and especially *kvag1-1* single knock-out plants, in response to phosphate limitation. Mutants and wild type (Col-0) plants were grown on ½ MS media containing varying concentrations of phosphate (0.75 mM, 0.4 mM, 0.2 mM, 0.1 mM and 0.0 mM), and their development and morphological characteristics were analysed.

In general, the single mutants and the wild type exhibited similar developmental characteristics. They exhibited retarded growth, small dark green rosette leaves, bushy root architecture (Figure 19) and retarded flowering, with one shoot and few siliques. These features were more severe in plants grown under phosphate starvation, in media with 0.1 and 0.0 mM phosphate concentrations. Grown on such phosphate deficiency conditions, the plants overall size was severely reduced (Figure 19). There were no detectable differences in root length, length or number of secondary roots, or number of leaves between the wild type and the knock-out plants. Under phosphate starvation (0.2, 0.1 and 0.0 mM phosphate) both wild type and mutants died before reaching reproductive maturity.



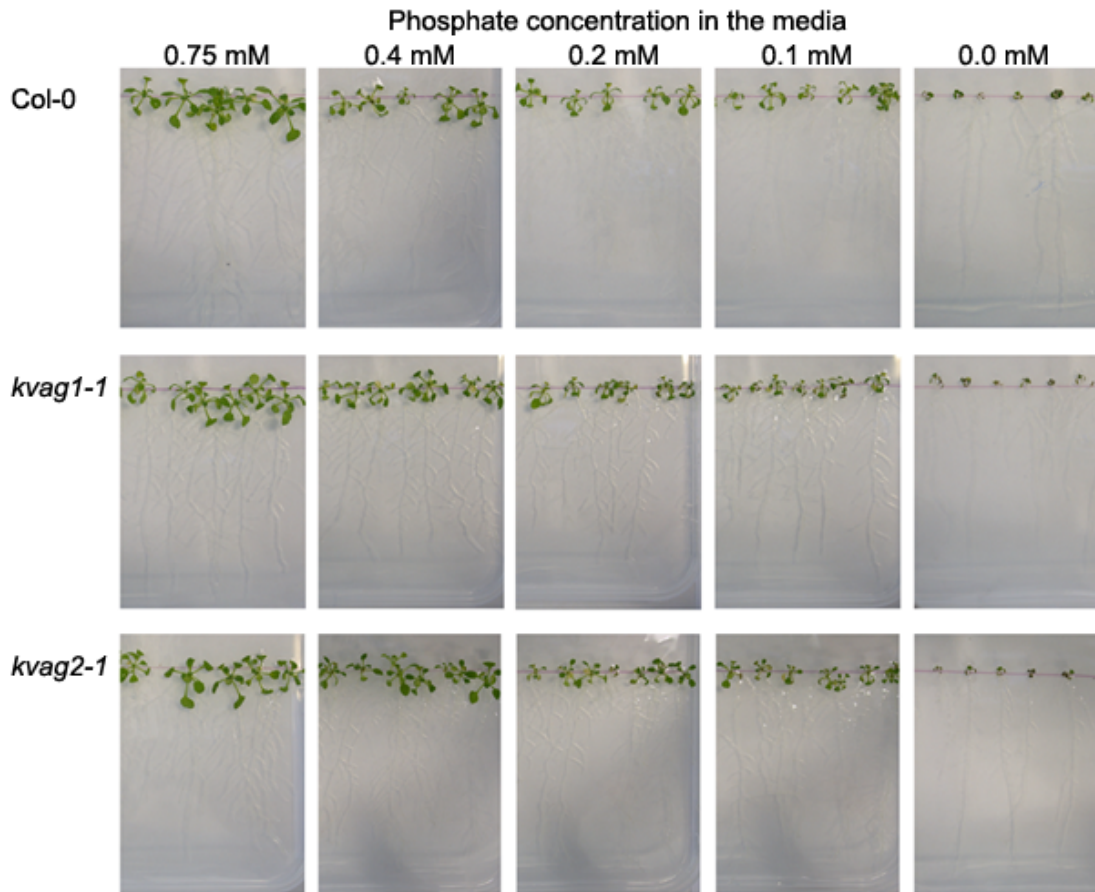


**Figure 19.** Growth of *kvag1-1* and *kvag2-1* under phosphate deficiency.

Wild type Col-0 and single *kvag1-1* and *kvag2-1* knock-out plants grown under different phosphate concentrations; 15-day-old plants.

#### 3.3.5.4. Analysis of *KVAG1* and *KVAG2* Gene Expression under Phosphate Limiting Conditions by RT-PCR

To inspect a possible deregulation of expression of *KVAG1* and *KVAG2* under phosphate limitation, a semi-quantitative RT-PCR was performed using total RNA extracted from wild type plants grown under different phosphate concentrations. The results demonstrated that *KVAG1* and *KVAG2* transcripts in root tissues under phosphate deficiency (0.4 and 0.2 mM phosphate) closely match the transcript levels in roots from plants grown on sufficient phosphate (0.75 mM, Figure 20). The amount of *KVAG* transcripts from phosphate starved roots (0.1 mM) was fainter, and also the amount of actin transcript in this condition, indicating that the RNA template had a lower quality. Similarly, plants grown on 0.0 mM phosphate were very small and the RNA extracted from them was not suitable for

cDNA synthesis. In the shoots, *KVAG1* and *KVAG2* transcripts behaved similarly, showing increase at the onset of phosphate deficiency (0.4 mM, Figure 20). However, transcript amounts decreased, near control levels, in more phosphate deprived plants (grown at 0.2 and 0.1 mM). This shows that mainly moderate phosphate deficiency might alter transcript regulation of the *KVAG1* and *KVAG2* gene products in the shoots. Interestingly, severe reduction of phosphate seems to have little impact on the expression of both genes.

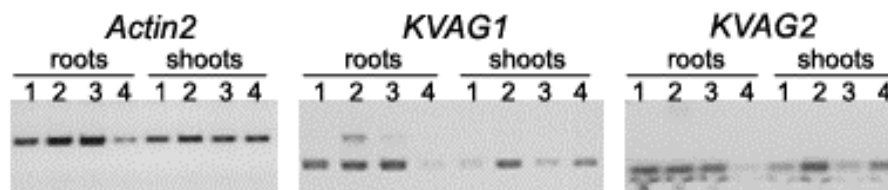


**Figure 20.** Analysis of *KVAG1* and *KVAG2* expression in wild type plants grown under phosphate deficiency.

Semi-quantitative RT-PCR, 28 cycles, performed with mRNA from 15-day-old wild type (Col-0) plants grown under phosphate limiting conditions. 1 = 0.75 mM, 2 = 0.4 mM, 3 = 0.2 mM, 4 = 0.1 mM phosphate concentration in the media. *Actin2* as control for a housekeeping gene.

The characteristics of the mutants are summarized in Table 5. Essentially, plants that lack functional members of the KV/A/G subfamily of NST/pPT carriers display phenotypes that resemble the wild type (i.e. leaf, root and flower morphologies and developmental characteristics). Investigation of the lipid composition in leaves from the *kvag1-1* and *kvag2-1* mutants, lacking one putative plastidic KVAG transporter each, indicated a possible association of these two proteins in the biosynthesis of phospholipids. Further studies regarding the lipid and fatty acid properties of double knock-out mutants from these two genes, and knock-outs from the other members of the KV/A/G subfamily, are expected to reveal whether this family might be involved in the synthesis of lipids of eukaryotic origin.

**Table 5.** Characteristics of the KVAG T-DNA insertion lines.

Summary of the molecular and phenotypic characterization of KVAG mutants. a = RT-PCR product in homozygous plants (refer to section 3.3.4). n.d. = not determined.

T-DNA insertion Line	Homozygosity	Position of T-DNA insertion	Knock-out (by RT-PCR)	No. of T-DNA insertions	Phenotype
<i>kvag1-1</i>	Yes	Intron +853	Yes	1	Reduced phospholipid content in leaves
<i>kvag2-1</i>	Yes	Intron +898	Yes	1	Reduced phospholipid content in leaves
<i>kvag2-2</i>	Yes	n.d.	No	n.d.	Like wild type
<i>kvag3-1</i>	Yes	Intron +869	Yes	More than 1	Like wild type
<i>kvag3-2</i>	No	n.d.	n.d.	n.d.	Dwarfish, yellowish leaves
<i>kvag4-1</i>	Yes	Intron +1444	Yes	1	Like wild type
<i>kvag5-1</i>	Yes	Exon +304	Yes	More than 1	Like wild type
<i>ugt1-1</i>	Yes	Exon +1332	No	1	Like wild type
<i>kvag2-1</i> x <i>kvag1-1</i>	Yes Yes	Intron +898 Intron +853	Yes No <sup>a</sup>	1 1	Like wild type
<i>pho1.2</i>	Yes	Premature stop codon in 5 <sup>th</sup> exon	Yes	No T-DNA	Dwarfish, dark green leaves, few siliques
<i>pho1.2</i> x <i>kvag1-1</i>	Yes Yes	5 <sup>th</sup> exon Intron +853	Yes n.d.	No T-DNA 1	Stunted growth, dark green leaves, retarded development
<i>pho1.2</i> x <i>kvag2-1</i>	Yes Yes	5 <sup>th</sup> exon Intron +898	Yes Yes	No T-DNA 1	Dwarfish, dark green leaves, like <i>pho1.2</i>

### **3.4 Intracellular Localization of KVAG Proteins: Expression of KVAG::GFP Fusions *in planta***

The *in silico* analysis of the deduced amino acid sequences of KVAG1 and KVAG2 predicted plastidic targeting signals for these two proteins (section 3.1.1). In order to assess this putative plastidial signal peptide for its effective organellar targeting role in both proteins, analyses of plant cells transiently expressing these KVAG proteins fused to the reporter GFP were carried out. In addition, the same approach was employed for studying the intracellular localization of other members of the KV/A/G subfamily.

The amino terminal region of KVAG2 (the first 161 amino acids comprising the predicted plastid target) was amplified from cDNA and cloned into the pGWB5 vector, thereby fusing it to the amino terminus of GFP. Transient expression of this N<sub>161</sub>-KVAG2::GFP construct rendered a diffused cytoplasmic fluorescence in tobacco BY2 protoplasts (Figure 21). This GFP expression was repeatedly observed in several transformed cells and thus clearly contradicted the expression results of specific plastid labelling in protoplasts transformed with the triose phosphate/phosphate transporter (TPT::GFP) (Figure 21). Thus, the KVAG2 amino terminal region by itself was not able to target the reporter protein to the plastids. This indicated that the KVAG2 predicted plastid signal might not be functional in tobacco or is insufficient for targeting the reporter protein to this organelle.

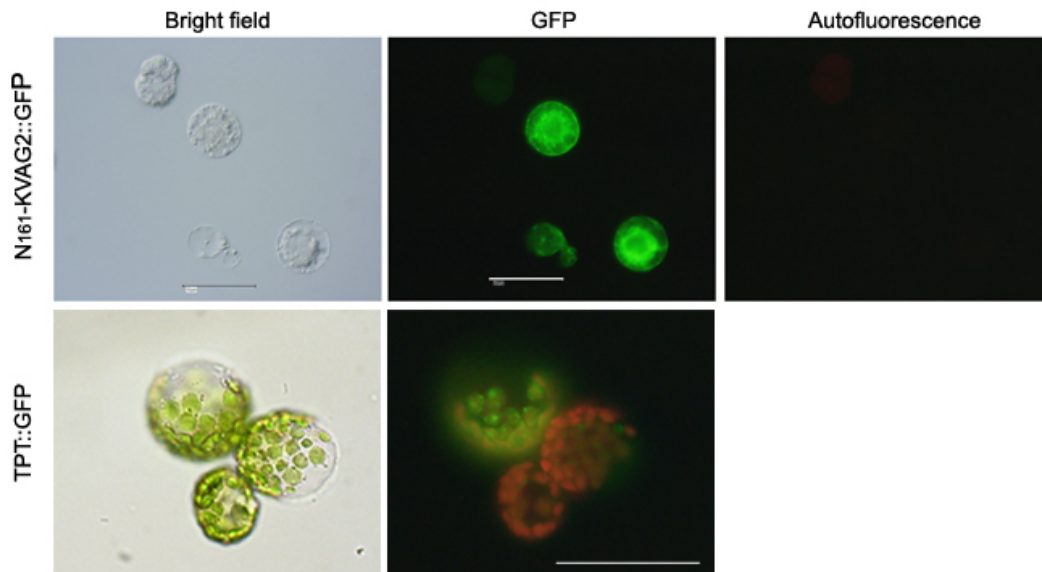


**Figure 21.** Intracellular localization of N<sub>161</sub>-KVAG2::GFP.

Tobacco BY2 protoplasts transiently expressing the amino terminal region of KVAG2 (first 161 residues) fused to GFP. For comparison the expression of the plastidic TPT protein fused to GFP in protoplasts from tobacco Samsun plants. Bright field = white light, GFP = blue light, Autofluorescence = green light. Bars = 50  $\mu$ m.

Consequently, the full length cDNA of *KVAG2* was amplified and cloned into the pGWB5 vector (35S-KVAG2::GFP). This construct was transiently expressed in tobacco Samsun protoplasts as they present clearly distinguishable chloroplasts. The GFP reporter protein was not observed in plastids; instead, it labeled small vesicles dispersed across the cytoplasm forming a dotted pattern (Figure 23). These vesicles were highly motile and moved along defined narrow paths through the cytoplasm. This kind of pattern is comparable to reports of Golgi apparatus labeling (Abe *et al.*, 2004; Gilson *et al.*, 2004; Handford *et al.*, 2004; Baldwin *et al.*, 2001). Moreover, expression of a mouse sialyltransferase (ST), a Golgi resident protein, fused to GFP (35S-ST::GFP) in BY2 protoplasts presented a similar expression pattern with vesicles of comparable size (Figure 23). Labeling of the ER, accomplished by expression of GFP tagged with an ER retention signal (35S-mGFP-ER) in tobacco leaf epidermal cells (Figure 23) and protoplasts, showed a network of fibers across the cytoplasm differing from the Golgi dotted pattern. Therefore, the localization of KVAG2 fused to GFP matched the labeling patterns observed for the Golgi apparatus and not the ER.

The localization of GFP fused to the putative KVAG1 plastidic signal peptide alone was not determined. Instead, the full *KVAG1* cDNA was amplified and cloned into the pGWB5 vector to determine the intracellular localization of this protein. In addition, the cDNAs from *KVAG3*, *KVAG4* and *KVAG5* were also cloned in order to analyze their intracellular localization following the same procedure. Interestingly, the amplification product of the *KVAG5* cDNA was approximately 100 bp shorter than the annotated model cDNA (920 bp observed *versus* 1025 bp expected, Figure 22). Sequence analysis revealed that this fragment lacks the second predicted exon (Figure 3). This further supports the previous misannotation of the *KVAG5* gene. The transient expression of 35S-KVAG1::GFP, 35S-KVAG3::GFP, 35S-KVAG4::GFP and 35S-KVAG5::GFP in tobacco (protoplasts or leaf epidermal cells) showed a similar pattern to that observed for 35S-KVAG2::GFP and the ST Golgi marker (Figure 23).

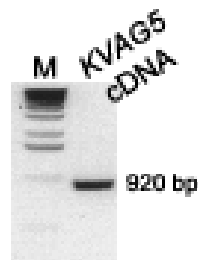


**Figure 22.** Amplification of *KVAG5* cDNA.

The *KVAG5* cDNA product (920 bp) is 100 bp shorter than predicted by annotation models (1025 bp). M = DNA molecular weight marker (Fermentas).

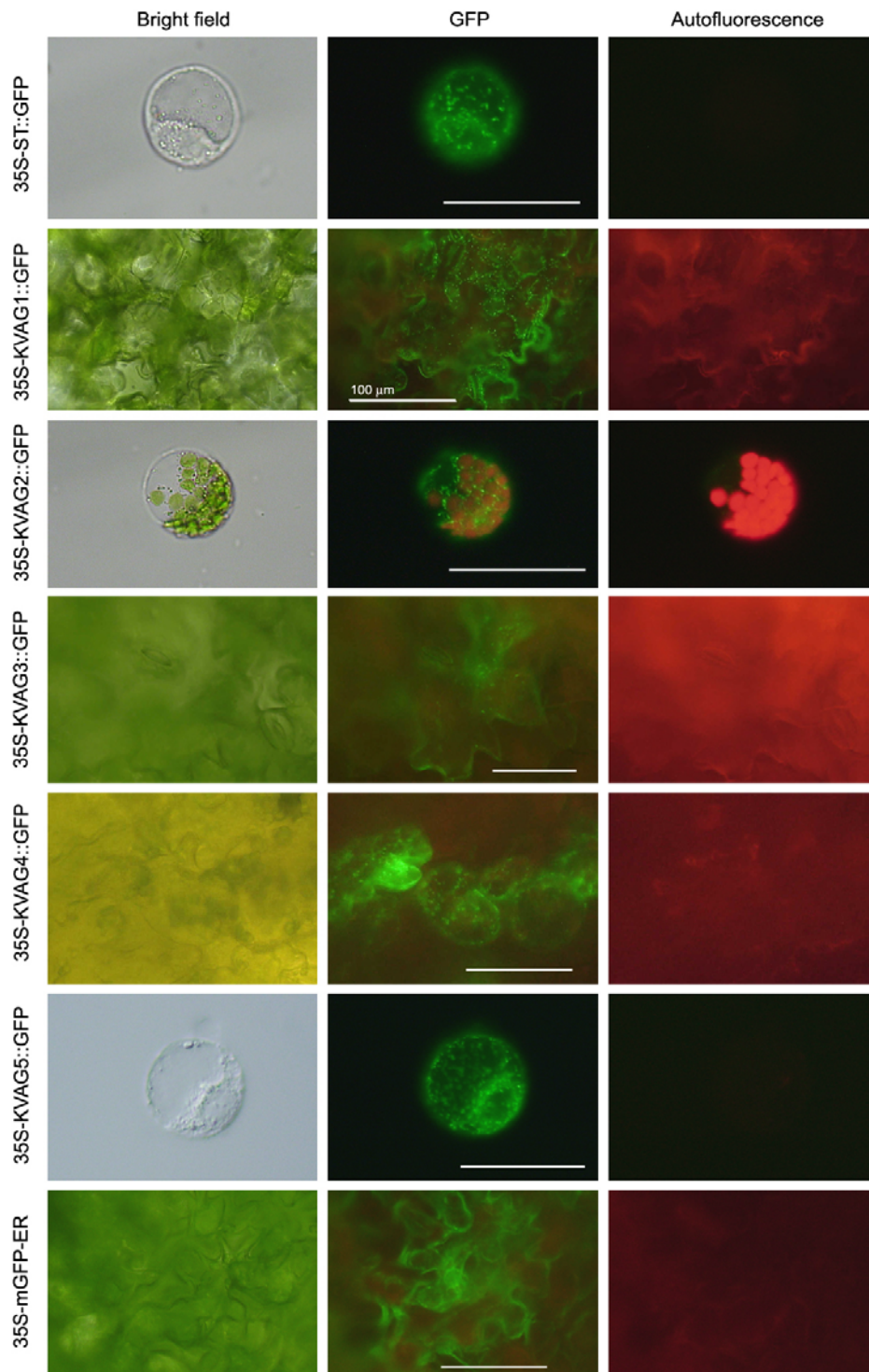


**Figure 23.** Intracellular localization of 35S-KVAG::GFP proteins *in planta*.

35S-ST::GFP, 35S-KVAG2::GFP and 35S-KVAG5::GFP constructs expressed in tobacco protoplasts (BY2 or Samsun). 35S-KVAG1::GFP, 35S-KVAG3::GFP, 35S-KVAG4::GFP and 35S-mGFP-ER constructs expressed in *N. benthamiana* epidermal cells. 35S-ST::GFP = mouse ST as Golgi marker protein. 35S-mGFP-ER = GFP targeted to the ER. Bright field = white light, GFP = blue light, Autofluorescence = green light. Bars = 50 µm, except when differently stated.

To verify the Golgi localization of the KVAG proteins, tobacco cells expressing the GFP fusion proteins were treated with Brefeldin A (BFA, 100 µg/ml). BFA is a fungal toxin that affects specifically the structural stability of the Golgi apparatus. It causes disassembly of the Golgi, with most of the cisterna being absorbed into the ER and the fusion of the trans-Golgi network with elements of the endocytic pathway (Nebenfuehr *et al.*, 2002). After BFA treatment the 35S-KVAG::GFP labeled structures showed severe distortion of the dotted pattern (Figure 24). The GFP signal was seen dispersed in the cytoplasm. Furthermore, it was also detected in bigger and less motile structures forming clear aggregates. Protoplasts transiently expressing the mammalian ST behaved in the same manner upon BFA treatment, while there was no change on the fluorescence pattern of 35S-mGFP-ER transfected cells (Figure 24). The stability of other cellular compartments, i.e. plastids, was unaffected by BFA.

The intracellular BFA sensitivity displayed by the GFP-labelled compartment suggested that all KVAG proteins, including KVAG1 and KVAG2 initially predicted as plastid localized proteins, are located in the Golgi apparatus.



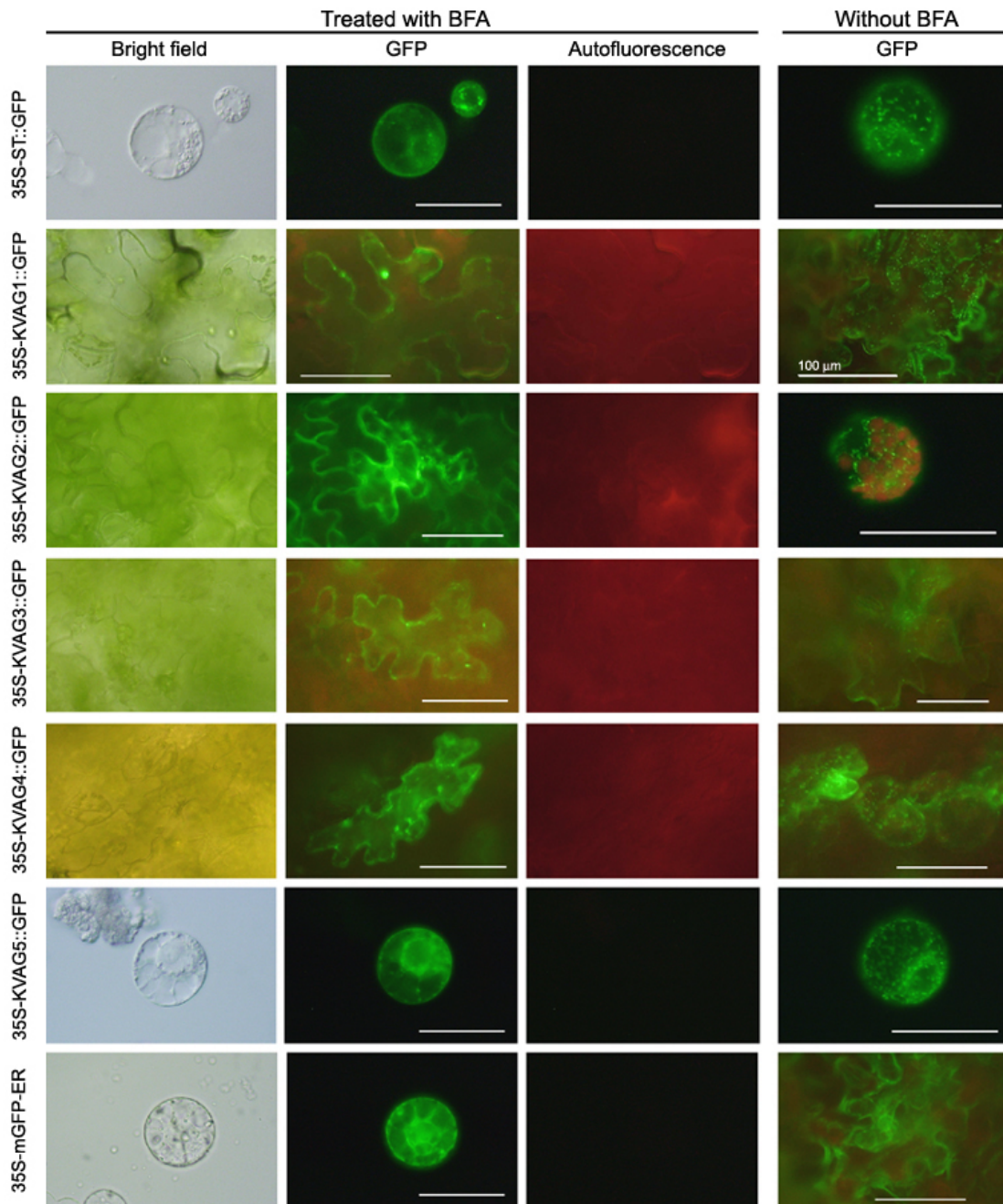


**Figure 24.** Distribution of 35S-KVAG::GFP proteins after BFA treatment.

Transiently transformed cells treated with BFA. BY2 protoplasts transfected with 35S-ST::GFP, 35S-KVAG5::GFP and 35S-mGFP-ER; *N. benthamiana* leaf epidermal cells transfected with 35S-KVAG1::GFP, 35S-KVAG2::GFP, 35S-KVAG3::GFP and 35S-KVAG4::GFP. Untreated cells (Without BFA) are shown for comparison. 35S-ST::GFP = mouse ST as Golgi marker protein; 35S-mGFP-ER = GFP targeted to the ER. Bright field = white light, GFP = blue light, Autofluorescence = green light. Bars = 50  $\mu\text{m}$ , except when differently stated.

### 3.5 Expression of KVAG Proteins in a Heterologous System and Measurements of Transport Activity

To investigate the transport activity of KVAG1 and KVAG2, high amounts of the proteins were required. For this purpose, the proteins were heterologously overexpressed in the heterologous system of *S. cerevisiae*, strain InvSC1. The cDNA entry clones (employed for GFP fusions and intracellular localization *in planta*, section 3.4) were recombined into the pYES-DEST52 yeast expression vector and thereby fused to a C terminal histidine tag (6 x histidine). This tag permitted the purification of the expressed proteins by Ni-NTA affinity chromatography and detection by a histidine-tag specific antibody. Transformed yeasts were selected and grown in SC medium lacking uracil, and protein overexpression was induced by galactose. For transport experiments the proteins were reconstituted into phosphatidylcholine membranes or liposomes. These artificial proteoliposomes were submitted to transport measurements using radiolabeled substrates.

As a positive control for transport of nucleotide sugars (UDP-Gal), the full length cDNA of UDP-GalT1 was also cloned into pYES-DEST52 in addition to KVAG1 and KVAG2. UDP-GalT1 is a specific UDP-Gal transporter that also belongs to the KV/A/G subfamily of NST/pPT homologous proteins (Bakker *et al.*, 2005). Recently, UDP-GalT3 (At4g39390) a member of the KT subfamily, was identified as a highly specific UDP-Gal/UMP antiporter (Rollwitz *et al.*, *in prep.*). Therefore, the UDP-GalT3 protein overexpressed in yeast was employed as a second positive control for transport measurements. The full cDNAs of KVAG4 and KVAG5 (from section 3.4) were also cloned into pYES-DEST52, and transformed yeast clones were identified. A summary of the cDNAs cloned for protein expression is presented in Table 6.

**Table 6.** Characteristics of the KVAG cDNAs cloned for protein expression in yeast. The plasmid template was obtained from the Riken Institute.

<b>Protein</b>	<b>cDNA size (bp)</b>	<b>Protein size (kDa)</b>	<b>mRNA / cDNA source</b>
KVAG1	1077	36	Plasmid
KVAG2	1065	35	Flower
KVAG4	918	30	Seedling
KVAG5	918	30	Root
UDP-GalT1	1005	33	Plasmid
UDP-GalT3	1011	33	Seedling

### 3.5.1 Analysis of KVAG Heterologous Protein Expression

To evaluate the heterologous overexpression of KVAG proteins in yeast, the cells were grown in the presence of galactose and harvested at different time points, ranging from 4 to 24 hours after induction. Yeast membrane proteins were separated by SDS-PAGE and analyzed by Coomassie staining and western blots. The western blots, visualized by immune-localization with an anti-histidine-tag antibody, showed clear protein expression upon induction for KVAG1, KVAG2 and UDP-GalT1 in isolated membranes (Figure 25). The expressed proteins were detected between 4 to 8 hours after induction. UDP-GalT3 was also expressed in yeast membranes upon induction (Figure 25). As expected, no signal was detected in either protein fractions from un-induced cells (time point 0 hours, Figure 25) or from cells transformed with an empty vector (not shown).

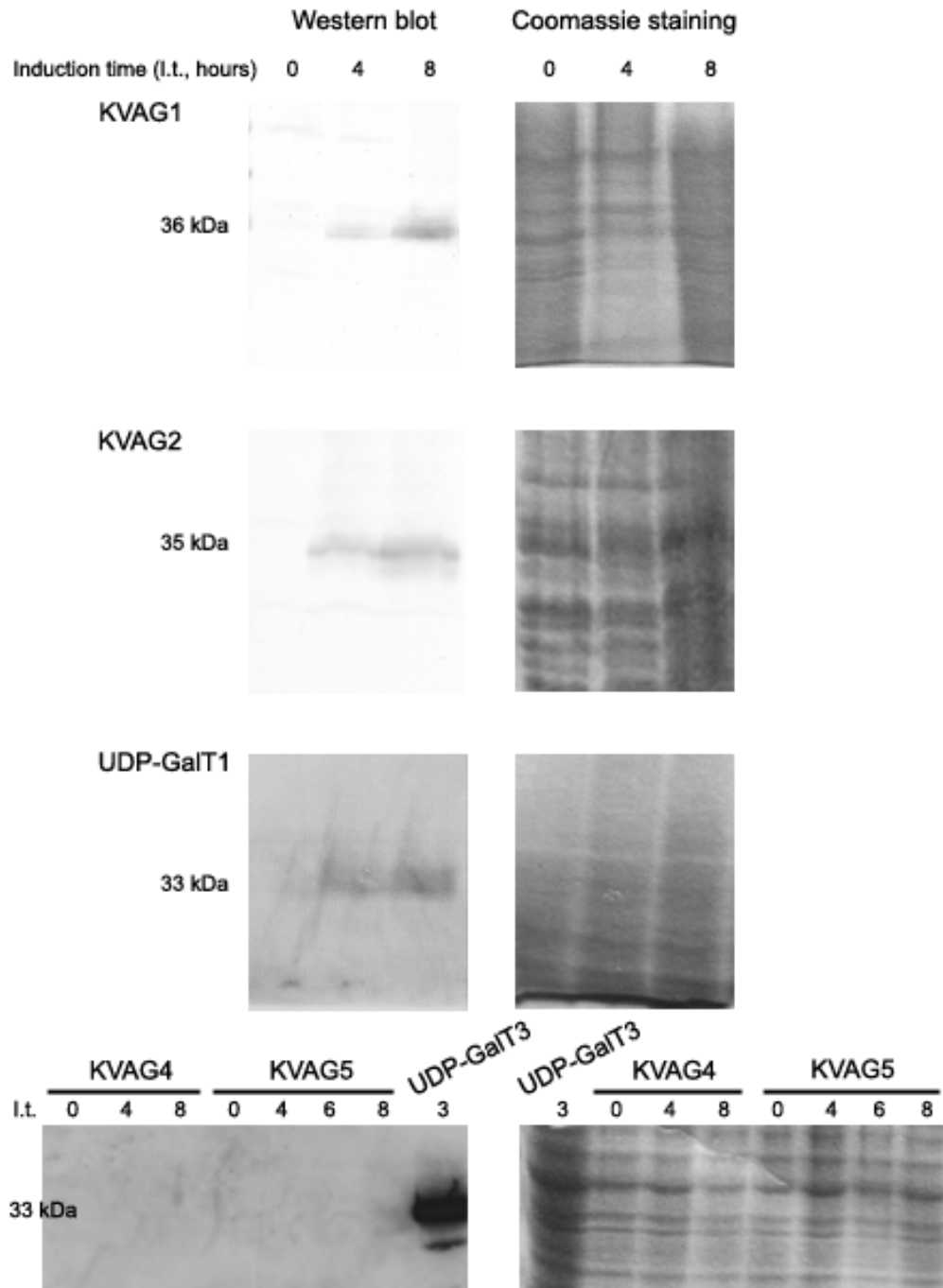


**Figure 25.** SDS polyacrylamide gel electrophoresis and western blots of heterologously expressed membrane proteins.

Induction time (I.t.): 0 hours, before protein induction; 4, 6 and 8 hours, after galactose induction. Western blots immune-visualized with anti-histidine-tag antibody.

Yeast clones containing the *KVAG4* and *KVAG5* constructs did not express the recombinant protein after induction (10 clones analyzed for each construct, one representative example in Figure 25). The soluble protein fractions revealed no

detectable signals for histidine tagged proteins either, indicating that the recombinant proteins were not lost during the process of membrane isolation. What might cause the lack of expression of these two proteins in yeast is unknown. Since KVAG4 and KVAG5 could not be expressed heterologously, the subsequent functional assays were performed solely with the KVAG1, KVAG2, UDP-GalT1 and UDP-GalT3.

### **3.5.2 Measurements of Transport Activity of the Heterologously Expressed KVAG Proteins**

In the last years, the reconstitution of proteins into artificial membranes or liposomes became a powerful and commonly used tool to investigate the transport activity of proteins imbedded in cellular membranes (Flügge, 1998; Hanke *et al.*, 1999; Eicks *et al.*, 2002; Knappe *et al.*, 2003b; Segawa *et al.* 2005). In the current study it was used to assay transport activity of proteins by measuring the import of a radiolabeled substrate into the lumen of liposomes. Because NSTs and pPTs have been described as antiporter proteins (Capasso and Hirschberg, 1984; Flügge, 1999; Bakker *et al.*, 2005), the substrate/counter-substrate transport activity was also evaluated.

#### **3.5.2.1 Protein Solubilization from the Yeast Membrane Fraction**

Reconstitution of hydrophobic proteins into liposomes requires separation of the proteins from surrounding membranes first. Thus, the solubilization of the KVAG proteins was surveyed to optimize protein isolation. Different detergents were tested for their capacity to solubilize the proteins imbibed in the membranes (1% final concentration of detergents; nonionic: Triton X-100, Tween20, DM; anionic: sodium deoxycholate (DOC); and zwiterionic: CHAPSO). After detergent treatment, the samples were centrifuged to separate the protein solution (supernatant fraction) from the remaining membranes (pellet fraction). The supernatant and pellet fractions were analyzed by western blot and the solubilization behavior of the protein of interest was evaluated (Figure 26 for KVAG2).

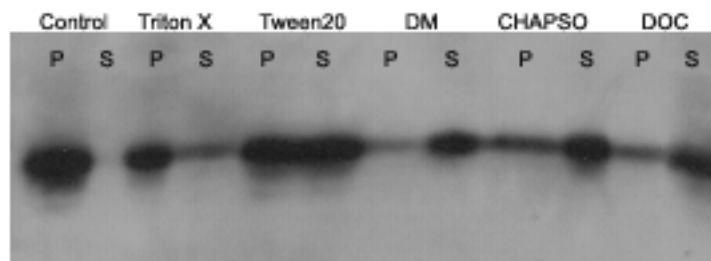


**Figure 26.** KVAG2 protein solubilization using different detergents.

P = pellet fraction containing membranes, S = supernatant fraction containing solubilized proteins. Control = sample without detergent treatment, Triton X = Triton X-100, DM = n-Dodecyl- $\beta$ -D-maltoside, DOC = sodium deoxycholate.

The recombinant protein remained entirely in the pellet fraction in the absence of detergents (control lanes in Figure 26). The KVAG2 protein was partially solubilized with all detergents tested. However, DM, CHAPSO and DOC rendered higher amounts of soluble recombinant protein than Triton X-100 and Tween20 (compare the supernatant vs. pellet signals in each treated sample, Figure 26). DM solubilized most of the recombinant protein as demonstrated by the faint signal that was detected in the pellet (Figure 26), while considerable amounts of protein were still found in the pellet fraction from CHAPSO and DOC treated samples. Consequently, DM was further used for protein solubilization prior to protein reconstitution into liposomes.

### 3.5.2.2 Measurements of Transport Activity Using Whole Yeast Membrane Proteins Reconstituted into Liposomes

The yeast membrane fractions enriched with UDP-GalT1, UDP-GalT3, KVAG1 and KVAG2 were reconstituted into liposomes and subjected to transport kinetic assays. The liposomes were preloaded with buffer with or without a putative substrate (CDP-choline, CDP-ethanolamine or nucleotide sugar diphosphates) prior to protein reconstitution. The transport activity of the protein was determined by measuring the incorporation of a radiolabeled nucleoside monophosphate (CMP, UMP or GMP) into the liposomes. As negative control yeast membrane fractions from cells transformed with an empty vector were used. The radioactivity incorporated into these proteoliposomes corresponds to the background transport

activity of endogenous yeast proteins. As another negative control, Liposomes without reconstituted proteins were treated identically but yielded no radioactive incorporation, confirming the lack of protein unrelated substrate transport into the artificial vesicles.

The two positive controls, UDP-GalT1 and UDP-GalT3, were assayed for UMP and UDP-Gal/UMP transport. Uniport transport of radiolabeled UMP was low in UDP-GalT1 and UDP-GalT3 proteoliposomes. These uptake levels were similar to the values observed for the empty vector control (Figure 27). The transport of radiolabeled UMP in exchange for UDP-Gal in UDP-GalT1 liposomes was even reduced compared to the empty vector control (Figure 27). Thus, no activity associated with UDP-GalT1 was detected although UDP-GalT1 was previously characterized as a selective UDP-Gal transporter (Bakker *et al.*, 2005). Similar transport experiments performed in our laboratory using UDP-GalT2, another UDP-Gal/UMP transporter (Bakker *et al.*, 2005) and member of the KT subfamily, also did not show UDP-Gal/UMP transport activity (I. Rollwitz, *pers. comm.*). In contrast, UDP-GalT3 revealed high UDP-Gal/UMP transport activity (24.76 nmol/min, average from 5 experiments, Figure 27). This transport was five times higher than the empty vector control indicating that the overexpressed carrier mainly transports the substrate and that the method itself is functioning. This activity was also significantly higher (near 12 fold increase) when compared to UMP unitransport, confirming UDP-GalT3 as a highly specific UDP-Gal/UMP antiporter (Figure 27).

The characterization of the loss-of-function mutants for KVAG1 and KVAG2 indicated a possible involvement of these proteins in the phospholipid biosynthesis pathway (section 3.3.5.1). Activated choline and ethanolamine are the precursors for phospholipid biosynthesis in the lumen of the ER. It is known that their activation (coupling to cytidine diphosphate) occurs in the cytosol (Buchanan *et al.*, 2000) and thus requires an import mechanism into the endomembrane system. The two activated phospholipid precursors, CDP-choline and CDP-ethanolamine, were used for transport experiments by the KVAG2 protein. Radiolabeled CMP was used as counter-substrate. Similar experiments using KVAG1 are currently under progress.

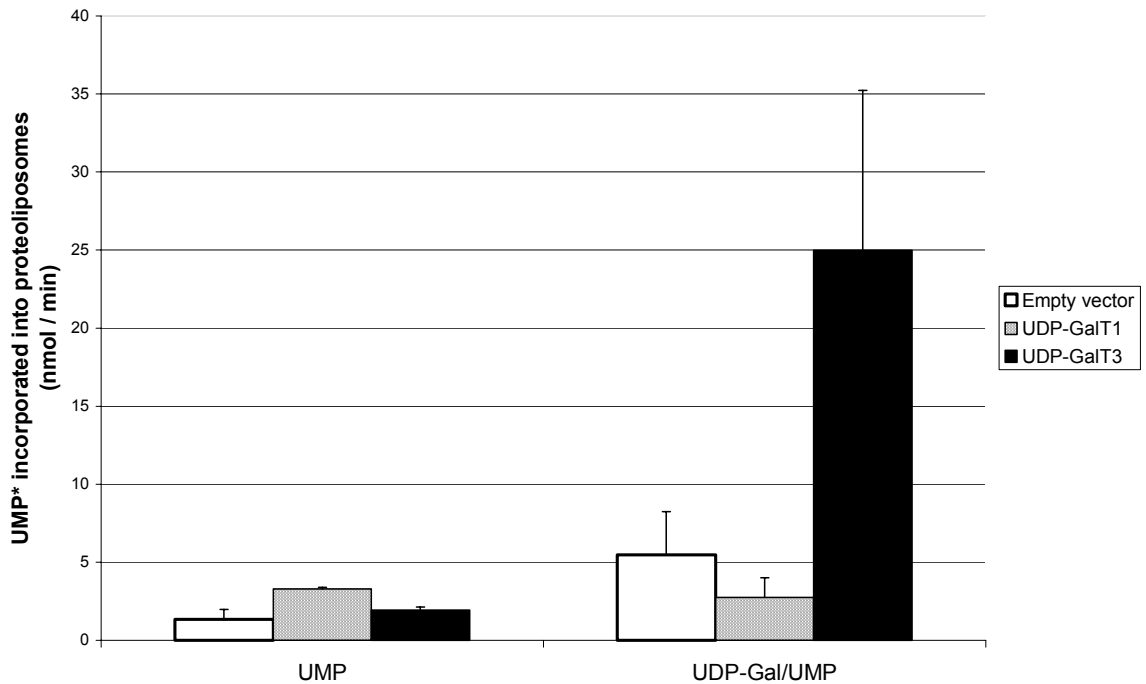


**Figure 27.** Transport activity of UDP-GalT1 and UDP-GalT3 reconstituted into liposomes. Empty vector and UDP-GalT3, n = five independent experiments; UDP-GalT1, n = three independent experiments. UMP\* = <sup>33</sup>P radiolabeled UMP.

The transport activity of phospholipid precursors by KVAG2 were comparable to the transport measured in the background control (empty vector, Figure 28). There was no significant import of CMP or exchange of CDP-choline against CMP displayed by KVAG2 (Figure 28). Transport of CDP-ethanolamine/CMP (1.31 nmol/min) was higher in comparison to the empty vector (0.6 nmol/min), but still below uptake of CMP in the absence of a counter substrate (2.12 nmol/min). Thus, the results indicate that KVAG2 does not transport CMP, CDP-choline or CDP-ethanolamine under these conditions.



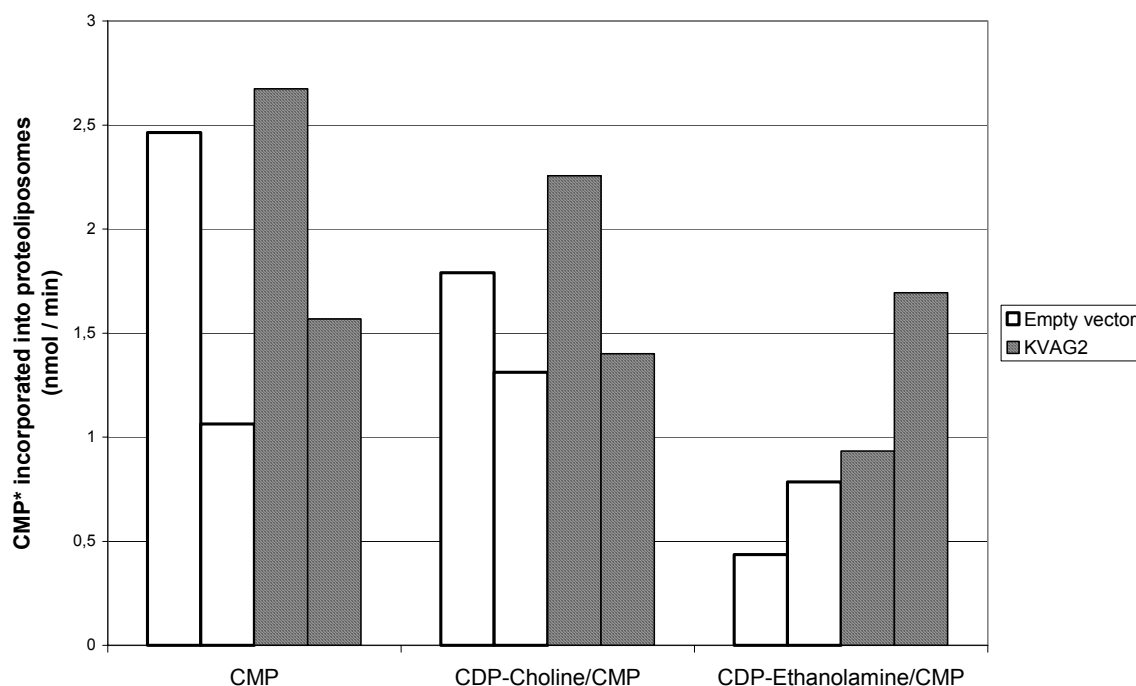


**Figure 28.** Transport activity of phospholipid precursors by KVAG2 reconstituted into liposomes.

Two independent experiments. CMP\* =  $^{33}\text{P}$  radiolabeled CMP.

Nucleotide sugars are the usual substrates of NSTs. These metabolites serve as sugar donors for the glycosyltransferases in the Golgi and ER to modify a wide array of proteins, polysaccharides and lipids. Due to the structural similarities of KVAG proteins with NSTs, the transport activity of KVAG1 and KVAG2 reconstituted into liposomes was assayed with a panel of nucleotide sugars. These substrates were chosen based on their natural occurrence in plants, and included UDP- and GDP- activated sugars (UDP-Glc, UDP-Gal, UDP-GlcNAc, UDP-N-acetyl galactosamine (UDP-GalNAc), UDP-Glucuronic acid (UDP-GlcA), UDP-Arabinose (UPD-Ara), UDP-Xyl, GDP-Glucose (GDP-Glc), GDP-Fuc, and GDP-Man).

Comparisons with the specific UDP-Gal/UMP activity of UDP-GalT3 showed that neither KVAG1 nor KVAG2 presented high specific transport rates for any of the nucleotide sugars tested (Figure 29). The exchange of nucleotide sugars for radiolabeled monophosphates in KVAG liposomes ranged between 1.5 and 11 nmol/min, compared to >25 nmol/min in UDP-GalT3 proteoliposomes (Figure 29).

UMP or GMP unitransport was also not significantly high in liposomes containing KVAG proteins. The transport of most nucleotide sugars by KVAG1 and KVAG2 did not significantly surpass the background transport activities (compared to the empty vector, Figure 29). The exceptions were transport of UDP-GlcA/UMP and GDP-Fuc/GMP by KVAG2. In both cases, the KVAG2 transport of these nucleotide sugars represented a two fold increase compared to the same substrates transported by proteins from yeast transformed with the empty vector (Figure 29). However, the significance of these data is affected by considerable experimental variability, indicated by high standard deviation ( $sd \pm 4.32$ ). Thus, the evidence supporting UDP-GlcA/UMP mediated transport by KVAG2 is weak. However, the transport experiment of GDP-Fuc/GMP by KVAG2 yielded a 2.5 fold increase compared to the empty vector ( $sd \pm 1.2$ ), although this activity is still low compared to the positive control UDP-GalT3 (Figure 29).

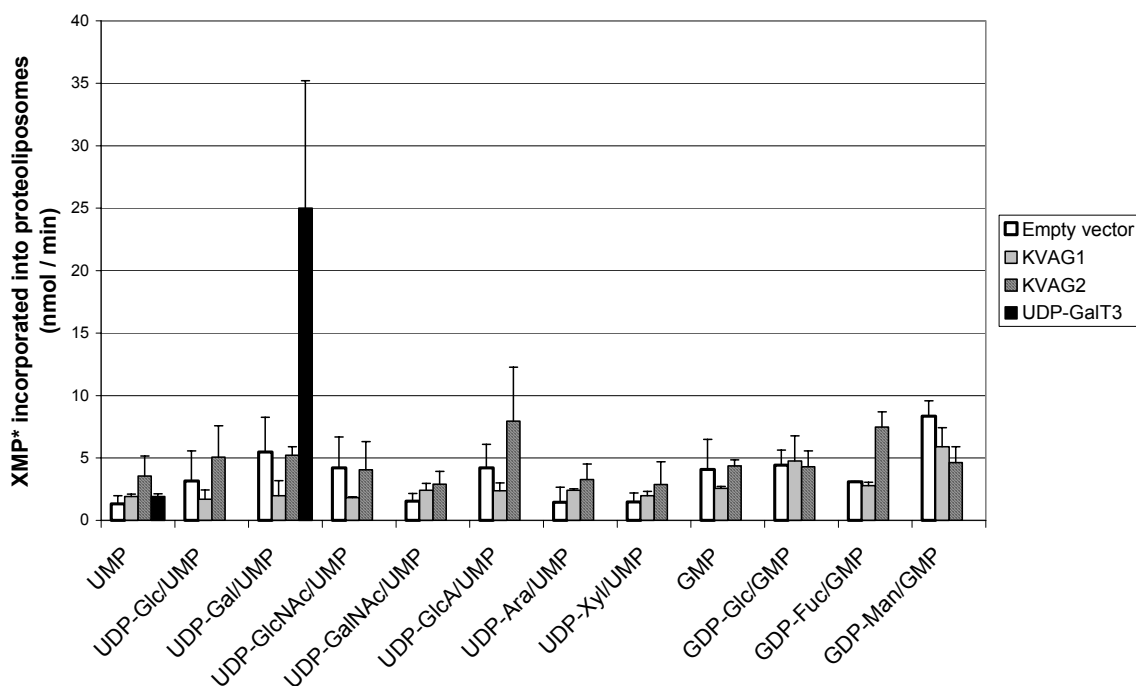


**Figure 29.** Transport activity of nucleotide sugars by KVAG1 and KVAG2 reconstituted into liposomes.

n = two to four independent experiments. XMP\* =  $^{33}\text{P}$  radio-labeled UMP and GMP.

### 3.5.2.3 Measurements of Transport Activity Using Purified KVAG2 Protein Reconstituted into Liposomes

The KVAG2 protein overexpressed in yeast membranes and reconstituted into liposomes showed slight GDP-Fuc/GMP and UDP-GlcA/UMP transport activities. To verify this, the KVAG2 protein was isolated from yeast membrane proteins by affinity chromatography on Ni-NTA agarose matrix. Analysis of the flow-through, wash and elution fractions by SDS-PAGE confirmed efficient KVAG2 purification to homogeneity (Figure 30). The isolated protein was reconstituted into liposomes and used for transport activity measurements of nucleotide sugars. The results from these experiments reduced the background transport especially for radiolabeled GMP uptake (Figure 31). However, the transport of UDP-GlcA/UMP ( $1.55 \pm 0.39$  nmol/min) and GDP-Fuc/GMP ( $1.87 \pm 1.39$  nmol/min) did not reach the levels observed in the whole membrane protein liposomes ( $7.94 \pm 4.32$  and  $7.48 \pm 1.2$  nmol/min, respectively, Figure 29). Transport of UDP-GlcA and GDP-Fuc was minimal and showed no difference with other nucleotide sugar transport activities (Figure 31). Moreover, the incorporated radioactivity in KVAG2 proteoliposomes remained ten times lower than the radiolabeled UMP measured in liposomes containing the purified UDP-GalT3. Thus, these results indicate that KVAG2 does not significantly transport UDP-GlcA, GDP-Fuc and no other nucleotide sugar in the conditions tested.

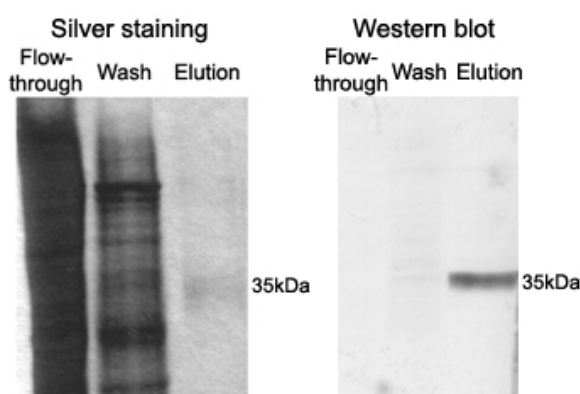


**Figure 30.** SDS-polyacrylamide gel electrophoresis analysis of purified KVAG2.

Analysis of the flow-through, wash and elution fractions obtained during KVAG2 Ni-NTA protein purification. 12% SDS polyacrylamide gel stained with silver nitrate and corresponding western blot.

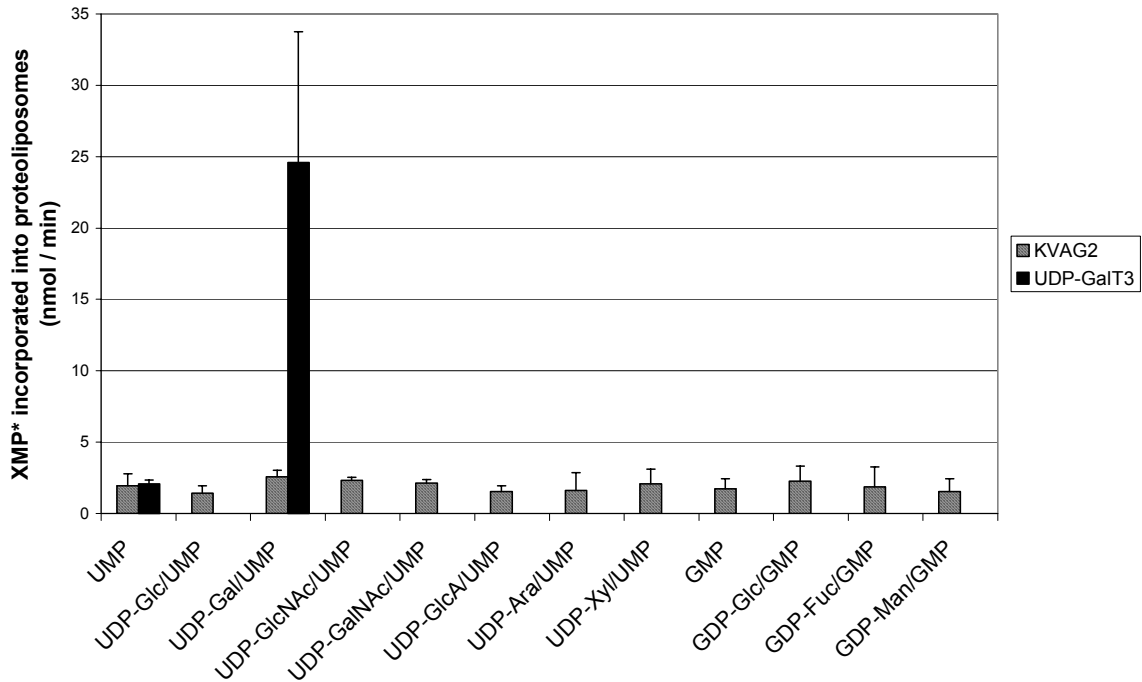


**Figure 31.** Transport activity of nucleotide sugars by purified KVAG2 reconstituted into liposomes.

KVAG2, n = at least two independent experiments; UDP-GalT3, n = three independent experiments. XMP\* =  $^{33}\text{P}$  radio-labeled UMP and GMP.

### 3.5.2.4 Measurements of Transport Activity Using Yeast Golgi Vesicles Enriched with KVAG Proteins

The low substrate transport activity observed by the KVAG proteins might be a consequence of denaturing conditions used in the process of proteoliposome preparation. The action of detergents, used to separate proteins from the yeast membranes, might affect the three dimensional structure of the protein and thus impair its functional properties. To omit this potentially unfavorable step, the Golgi-rich microsomal fractions from yeast cells overexpressing the recombinant proteins were isolated and used for transport measurements.

Initially, import of the radiolabeled nucleoside monophosphates, UMP and GMP, into Golgi vesicles was measured. High concentration (20  $\mu\text{M}$ ) of these two substrates in the external solution was expected to induce a transporter mediated influx towards the lumen of the Golgi vesicles. However, the UDP-GalT3, KVAG1

and KVAG2 microsomal vesicles did not show increase in UMP or GMP uptake in comparison to control vesicles (empty vector, Figure 32). There was a general increase in UMP and GMP uptake in the microsomes when compared to the import measured in the proteoliposomes method (compare Figures 29 and 32), also detectable in the empty vector Golgi vesicles. Therefore, this increase in nucleoside monophosphates uptake appears to be the result of higher amounts of endogenous yeast Golgi-membrane associated proteins rather than to the actual activity of NST/pPT transporters.

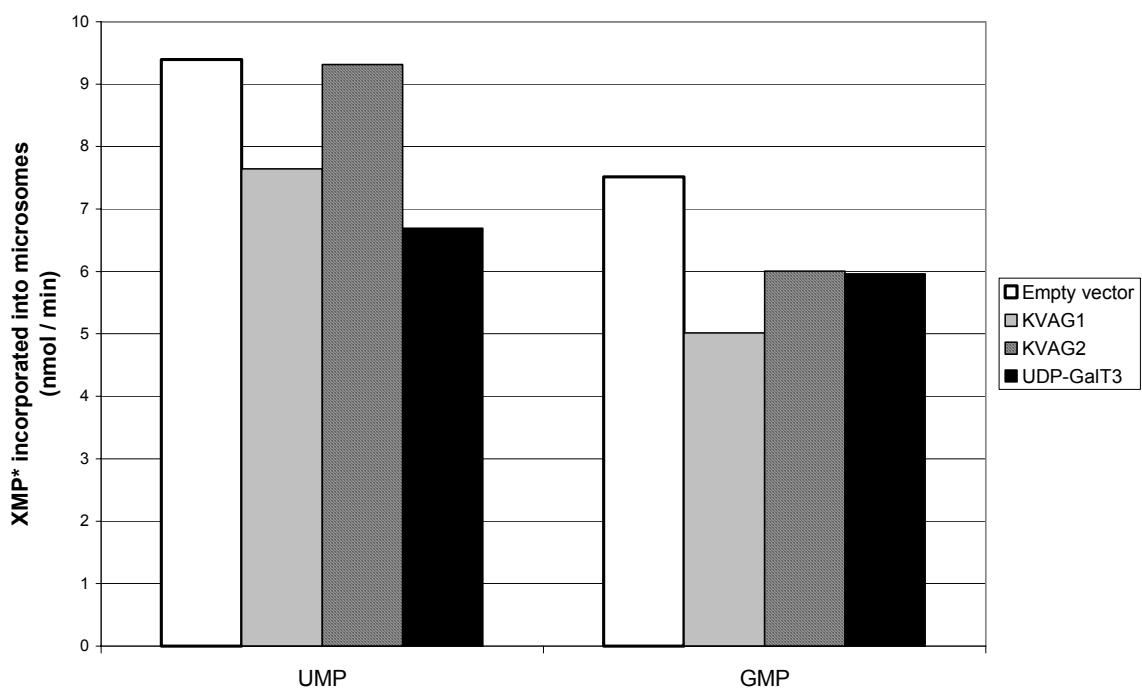


**Figure 32.** Uptake of nucleoside monophosphates into Golgi microsomal vesicles enriched with KVAG proteins.

Data from one representative experiment. XMP\* =  $^{33}\text{P}$  radio-labeled UMP and GMP.

Most nucleotide sugars naturally occur in the cytoplasm but are needed in the lumen of the ER and Golgi for glycosylation of different molecules. The uptake of nucleotide sugars into the Golgi apparatus has been shown in several cases as the result of exchanging these substrates with luminal nucleoside monophosphates (Capasso and Hirschberg, 1984; Segawa *et al.*, 2005). Because the experiments performed here used the radiolabeled nucleoside monophosphates as substrates, availability of the specific counter-substrates (the

nucleotide sugars) in the luminal side became a major constraint for measuring KVAG transport activity. This fact may explain why UMP import by UDP-GalT3 imbibed in Golgi membranes did not reflect its high UDP-Gal/UMP transport activity (compare with measurements in proteoliposomes transport, Figures 29 and 31). To circumvent this limitation, preloading of the UDP-GalT3 and control microsomal vesicles with UDP-Gal was assayed. Transport measurements were performed by incubating the preloaded Golgi microsomes with the radiolabeled UMP (Figure 33).

The nucleotide sugar preloading treatment of Golgi vesicles (brief sonication of microsomes in the presence of UDP-Gal, followed by high speed centrifugation and microsomal pellet resuspension) had negative consequences for uptake of radiolabeled UMP. This was evident by nearly 50% reduction of incorporated substrate in both the control and UDP-GalT3 vesicles (“Sonicated” in Figure 33). Nevertheless, Golgi vesicles preloaded with UDP-Gal recovered UMP uptake to untreated levels (“Sonicated+UDP-Gal/UMP” in Figure 33). This implied that preloading with the nucleotide sugar induced UDP-Gal/UMP transport to a certain extent although there were no significant differences between control and UDP-GalT3 enriched Golgi vesicles (Figure 33).

The amount of radiolabeled UMP transported inside UDP-GalT3 vesicles was more than threefold below the activity observed for the same UDP-GalT3 protein when isolated from the Golgi microsomes and reconstituted into liposomes (“Liposomes+UDP-Gal/UMP” in Figure 33). This fact indicates that the stability and integrity of the proteins within the Golgi membranes were conserved, and hence, their potential functions. However, employing a radiolabeled nucleoside monophosphate as the measurable substrate of transport appears to be inadequate in this microsomal system. The microsomal vesicles contain the Golgi machinery and carrier proteins in a natural manner. Consequently, the preloaded UDP-Gal is most likely used inside the Golgi by endogenous glycosyltransferases, again depleting the luminal source of counter-substrate. Moreover, after galactose release, UDP is likely dephosphorylated increasing the luminal pool of UMP and thus preventing external UMP uptake. A more direct way to assess the putative

nucleotide sugar transport of these proteins would require the use the classical radiolabeled nucleotide sugars as the import substrates into the vesicles.

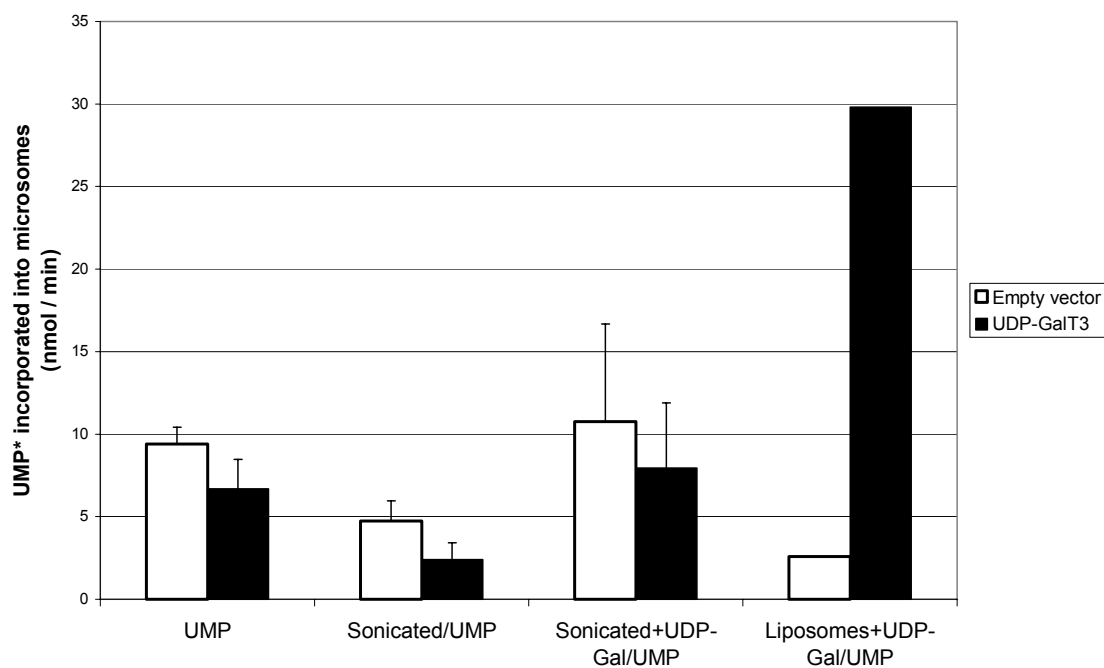


**Figure 33.** Uptake of UMP into UDP-GalT3 enriched Golgi vesicles preloaded with UDP-Gal.

n = three independent experiments (except for Liposomes+UDP-Gal/UMP where one representative experiment was performed). UMP\* = <sup>33</sup>P radio-labeled UMP.

## 4. Discussion

Recently, many uncharacterized proteins from different organisms have been identified based on sequence similarities to NSTs and pPTs (Berninsone *et al.*, 2001; Norambuena, *et al.*, 2002; Baldwin *et al.*, 2001; Knappe *et al.*, 2003a; Handford *et al.*, 2004; Bakker *et al.*, 2005). These proteins share common structural features like protein size, number of TMDs, and distribution and conservation of putative substrate binding residues (Jack *et al.*, 2001; Martinez-Duncker *et al.*, 2003; Knappe *et al.*, 2003a). Still, very little is known about the substrates they transport and their physiological function. Among these new NST/pPT homologous proteins, the KVAG1 and KVAG2 proteins, grouped within the KV/A/G subfamily of *Arabidopsis* proteins, are the only ones presenting putative plastid targeting sequences. Members of the pPT subfamily, the closest homologues of the KVAG proteins, are transporters of the inner membrane of plastids that perform the relocation of carbon metabolites (e.g. triose phosphate, phosphoenolpyruvate, glucose-6-phosphate) between the cytosol and plastids (Flügge, 1999; Flügge *et al.*, 2003; Weber *et al.*, 2005). The proposed function of the KVAG1 and KVAG2 proteins in plastids was to mediate the import of lipid precursors, like nucleotide sugars or sugar phosphates, used for the synthesis of plastid exclusive lipids like MGDG, DGDG or SQDG (Knappe *et al.*, 2003a). These precursors are likely synthesized in the cytosol (Coates *et al.*, 1980; Bonin *et al.*, 1997), which requires an import mechanism to supply the machinery of lipid synthesis in plastids with the appropriate substrates.

### Expression and Cellular Localization of the KVAG Proteins

KVAG1 and KVAG2 contain amino terminal extensions that were predicted as plastidial targeting sequences by three prediction programs: TargetP\_v1, ChloroP\_v1.1, and PCLR\_v0.9 (data compiled in Aramemnon database, Schwacke *et al.*, 2003). However, *in planta* transient expression of chimeras, where GFP was fused to the full cDNA of KVAG1 and KVAG2, did not result in plastid labeling (Figure 23). Instead, highly motile small vesicles were GFP labeled across the cytoplasm. The predicted plastid signals in KVAG1 and KVAG2 contain high frequency of serine/threonine and basic residues, features generally found in



prototype transit peptides (Schein *et al.*, 2001; Nassoury and Morse, 2005). However, related proteins from other species like rice (*Oryza sativa*) did not display plastidic targeting signals. Furthermore, the predicted KVAG plastid signals are shorter (20-35 less residues) in comparison to the targeting peptides from the known pPTs. Expression *in planta* of one of these predicted signals, the KVAG2 signal fused to GFP, also did not render specific plastid labeling (Figure 21), thus indicating that this amino terminal extension is not functional as a plastidial targeting sequence.

The numerous small vesicles observed in tobacco cells transiently expressing the KVAG::GFP fusion proteins formed a dotted pattern that resembled that of proteins localizing to the Golgi apparatus (Figure 23). This was inferred from the comparison with the expression pattern of a mammalian ST fused to GFP in tobacco cells. Furthermore, treatment with BFA displayed similar organellar sensitivity in 35S-KVAG::GFP and 35S-ST::GFP expressing cells, that revealed severe distortion of the dotted GFP pattern. Upon BFA treatment, the GFP labeled compartment formed clear aggregates that got dispersed through the cytoplasm after prolonged exposure to the toxin (Figure 24). This is in accordance with the reported effects of BFA in the Golgi apparatus of plant cells. BFA causes the loss of Golgi stacks as the result of continuous maturation of the *trans*-Golgi vesicles and the apparent fusion between the *cis*-Golgi with the ER (Ritzenthaler *et al.*, 2002; Baldwin *et al.*, 2001; Handford *et al.*, 2004; Norambuena *et al.*, 2005). BFA treatment prevents the formation of new *cis*-Golgi from budding vesicles from the ER, it therefore it appears as if the Golgi apparatus blends to the ER (Nebenfuhr *et al.*, 2002). Hence, the organelle behaviour in transfected tobacco cells treated with BFA confirmed localization of KVAG1 and KVAG2 proteins in the Golgi apparatus.

Two additional members of the KV/A/G subfamily, GONST5 and UDP-GalT1, were previously reported to be located in the Golgi membranes. GONST5 fused to GFP, co-localized with GONST1::YFP in onion epidermal cells. In addition, the dotted pattern of expression of GONST5 was sensitive to BFA (Handford *et al.*, 2004). UDP-GalT1 was indirectly shown to be expressed in the Golgi apparatus by complementation of CHO-Lec8 mutant cells defective in UDP-Gal import to the

Golgi lumen. UDP-Gal uptake experiments performed with Golgi microsomal fractions isolated from yeast cells expressing UDP-GalT1 also supported the Golgi localization of this protein (Bakker *et al.*, 2005). In the present study the remaining proteins of the KV/A/G subfamily, KVAG3, KVAG4 and KVAG5, fused to GFP, revealed similar patterns of Golgi localization *in planta* (Figure 23). Furthermore, the GFP labeled organelle also showed sensitivity to BFA (Figure 24). This strongly indicates that all members from the KV/A/G subfamily of NST/pPT homologous proteins are localized in the Golgi apparatus.

### **KVAG Transport of Nucleotide Sugars and Other Substrates**

During the last five years several plant NSTs have been identified, most of them are localized in the Golgi membranes (Baldwin *et al.*, 2001; Norambuena *et al.*, 2002; Handford *et al.*, 2004; Bakker *et al.*, 2005; Norambuena *et al.*, 2005). They are most likely involved in the supply of nucleotide sugars for the modification of different glycoconjugates. The substrate affinities of these transporters were typically determined by analysis of the nucleotide sugar uptake in microsomal Golgi fractions enriched with the NST. Because of its low background transport of nucleotide sugars, except for GDP-Man and UDP-Glc (Berninsone *et al.*, 1997; Norambuena *et al.*, 2002, Bakker *et al.*, 2005), yeast has been chosen as a suitable heterologous system of NST protein analysis. However, the presence of additional endogenous proteins, like multifunctional glycosyltransferases, might interfere in the determination of the NSTs transport activity (Handford *et al.*, 2004; Segawa *et al.*, 2005). This limitation can be overcome by performing transport experiments using phosphatidylcholine vesicles that contain the isolated membrane proteins (proteoliposomes). This system facilitates the manipulation of both, substrate and counter-substrate concentrations, without interference from additional transporters and metabolic enzymes (i.e. glycosyltransferases or pyrophosphatases). This technique has been successfully applied to determine the substrate specificity of LPG2 in *Leishmania donovani* (Segawa *et al.*, 2005), the rat UDP-GalNAc and GDP-Fuc transporters (Puglielli *et al.*, 1999; Puglielli and Hirschberg, 1999) and that of different pPTs (Loddenkötter *et al.*, 1993; Fischer *et al.*, 1997; Eicks *et al.*, 2002; Knappe *et al.*, 2003b).

UDP-GalT3 was recently discovered as a NST with high affinity for UDP-Gal/UMP transport (Rollwitz *et al.*, *in prep.*, Figures 27 and 31). The experimental setting for functional characterization of UDP-GalT3 used proteoliposomes preloaded with UDP-Gal in exchange with external radiolabeled UMP. This substrate setting is opposite to the one used by Segawa and collaborators (2005), as they measured the LPG2 import of radiolabeled nucleotide sugars in exchange for the nucleoside monophosphates. These experimental settings and their corresponding results confirm the notion that the membrane proteins are randomly incorporated into liposomes, some facing the inside and some facing the outside of the vesicles (Segawa *et al.*, 2005). Thus, the transport of substrates across liposomal membranes occurs in both directions, and labeling of either the nucleotide sugar or the monophosphate is therefore suitable for measuring protein transport activity.

The Golgi localized KVAG1 and KVAG2 proteins might function as NSTs, as shown for their close homologues GONST5, UDP-GalT1, UDP-GalT2 and UDP-GalT3 (Handford *et al.*, 2004; Bakker *et al.*, 2005; Rollwitz *et al.*, *in prep.*). Moreover, the *KVAG1* and *UDP-GalT3* genes were recently found to co-express with primary cell wall and cellulose biosynthesis related genes (i.e. *cellulose synthase 1, 3 and 6*) (Persson *et al.*, 2005). Plant primary cell wall components include polysaccharides and glycoproteins that are highly glycosylated. It is therefore assumed that high amounts of nucleotide sugars are needed inside the Golgi cisternae to support glycosylation (Fry, 2004). However, when proteoliposomes containing KVAG1 were subjected to transport experiments with nucleotide sugars, no specific affinity for any of the substrates was observed (Figure 29). Experiments with KVAG2 reconstituted into liposomes presented similar results (Figures 29 and 31). No significant transport activity was detected for either protein when using UDP-Glc, UDP-Gal, UDP-GlcNAc, UDP-GalNAc, UDP-GlcA, UDP-Ara, UDP-Xyl, GDP-Glc, GDP-Fuc or GDP-Man in exchange to the corresponding nucleoside monophosphates.

These results raised three crucial functional and methodological questions: Are the functional properties of the KVAG proteins severely affected during the process of protein solubilization and reconstitution into liposomes, thus impairing proper function? Do the two KVAG proteins transport different substrates that were not

included in the previous assays? Are there cofactors or protein partners missing in the liposome artificial system that prevent full activity of the KVAG proteins?

In principle, it is reasonable to think that the KVAG proteins reconstituted into liposomes still conserve their functional characteristics based on comparisons with successful functional characterizations of related proteins (i.e. pPTs, LPG2 and UDP-GalT3) (Loddenkötter *et al.*, 1993; Fischer *et al.*, 1997; Eicks *et al.*, 2002; Segawa *et al.*, 2005; Rollwitz *et al.*, *in prep.*). However, the failed attempts to measure KVAG activity in isolated microsomal vesicles using radiolabeled monophosphates (Figures 32 and 33), did not disclose if protein solubilization with detergents, prior to proteoliposomes generation, interfered with the stability and functional properties of the KVAG proteins. As inferred from the control experiments with UDP-GalT3, the direct microsomal nucleotide sugar transport can only be performed using the radiolabeled nucleotide sugars. This approach is therefore limited to substrates available as radiolabeled compounds.

The investigation of the T-DNA insertional mutants suggested other possible substrates transported by KVAG1 and KVAG2. Analyses of leaf lipids from the *kvag1-1* and *kvag2-1* knock-out mutants revealed a small but significant reduction in the phospholipids content (Figure 16) accompanied by reductions in C18 fatty acid chains (Table 4). This phenotype indicated a possible deficiency in the synthesis of lipids that originate from the eukaryotic biosynthesis pathway. A decreased supply of the phospholipid precursors CDP-choline and/or CDP-ethanolamine to the endomembrane lumen (i.e. ER), in the absence of specific transporters, might explain the reduced content of phospholipids in the mutants. However, the transport of these additional substrates, CDP-choline and CDP-ethanolamine, by the KVAG2 protein in liposomes was low (~1.5 nmol/min). CDP-ethanolamine/CMP transport was higher in KVAG2 proteoliposomes than in the control proteoliposomes (Figure 28), but the values were still very close to the unitransport of CMP displayed by the control. This indicates that KVAG2 alone does not present specificity for phospholipids precursors under these conditions. These findings also correlate with the association of this protein to the Golgi apparatus instead of the membranes of the ER.

Like KVAG2, KVAG1 was also present in the Golgi membranes and not the ER (Figure 23). The analysis of transport of CDP-choline and CDP-ethanolamine by this protein is nevertheless interesting since this carrier is expressed in actively developing organs where phospholipids and other components are highly needed for new membrane formation. This putative function of KVAG1 is also suggested by the pronounced dwarfism and retarded development observed in *pho1.2* plants that additionally lack KVAG1 (Figure 18). Reduction of phospholipids from the cell membranes and corresponding functional replacement (to a limited extent) by non-phosphorous galactolipids and sulfolipids, represents one of the numerous adaptations that plants have evolved to sustain survival under low phosphate availability (Essigmann *et al.*, 1998; Doermann and Benning, 2002; Poirier and Bucher, 2002). Thus, the putative involvement of KVAG1 in phospholipid synthesis would impose further restrictions in the formation of new membranes (and overall plant growth) in the *pho1.2* phosphate deprived shoots. However, analysis of the single *kvag1-1* mutant grown under phosphate limitation showed plant architecture and development indistinguishable from wild type plants grown under identical conditions (Figure 19). Furthermore, the regulation of *KVAG1* gene expression was not associated to phosphate depletion in the medium (Figure 20). These observations indicate that even if the KVAG1 transporter is involved in phospholipid biosynthesis it is not essential for this metabolic pathway.

Whether NSTs require additional cofactors or protein partners for proper function is still obscure. However, experiments with LPG2 proteoliposomes and presence/absence of  $Mg^{2+}$  and  $Mn^{2+}$  in the assay buffer, showed that the transport of GDP-Man was unaffected by these ions (Segawa *et al.*, 2005). Another NST, the yeast VRG4, also does not require metal ions for its activity (Gao *et al.*, 2001). Furthermore, Segawa and collaborators (2005) showed that the higher uptake of nucleotide sugars detected in Golgi microsomes incubated with  $Mg^{2+}$  was due to the presence of endogenous protein contaminants (i.e. glycosyltransferases). Thus, it appears that NSTs do not require metal ions to perform transport.

Although C-terminal protein tags have been speculated to be detrimental for the activity or assembly of proteins complexes like in the case of NSTs, the KVAG proteins were extended by a C-terminal histidine-tag to facilitate their recognition

and isolation. In a similar manner, the LPG2 and all plant NSTs that have been functionally characterized until now were attached to C-terminal tags (Segawa *et al.*, 2005; Rollwitz *et al.*, *in prep.*; Norambuena *et al.*, 2002; Handford *et al.*, 2004; Bakker *et al.*, 2005; Norambuena *et al.*, 2005). Thus, it does not seem likely that the histidine C-terminal extension interferes with KVAG transport assembly and/or activity. The possibility that KVAG1 and KVAG2 require additional protein partners for proper function (formation of functional heterodimers) is not very likely, considering the fact that the NSTs identified so far seem to work as homodimers. However, it cannot be completely ruled out. Testing this possibility in the future would involve carefully designed transport experiments in which two proteins are reconstituted together in the same liposomes. Putative partners should be chosen following criteria like expression patterns *in planta* rather than sequence identity, as it was shown that closely related proteins might be expressed in different organs.

### **KVAG Mutant Analyses**

*Arabidopsis* T-DNA insertion knock-out plants were identified for six of the genes of the KV/A/G subfamily. Under ambient conditions, the single gene mutants and individual plants with double *kvag1-1 x kvag2-1* gene knock-outs presented similar developmental and morphological characteristics in comparison to the wild type. Furthermore, the phenotype of the *kvag1-1* and *kvag2-1* single mutants grown on limited phosphate availability also resembled that of the wild type under the same stress conditions (Figure 19). As mentioned above, a potential defect in the synthesis of phospholipids in single *kvag1-1* and *kvag2-1* mutant plants was detected only through analyses of their lipid composition. One hypothesis is that KVAG1 and KVAG2 are transporters of the phospholipids precursors in the ER, but so far there is no functional evidence to support this possibility. Moreover, these proteins were found to localize in the Golgi apparatus, whereas the proposed function mainly takes place at the ER (Dowhan, 1997; Buchanan *et al.*, 2000).

Most of the currently known NSTs are involved in the glycosylation of cell wall polysaccharides and glycoproteins in the Golgi apparatus (Ma *et al.*, 1997;

Hirschberg *et al.*, 1998; Baldwin *et al.*, 2001; Norambuena *et al.*, 2002; Handford *et al.*, 2004; Norambuena *et al.*, 2005). In this respect, quantitative analyses of the cell walls components from the different *Arabidopsis* mutants might reveal deficiencies in glycosyl residues and therefore provide insights on the putative substrate(s) of the corresponding NSTs.

## 5. Conclusion

The characterization of several NSTs and pPTs proteins in animals, fungi and plants and the recent sequencing of genomes allowed the identification of new NST/pPT homologous proteins in different organisms. The newly identified putative proteins show similar structural characteristics to known NSTs and pPTs, including the number and distribution of TMDs and several conserved residues. Only few of these novel proteins have been characterized, and all are functional NSTs localized on the Golgi apparatus. In *Arabidopsis* there is a high number of these NST/pPT like proteins (more than 40 members) and functional studies have been performed for only a few of them. The majority of the *Arabidopsis* NST/pPT homologous proteins split into three subfamilies according to sequence similarity: the KT, KD and KV/A/G subfamilies. Recent work led to the identification of two members of the KT and two of the KV/A/G subfamilies as UDP-Gal and GDP-Man transporters. Interestingly, two proteins from the KV/A/G subfamily, KVAG1 and KVAG2, contain predicted plastid targeting signals and therefore were thought to transport nucleotide sugars to the lumen of plastids, supplying the sugar donors for specific plastidial lipid glycosylation.

Expression of the cDNA of the two putative plastidic proteins, fused to GFP, in plant cells revealed the localization of both proteins in the Golgi apparatus and not in plastids. This was further confirmed by comparisons with the Golgi specific labeling pattern displayed by 35S-ST::GFP and the sensitivity to BFA of the labeled organelle. Similar expression studies revealed that all members of the KV/A/G family are located in the membranes of the Golgi apparatus. In accordance with the proteins intracellular localization and their putative role, the KVAG1 and KVAG2 mediated transport of different nucleotide sugars was assayed, after heterologous protein expression in yeast and reconstitution into liposomes. In these experiments no significant transport activity was detected for any of the substrates tested. It is unlikely that the functional properties of these proteins are affected through protein solubilization and liposome preparation, as the UDP-GalT3 displayed high transport rates of UDP-Gal, and other homologous proteins have also been studied following the same approach (LPG2, members of



the pPT). Therefore, different substrates must be transported by the KVAG1 and KVAG2 proteins.

The analysis of leaf lipids from the single mutants *kvag1-1* and *kvag2-1* revealed a small reduction on the phospholipid levels. This suggested the putative involvement of KVAG1 and KVAG2 in the synthesis of phospholipids. Phospholipids are mainly synthesized in the lumen of the ER, and require the import from the cytosol of the phospholipid precursors CDP-choline and CDP-ethanolamine. The phospholipid precursor molecules are similar to the nucleotide sugars and possible substrates for NST/pPT homologous proteins. However, transport experiments with KVAG2 and CDP-choline and CDP-ethanolamine as substrates did not show significant transport activity. The experiments have not been performed with KVAG1 yet, but these are of great interest as the lack of this protein in the *pho1.2* phosphate shoot deficient mutant showed a more severe dwarfish phenotype and delay in development. Because the *KVAG1* gene is more or less ubiquitously expressed in developing organs, the lack of it might cause considerable alterations in the growth and development of the double *pho1.2 x kvag1-1* mutant. The knock-out mutants for the other members of the KV/AG subfamily, *kvag3-1*, *kvag4-1*, *kvag5-1* and *ugt1-1*, did not show major differences in phenotype and performance compared to the wild type.

**6. Abbreviations**

A	Ampere
<i>A. tumefaciens</i>	<i>Agrobacterium tumefaciens</i>
aa	amino acids
AGI	<i>Arabidopsis</i> Genome Initiative number
APS	Ammonium persulphate
<i>Arabidopsis</i>	<i>Arabidopsis thaliana</i>
AtUTr1 & 2	<i>Arabidopsis</i> UDP-Glucose transporter 1 & 2
BCIP	5-Bromo-4-chloro-3-indoylphosphate
BFA	Brefeldin A
bp	base pairs
BSA	Bovine serum albumin
BY2	Bright yellow 2
°C	Centigrade
cDNA	complementary DNA
CHO-Lec8	Chinese hamster ovary cell line deficient in UDP-Gal transport into the Golgi
cm	centimetre
CMP	Citidine monophosphate
CMP-Sia	CMP-Sialic acid
Col-0	Columbia 0
CSPD	Disodium 3-[4-methoxyspiro {1, 2-dioxetane-3, 2'-(5'chloro) tricyclo [3.3.1.1 <sup>3,7</sup> ] decan} -4-yl] phenyl phosphate
DNA	Desoxyribonucleic acid
dd	double distilled
DEPC	Diethylpyrocarbonate
DGDG	Digalactosyl-diacylglycerol
DM	n-Dodecyl- $\beta$ -D-maltoside
Dm	<i>Drosophila melanogaster</i>
DMF	Dimethylformamide
DMSO	Dimethyl-sulfoxide
dNTPs	deoxynucleotides
DOC	Deoxycholate
DTT	Di-thiotreitol
<i>E. coli</i>	<i>Escherichia coli</i>
EDTA	Ethylendiaminetetraacetic acid
ER	Endoplasmic reticulum
ESTs	Expressed sequenced tags
GDP-Ara	Guanidin diphosphate-Arabinose
GDP-Fuc	Guanidin diphosphate-Fucose
GDP-Glc	Guanidin diphosphate-Glucose
GDP-Man	Guanidin diphosphate-Mannose
GFP	Green fluorescent protein
GMP	Guanidin monophosphate
GONST1 to 5	Golgi nucleotide sugar transporter 1 to 5
GPT	Glucose 6-phosphate/phosphate transporter
GUS	$\beta$ -glucuronidase
HEPES	N-2-Hydroxyethylpiperazin-N'-2-ethansulfonic acid
Hs	<i>Homo sapiens</i>

KD	Subfamily of NST/pPT homologous proteins
kDa	kiloDaltons
kg	kilograms
KT	A subfamily of NST/pPT homologous proteins
kV	kilovolt
KVAG	A subfamily of NST/pPT homologous proteins
LB	Luria-Bertani medium
Lm	<i>Leishmania mexicana</i>
M	molar
MES	4-Morpholinoethan-sulphonic acid
mg	milligram
MGDG	Monogalactosyl-diacylglycerol
μCi	microCurie
μF	micro Faraday
μg	microgram
μl	microlitre
min	minute
ml	millilitre
mM	millimolar
MOPS	(3-N-Morpholin)propan-sulfonic acid
mRNA	messenger RNA
MS	Murashige and Skog 10 medium
<i>N. benthamiana</i>	<i>Nicotiana benthamiana</i>
NAA	Naphthyl-acetic acid
NBT	p-Nitro-blue-tetrazolium-chloride
ng	nanogram
Ni-NTA	Ni <sup>2+</sup> -nitrilotriacetic acid
NST	Nucleotide sugar transporter
O/N	overnight
Ω	Ohm
ORF	Open reading frame
PCR	Polymerase chain reaction
PEG	Polyethylenglycol
Pi	Inorganic phosphate
PMSF	Phenyl-methyl-sulfonyl-fluoride
pPT	Plastidic phosphate transporter
PPT	Phosphoenolpyruvate-phosphate/phosphate transporter
RNA	Ribonucleic acid
rpm	Revolutions per minute
RT	Room temperature
RT-PCR	Reverse transcribed PCR
<i>S. cerevisiae</i>	<i>Saccharomyces cerevisiae</i>
SC	Synthetic complete medium
sd	Standard deviation
SDS	Sodium docecyl sulphate
SDS-PAGE	SDS-polyacrylamide gel electrophoresis
sec	seconds
Sp	<i>Saccharomyces pombe</i>
SQDG	Sufoquinovosyl-diacylglycerol
SSC	Tri-sodium citrate

---

TBS	Tris buffer saline
T-DNA	Transference DNA
TE	Tris/EDTA
Temed	N,N,N',N'-Tetramethylethyldiamine
TMD	Transmembrane domain
Tris	Tris-(hydroxymethyl)-aminomethan
TTP	Triose-phosphate/phosphate transporter
U	Units (enzymatic)
UDP-Ara	Uridine diphosphate-Arabinose
UDP-Gal	Uridine diphosphate-Galactose
UDP-GalT1 & 2	UDP-Galactose transporter 1 & 2
UDP-Glc	Uridine diphosphate-Glucose
UDP-GlcA	Uridine diphosphate-Glucuronic acid
UDP-GlcNAc	Uridine diphosphate-N-acetyl-glucuronic acid
UDP-Xyl	Uridine diphosphate-Xylose
UMP	Uridine monophosphate
UV	Ultraviolet
v/v	volume/volume
w/v	weight/volume
WT	Wild type
xg	times gravity
X-Gluc	D-Glucuronic acid
XPT	Xylulose-phosphate/phosphate transporter
YFP	Yellow fluorescent protein
YPD	Yeast extract peptone dextrose medium

## 7. References

**Abe, M., Noda, Y., Adachi, H., Yoda, K.** (2004) Localization of GDP-mannose transporter in the Golgi requires retrieval to the endoplasmic reticulum depending on its cytoplasmic tail and coatomer. *J. Cell Sci.* 117: 5687-5696.

**Abeijon, C., Chen, L.** (1989) Topography of glycosylation in yeast: Characterization of GDP-mannose transport and luminal guanosine diphosphatase activities in Golgi-like vesicles. *Proc. Natl. Acad. Sci. USA* 86: 6935-6939.

**Abeijon, C., Robbins, P.W., Hirschberg, C.B.** (1996) Molecular cloning of the Golgi apparatus uridine diphosphate-*N*-acetylglucosamin transporter from *Kluyveromyces lactis*. *Proc. Natl. Acad. Sci. USA* 93: 5963-5968.

**Alexander, M.P.** (1969) Differential staining of aborted and nonaborted pollen. *Stain Tech.* 44(3): 117-122.

**Alonso, J.M., Stepanova, A.N., Leisse, T.J., Kim, C.J., Chen, H., Shinn, P., Stevenson, D.K., Zimmerman, J., Barajas, P., Cheuk, R., Gadrinab, C., Heller, C., Jeske, A., Koesema, E., Meyers, C.C., Parker, H., Prednis, L., Ansari, Y., Choy, N., Deen, H., Geralt, M., Hazari, N., Hom, E., Karnes, M., Mulholland, C., Ndubaku, R., Schmidt, I., Guzman, P., Aguilar-Henonin, L., Schmid, M., Weigel, D., Carter, D.E., Marchand, T., Risseeuw, E., Brogden, D., Zeko, A., Crosby, W.L., Berry, C.C., Ecker, J.R.** (2003) Genome-Wide Insertional Mutagenesis of *Arabidopsis thaliana*. *Science* 301: 653-657.

**Aoki, K., Ishida, N., Kawakita, M.** (2003) Substrate recognition by nucleotide sugar transporters. Further characterization of substrate recognition regions by analyses of UDP-galactose/CMP-sialic acid transporter chimeras and biochemical analysis of the substrate specificity of parental and chimeric transporters. *J. Biol. Chem.* 278(25): 22887-22893.

**Ashikov, A., Routier, F., Fuhlrott, J., Helmus, Y., Wild, M., Gerardy-Schahn, R., Bakker, H.** (2005) The human solute carrier gene SLC35B4 encodes a

bifunctional nucleotide sugar transporter with specificity for UDP-xylose and UDP-N-Acetylglucosamine. *J. Biol. Chem.* 280(29): 27230-27235.

**Bakker, H., Routier, F., Oelmann, S., Jordi, W., Lommen, A., Gerardy-Schahn, R., Bosch, D.** (2005) Molecular cloning of two *Arabidopsis* UDP-galactose transporters by complementation of a deficient Chinese hamster ovary cell line. *Glycobiology* 15(2): 193-201.

**Baldwin, T.C., Handford, M.G., Yuseff, M.I., Orellana, A., Dupree, P.** (2001) Identification and characterization of GONST1, a Golgi-localized GDP-mannose transporter in *Arabidopsis*. *Plant Cell* 13: 2283-2295.

**Berendzen, K.W., Searle, I., Ravenscroft, D., Koncz, C., Batschauer, A., Coupland, G., Somssich, I.E., Uelker, B.** (2005) A rapid and versatile combined DNA/RNA extraction protocol and its application to the analysis of a novel DNA marker set polymorphic between *Arabidopsis thaliana* ecotypes Col-0 and *Landsberg erecta*. *Plant Methods* 1:4 doi:10.1186/1746-4811-1-4.

**Berninsone, P., Eckhardt, M., Gerardy-Schahn, R., Hirschberg, C.B.** (1997) Functional expression of the murine Golgi CMP-sialic acid transporter in *Saccharomyces cerevisiae*. *J. Biol. Chem.* 272: 12616-12619.

**Berninsone, P., Hwang, H.Y., Zemtseva, I., Horvitz, H.R., Hirschberg, C.B.** (2001) SQV-7, a protein involved in *Caenorhabditis elegans* epithelial invagination and early embryogenesis, transports UDP-glucuronic acid, UDP-N-acetylgalactosamine, and UDP-galactose. *Proc. Natl. Acad. Sci. USA* 98: 3738-3743.

**Birnboim, H.C., Doly, J.** (1979) A rapid alkaline extraction procedure for screening recombinant plasmid DNA. *Nucl. Acids. Res.* 7: 1513-1523.

**Blum, H., Beier, H., Gross, H.J.** (1987) Improved silver staining of plant proteins, RNA and DNA in polyacrylamide gels. *Electrophoresis* 8: 93-99.

**Bonin, C.P., Potter, I., Vanzin, G.F., Reiter, W.D.** (1997) The *MUR1* gene of *Arabidopsis thaliana* encodes an isoform of GDP-D-mannose-4,6-dehydratase, catalyzing the first step in the *de novo* synthesis of GDP-L-fucose. Proc. Natl. Acad. Sci. USA 94: 2085-2090.

**Buchanan, B.B., Gruissen, W., Jones, R.L. eds.** (2000) Biochemistry and Molecular Biology of Plants. American Society of Plant Physiologists.

**Capasso, J.M., Hirschberg, C.B.** (1984) Mechanisms of glycosylation and sulfation in the Golgi apparatus: evidence for nucleotide sugar/nucleoside monophosphate and nucleotide sulphate/nucleoside monophosphate antiports in the Golgi apparatus membrane. Proc. Natl. Acad. Sci. USA 81: 7051-7055.

**Chiaromonte, M., Koviach, J.L., Moore, C., Iyer, V.V., Wagner, C.R., Halcomb, R.L., Miller, W., Melançon, P., Kuchta, R.D.** (2001) Inhibition of CMP-sialic acid transport into Golgi vesicles by nucleoside monophosphates. Biochemistry 40: 14260-14267.

**Chung, C.T., Miller, R.H.** (1993) Preparation and storage of competent *Escherichia coli* cells. In R. Wu (ed.). Methods in Enzymology 218: 621-627.

**Clough, S.J., Bent, A.F.** (1998) Floral dip: a simplified method for *Agrobacterium*-mediated transformation of *Arabidopsis thaliana*. Plant J. 16: 735-743.

**Coates, S., Gurney, T., Sommers, L.W., Yeh, M., Hirschberg, C.B.** (1980) Subcellular localization of sugar nucleotide synthetases. J. Biol. Chem. 255: 9226-9229.

**Dean, N., Zhang, Y.B., Poster, J.B.** (1997) The *VRG4* gene is required for GDP-mannose transport into the lumen of the Golgi in the yeast *Saccharomyces cerevisiae*. J. Biol. Chem. 272: 31908-31914.

**Dörmann, P., Benning, C.** (2002) Galactolipids rule in seed plants. Trends Plant Sci. 7(3): 112-118.

**Dowhan, W.** (1997) Molecular basis for membrane phospholipids diversity: why are there so many lipids? *Annu. Rev. Biochem.* 66: 199-232.

**Eckhardt, M., Mühlenhoff, M., Bethe, A., Gerardy-Schahn, R.** (1996) Expression cloning of the Golgi CMP-sialic acid transporter. *Proc. Natl. Acad. Sci. USA* 93: 7572-7576.

**Eckhardt, M., Gotza, B., Gerardy-Schahn, R.** (1999) Membrane topology of the mammalian CMP-sialic acid transporter. *J. Biol. Chem.* 274(13): 8779-8787.

**Eggermont, K., Goderis, I.J., Broekaert, W.F.** (1996) High-throughput RNA extraction from plant samples based on homogenisation by reciprocal shaking in the presence of a mixture of sand and glass beads. *Plant Mol. Biol. Rep.* 14: 273-279.

**Eicks, M., Maurino, V., Knappe, S., Flügge, U-I., Fischer, K.** (2002) The plastidic pentose phosphate translocator represents a link between the cytosolic and the plastidic pentose phosphate pathways in plants. *Plant Physiol.* 128: 512-522.

**Essigmann, B., Güler, S., Narang, R.A., Linke, D., Benning, C.** (1998) Phosphate availability affects the thylakoid lipid composition and the expression of *SQD1*, a gene required for sulfolipid biosynthesis in *Arabidopsis thaliana*. *Proc. Natl. Acad. Sci. USA* 95: 1950-1955.

**Fischer, K., Kammerer, B., Gutensohn, M., Arbinger, B., Weber, A., Häusler, R., Flügge, U-I.** (1997) A new class of plastidic phosphate translocators: a putative link between primary and secondary metabolism by the phosphoenolpyruvate/phosphate antiporter. *Plant Cell* 9: 453-462.

**Fliege, R., Flügge, U.I., Werdan, K., Heldt, H.W.** (1978) Specific transport of inorganic phosphate, 3-phosphoglycerate and triosephosphates across the inner membrane of the envelope in spinach chloroplasts. *Biochim. Biophys. Acta* 502: 232-247.



- Flügge, U.I., Fischer, K., Gross, A., Sebald, W., Lottspeich, F., Eckerskorn, C.** (1989) The triose phosphate-3-phosphoglycerate-phosphate translocator from spinach chloroplasts: Nucleotide sequence of a full-length cDNA clone and import of the in vitro synthesized precursor protein into chloroplasts. *EMBO J.* 8: 39-46.
- Flügge, U.I.** (1998) Metabolite transporters in plastids. *Curr. Opin. Plant Biol.* 1: 201-206.
- Flügge, U.I.** (1999) Phosphate translocators in plastids. *Annu. Rev. Plant Physiol. Plant Mol. Biol.* 50: 27-45.
- Flügge, U.I., Häusler, R., Ludewig, F., Fischer, K.** (2003) Functional genomics of phosphate antiporter systems of plastids. *Physiol Plant* 118: 475-482.
- Forsbach, A., Schubert, D., Lechtenberg, B., Gils, M., Schmidt, R.** (2003) A comprehensive characterization of single-copy T-DNA insertions in the *Arabidopsis thaliana* genome. *Plant Mol. Biol.* 52(1): 161-176.
- Freeze, H.H.** (2001) Update and perspectives on congenital disorders of glycosylation. *Glycobiology* 11(12): 37G-38G.
- Fry, S.C.** (2004) Primary cell wall metabolism: tracking the careers of wall polymers in living plant cells. *New Phytologist* 161: 641-675.
- Gallagher, S.R. ed.** (1992) *GUS Protocols. Using the GUS gene as a reporter of gene expression.* Academic Press, Inc., San Diego, California.
- Gao, X.D., Dean, N.** (2000) Distinct protein domains of the yeast Golgi GDP-mannose transporter mediate oligomer assembly and export from the endoplasmic reticulum. *J. Biol. Chem.* 275: 17718-17727.

**Gao, X.D., Nishikawa, A., Dean, N.** (2001) Identification of a conserved motif in the yeast Golgi GDP-mannose transporter required for binding to nucleotide sugar. *J. Biol. Chem.* 276: 4424-4432.

**Gelvin, S.** (2003) *Agrobacterium*-mediated plant transformation: the Biology behind the "gene-jockeying" tool. *Microb. Mol. Biol. Rev.* 67(1): 16-37.

**Gerardy-Schahn, R., Eckhardt, M.** (2004) Nucleotide-sugar transporters. In Ernst, S., Hart, G.W., & Sinay, P. (Eds.), *Oligosaccharides in Chemistry and Biology: a comprehensive handbook Vol II Biology of saccharides*. Wiley, New York, pp. 19-36.

**Gilson, P.R., Vergara, C.E., Kjer-Nielsen, L., Teasdale, R.D., Bacic, A., Gleeson, P.A.** (2004) Identification of a Golgi-localised GRIP domain protein from *Arabidopsis thaliana*. *Planta* 219: 1050-1056.

**Hamburger, D., Rezzonico, E., Petétot, J.M.C., Somerville, C., Poirier, Y.** (2002) Identification and characterization of the *Arabidopsis PHO1* gene involved in phosphate loading to the xylem. *Plant Cell* 14: 889-902.

**Handford, M.G., Sicilia, F., Brandizzi, F., Chung, J.H., Dupree, P.** (2004) *Arabidopsis thaliana* expresses multiple Golgi localised nucleotide-sugar transporters related to GONST1. *Mol. Gen. Genet.* 272: 397-410.

**Hanke, G., Bowsher, C.G., Jones, M.N., Tetlow, I., Emes, M.J.** (1999) Proteoliposomes and plant transport proteins. *J. Exp. Bot.* 50: 1715-1726.

**Hirschberg, C.B., Robbins, P.W., Abeijon, C.** (1998) Transporters of nucleotide sugars, ATP, and nucleotide sulphate in the endoplasmic reticulum and Golgi apparatus. *Annu. Rev. Biochem.* 67: 49-69.

**Hirschberg, C.B.** (2001) Golgi nucleotide sugar transport and leukocyte adhesion deficiency II. *J. Clin. Invest.* 108(1): 3-6.

**Jack, D.L., Yang, N.M., Saier, M.H.Jr.** (2001) The drug/metabolite transporter superfamily. *Eur. J. Biochem.* 268: 3520-3629.

**Jefferson, R.A.** (1987) Assaying chimeric genes in plants: the *GUS* gene fusion system. *Plant Mol. Biol. Rep.* 5(4): 387-405.

**Kammerer, B., Fischer, K., Hilpert, B., Schubert, S., Gutensohn, M., Weber, A., Flügge, U.I.** (1998) Molecular characterization of a carbon transporter in plastids from heterotrophic tissues: the glucose 6-phosphate/phosphate antiporter. *Plant Cell* 10: 105-117.

**Kasahara, M., Hinkle, P.C.** (1977) Reconstitution and purification of the D-glucose transporter from human erythrocytes. *J. Biol. Chem.* 252(20): 7384-7390.

**Kawakita, M., Ishida, N., Miura, N., Sun-Wada, G.H., Yoshioka, S.** (1998) Nucleotide sugar transporters: elucidation of their molecular identity and its implication for future studies. *J. Biochem.* 123: 777-785.

**Kelly, A.A., Dörmann, P.** (2004) Green light for galactolipid trafficking. *Curr. Opin. Plant Biol.* 7: 262-269.

**Knappe, S., Flügge, U.I., Fischer, K.** (2003a) Analysis of the plastidic *phosphate translocator* gene family in *Arabidopsis* and identification of new *phosphate translocator*-homologous transporters, classified by their putative substrate-binding site. *Plant Physiol.* 131: 1178-1190.

**Knappe, S., Löttgert, T., Schneider, A., Voll, L., Flügge, U.I., Fischer, K.** (2003b) Characterization of two functional *phosphoenolpyruvate/phosphate translocator (PPT)* genes in *Arabidopsis*: *AtPPT1* may be involved in the provision of signals for correct mesophyll development. *Plant J.* 36: 411-420.

**Kyhse-Andersen, J.** (1984) Electrophoretic transfer of multiple gels: a simple apparatus without buffer tank for rapid transfer of proteins from polyacrylamide to nitrocellulose. *J Biochem. Biophys. Methods* 10(3-4): 203-209.

**Laemmli, U.K.** (1970) Cleavage of structural proteins during the assembly of the head of Bacteriophage T4. *Nature* 227: 680-685.

**Lee, M.H., Min, M.K., Lee, Y.J., Jin, J.B., Shin, D.H., Kim, D.H., Lee, K.H., Hwang, I.** (2002) ADP-ribosylation factor 1 of *Arabidopsis* plays a critical role in intracellular trafficking and maintenance of endoplasmic reticulum morphology in *Arabidopsis*. *Plant Physiol.* 129: 1507-1520.

**Loddenkötter, B., Kammerer, B., Fischer, K., Flügge, U.I.** (1993) Expression of the functional mature chloroplast triose phosphate translocator in yeast internal membranes and purification of the histidine-tagged protein by a single metal-affinity chromatography step. *Proc. Natl. Acad. Sci. USA* 90: 2155-2159.

**Lübke, T., Marquardt, T., Etzioni, A., Hartmann, E., von Figura, K., Körner, C.** (2001) Complementation cloning identifies CDG-IIc, a new type of congenital disorders of glycosylation, as a GDP-fucose transporter deficiency. *Nat. Genet.* 28: 73-76.

**Lühn, K., Wild, M.K., Eckhardt, M., Gerardy-Schahn, R., Vestweber, D.** (2001) The gene defective in leukocyte adhesion deficiency II encodes a putative GDP-fucose transporter. *Nat. Genet.* 28: 69-72.

**Ma, D., Russel, D.G., Beverley, S.M., Turco, S.J.** (1997) Golgi GDP-mannose uptake requires *Leishmania* LPG2. A member of a eukaryotic family of putative nucleotide-sugar transporters. *J. Biol. Chem.* 272(6): 3799-3805.

**Martinez-Duncker, I., Mollicone, R., Codogno, P., Oriol, R.** (2003) The nucleotide-sugar transporter family: a phylogenetic approach. *Biochimie* 85: 245-260.

- Miège, C., Maréchal, E., Shimojima, M., Awai, K., Block, M., Otha, H., Takamiya, K.I., Douce, R., Joyard, J.** (1999) Biochemical and topological properties of type A MGDG synthase, a spinach chloroplast envelope enzyme catalyzing the synthesis of both prokaryotic and eukaryotic MGDG. *Eur. J. Biochem.* 265: 990-1001.
- Millar, A.A., Smith, M.A., Kunst, L.** (2000) All fatty acids are not equal: discrimination in plant membrane lipids. *Trends Plant Sci.* 5(3): 95-101.
- Miura, N., Ishida, N., Hoshino, M., Yamauchi, M., Hara, T., Ayusawa, D., Kawakita, M.** (1996) Human UDP-galactose translocator: molecular cloning of a complementary DNA that complements the genetic defect of a mutant cell line deficient in UDP-galactose translocator. *J. Biochem. (Tokyo)* 120(2): 236-241.
- Nassoury, N., Morse, D.** (2005) Protein targeting to the chloroplasts of photosynthetic eukaryotes: Getting there is half the fun. *Biochim. Biophys. Acta* 1743: 5-19.
- Nebenführ, A., Ritzenthaler, C., Robinson, D.G.** (2002) Brefeldin A: Deciphering an enigmatic inhibitor of secretion. *Plant Physiol.* 130: 1102-1108.
- Niewiadomski, P., Knappe, S., Geimer, S., Fischer, K., Schulz, B., Unte, U.S., Rosso, M.G., Ache, P., Flügge, U.I., Schneider, A.** (2005) The *Arabidopsis* plastidic glucose 6-phosphate/phosphate translocator GPT1 is essential for pollen maturation and embryo sac development. *Plant Cell* 17: 760-775.
- Norambuena, L., Marchant, L., Berninsone, P., Hirschberg, C.B.** (2002) Transport of UDP-galactose in plants. Identification and functional characterization of AtUTr1, an *Arabidopsis thaliana* UDP-galactose/UDP-glucose transporter. *J. Biol. Chem.* 277(36): 32923-32929.
- Norambuena, L., Nilo, R., Handford, M., Reyes, F., Marchant, L., Meisel, L., Orellana, A.** (2005) AtUTr2 is an *Arabidopsis thaliana* nucleotide sugar transporter

located in the Golgi apparatus capable of transporting UDP-galactose. *Planta* 222: 521-529.

**Persson, S., Wei, H., Milne, J., Page, G.P., Somerville, C.R.** (2005) Identification of genes required for cellulose synthesis by regression analysis of public microarray data sets. *Proc. Natl. Acad. Sci. USA* 102(24): 8633-8638.

**Poirier, Y., Bucher, M.** (2002) Phosphate transport and homeostasis in *Arabidopsis*. In C.R. Somerville, E.M. Meyerowitz (Eds.). *The Arabidopsis Book*. American Society of Plant Biologists, Rockville, MD.  
<http://www.aspb.org/publications/arabidopsis>

**Reyes, F., Marchant, L., Norambuena, L., Nilo, R., Silva, H., Orellana, A.** (2006) AtUTr1, a UDP-glucose/UDP-galactose transporter from *Arabidopsis thaliana*, is located in the endoplasmic reticulum and up-regulated by the unfolded protein response. *J. Biol. Chem.* 281(14): 9145-9151.

**Ritzenthaler, C., Nebenführ, A., Movafeghi, A., Stussi-Graud, C., Behnia, L., Pimpl, P., Staehelin, L.A., Robinson, D.G.** (2002) Reevaluation of the effects of Brefeldin A on plants cells using tobacco Bright Yellow 2 cells expressing Golgi-targeted green fluorescent protein and COPI antisera. *Plant Cell* 14: 237-261.

**Ronen, G., Cohen, M., Zamir, D., Hirschberg, J.** (1999) Regulation of carotenoid biosynthesis during tomato fruit development: expression of the gene for lycopene epsilon-cyclase is down-regulated during ripening and is elevated in the mutant Delta. *Plant J.* 17(4): 341-351.

**Ros, F., Kunze, R.** (2001) Regulation of *Activator/Dissociation* transposition by replication and DNA methylation. *Genetics* 157: 1723-1733.

**Saiki, R.K., Bugawan, T.L., Horn, G.T., Mullis, K.B., Erlich, H.A.** (1986) Analysis of enzymatically amplified beta-globin and HLA-DQ alpha DNA with allele-specific oligonucleotide probes. *Nature* 324(6093): 163-166.

**Schein, A.I., Kissinger, J.C., Ungar, L.H.** (2001) Chloroplast transit peptide prediction: a peek inside the black box. *Nucleic Acids Res.* 29(16): E82.

**Schumacher, K., Vafeados, D., McCarthy, M., Sze, H., Wilkins, T., Chory, J.** (1999) The *Arabidopsis* det3 mutant reveals a central role for the vacuolar H<sup>+</sup>-ATPase in plant growth and development. *Genes Dev.* 13(24): 3259-3270.

**Schwacke, R., Schneider, A., Van der Graaf, E., Fischer, K., Catoni, E., Desimone, M., Frommer, W.B., Flügge, U.I.** (2003) ARAMEMNON: a novel database for *Arabidopsis* integral membrane proteins. *Plant Physiol.* 131: 16-26.

**Segawa, H., Soares, R.P., Kawakita, M., Beverley, S.M., Turco, S.J.** (2005) Reconstitution of GDP-mannose transport activity with purified *Leishmania* LPG2 protein in liposomes. *J. Biol. Chem.* 280(3): 2028-2035.

**Streatfield, S.J., Weber, A., Kinsman, E.A., Häusler, R.E., Li, J., Post-Beittenmiller, D., Kaiser, W.M., Pyke, K.A., Flügge, U.I., Chory, J.** (1999) The phosphoenolpyruvate/phosphate translocator is required for phenolic metabolism, palisade cell development and plastid-dependent nuclear gene expression. *Plant Cell* 11: 1609-1621.

**Tietje, C., Heinz, E.** (1998) Uridine-diphospho-sulfoquinovose:diacylglycerol sulfoquinovosyltransferase activity is concentrated in the inner membrane of chloroplast envelopes. *Planta* 206: 72-78.

**Wagner, R., Apley, E.C., Gross, A., Flügge, U.I.** (1989) The rotational diffusion of chloroplast phosphate translocator and of lipid molecules in bilayer membranes. *Eur. J. Biochem.* 182: 165-173.

**Ward, J.M.** (2001) Identification of novel families of membrane proteins from the model plant *Arabidopsis thaliana*. *Bioinformatics* 17: 560-563.

**Weber, A., Schwacke, R., Flügge, U.I.** (2005) Solute transporters of the plastid envelope membrane. *Annu. Rev. Plant Biol.* 56: 133-164.

**Weber, K., Osborn, M.** (1969) The reliability of molecular weight determination by sodium dodecyl sulphate-polyacrylamid gel electrophoresis. *J. Biol. Chem.* 244: 4406-4409.

**Zimmermann, P., Hirsch-Hoffmann, M., Henning, L., Gruissem, W.** (2004) GENEVESTIGATOR. *Arabidopsis* microarray database and analysis toolbox. *Plant Physiol.* 136: 2621-2632.



## 8. Appendix

### 8.1. Antibiotics

The identification of recombinant organisms was facilitated with the use of antibiotics for positive selection. Table 7 lists the different antibiotics and the conditions used.

**Table 7.** List of antibiotics employed to select transformed organisms.

Antibiotic	Organism	Stock (mg/ml)	Solvent	Final concentration (µg/ml)
Ampycilin	<i>A. tumefaciens</i>	50	H <sub>2</sub> O	100
Kanamycin	<i>E. coli</i>	50	H <sub>2</sub> O	25
	<i>A. tumefaciens</i>			50
	Arabidopsis			100
Hygromycin	<i>E. coli</i>	50	H <sub>2</sub> O	25
	<i>A. tumefaciens</i>			50
Gentamycin	<i>A. tumefaciens</i> GV3101	25	H <sub>2</sub> O	25
Rifampicin	<i>A. tumefaciens</i> GV3101, GV2260	30	DMSO	150
Carbenicilin	<i>A. tumefaciens</i> GV2260	50	1M Tris pH8.0	100

### 8.2. Bacterial Growth Media

#### Luria-Bertani Medium (LB)

Bacto-Tryptone	1% (w/v)
Yeast extract	0.5% (w/v)
Sodium chloride (NaCl)	1% (w/v)

The pH was adjusted to 7.0 with NaOH and autoclaved. When preparing solid plates 1.5% (w/v) of agar was added before autoclaving.

**SOC Medium**

Tryptone	2% (w/v)
Yeast extract	0.5% (w/v)
NaCl	0.05% (w/v)
Magnesium (Mg <sup>++</sup> )	0.02 M
Sucrose	0.02 M

The pH was adjusted to 7.0 with NaOH and autoclaved. This is a rich medium used for recovering cells after transformation.

**YEB Medium**

Meat extract	0.5% (w/v)
Yeast extract	0.1% (w/v)
Peptone	0.5% (w/v)
Sucrose	0.5% (w/v)
Magnesium sulphate	0.05% (w/v)

When preparing solid plates 1.5% of Bacto-agar was added and autoclaved. This medium was used for growing *A. tumefaciens*.

**8.3. Yeast Growth Media****Yeast Extract Peptone Dextrose Medium (YPD)**

Yeast extract	1% (w/v)
Peptone	2% (w/v)
Dextrose (D-glucose)	2% (w/v)

The reagents were dissolved in double distilled water and autoclaved. When preparing solid YPD medium 2% agar was added and dextrose was omitted before autoclaving. Filter-sterilized dextrose was mixed to the still warm autoclaved medium.

**Synthetic Complete (SC) Minimal Medium for Yeast**

Yeast nitrogen base (without amino acids, with ammonium sulphate)	0.67%
Carbon source (glucose, raffinose or galactose)	2%
Amino acids	
Threonine	0.020%
Valine	0.015%
Leucine	0.010%
Phenylalanine	0.005%
Isoleucine, Lysine	0.003%
Adenine, Arginine, Histidine, Methionine, Tryptophan	0.002%
In selective medium Uracil (0.01%) was omitted.	

Stock solutions for the amino acids (10X Drop Out, autoclaved) and the carbon source (40%, filter-sterilized) were prepared in dd water. The nitrogen base was dissolved in 850 ml of water and autoclaved. When cooled to 50°C, 100 ml of Drop Out and 50 ml of the carbon source were added to the nitrogen base. Glucose or raffinose was used for regular growth of transforming yeast, whereas galactose was used to induce the overexpression of the protein of interest. When preparing plates 2% agar was added to the nitrogen base prior sterilization.

**8.4. Plant Growth Media****Half Strength Murashige and Skog 10 Medium (MS)**

## MS Macro-nutrients I

$\text{KH}_4\text{NO}_3$	10.3 mM
$\text{KNO}_3$	9.4 mM
$\text{MgSO}_4$	0.75 mM
$\text{KH}_2\text{PO}_4$	0.625 mM

## MS Macro-nutrients II

$\text{CaCl}_2$	1.49 mM
-----------------	---------

## MS Micro-nutrients

H <sub>3</sub> BO <sub>3</sub>	50.1 µM
MnSO <sub>4</sub>	35.2 µM
ZnSO <sub>4</sub>	14.95 µM
Na <sub>2</sub> MoO <sub>4</sub>	0.517 µM
CuSO <sub>4</sub>	0.05 µM
CoCl <sub>2</sub>	0.077 µM
KI	2.5 µM

## Vitamins

Myo-inositol	100 mg/l
Nicotinic acid	0.5 mg/l
Pyridoxine-HCl	0.5 mg/l
Thiamine-HCl	1.0 mg/l
Gycine	2.0 mg/l
FeNa EDTA	100 µM
MES	500 mg/l
Sucrose	1% (w/v)

The Macro I and II were prepared as 10X stock solutions, the FeNaEDTA as 100X and the vitamins as 1000X. Alternatively, a commercially vitamin mixture was used (McCown's Woody Plant Vitamin Mixture, Duchefa). The reagents were dissolved in dd water, the pH was adjusted to 5.7 with KOH and autoclaved. When preparing solid plates 0.6% plant agar or 0.8% Gelrite (Duchefa) was added before autoclaving. A practical alternative was to use the commercially available Murashige and Skog medium (Duchefa, with modified vitamins, 0.4% (w/v)) complemented with sucrose (1% w/v), when the media did not required alteration of the macro-nutrients concentrations. In media with reduced phosphate concentrations proportional KCl was added, to compensate the reduction on potassium due to lack of KH<sub>2</sub>PO<sub>4</sub>.

**BY2 Culture Medium**

MS with basic salts	0.44% (w/v)
Sucrose	3% (w/v)
myo-Inositol	100 mg/l
Thiamine-HCl	1 mg/l
2,4-Dichlorophenoxyacetic acid	0.2 mg/l
KH <sub>2</sub> PO <sub>4</sub>	255 mg/l

The pH was adjusted to 5.0 with KOH, autoclaved and stored in the dark.

**8.5 List of Primers****Table 8.** Primers used for genotyping the T-DNA mutant plants.

<b>T-DNA line</b>	<b>Primer name</b>	<b>Primer sequence (5' - 3')</b>
<i>kvag1-1</i>	Salk_34139for	CCGGCATCGTTCTTGCTTCTA
	Salk_34139rev	TGCTCCCTACTTTTTCACTTTTG
<i>kvag2-1 &amp; 2-2</i>	3g10290for	CATGCTCGAGGTAAGGAGCTA
	3g10290rev	AGCAATGACGGCTATTGGAG
<i>kvag3-1</i>	RT04160_35for	ATCGACATTAATCATCTCATGG
	RT04160 R	GCTCTTGCCGCAGTAGC
<i>kvag3-2</i>	Homoz04160for	CATTAGTGCTACTGCGGCAA
	Homoz04160rev	TATGGAGTACCCGCCAATTC
<i>kvag4-1</i>	GK380D03for	TTGAAGGGAAAAGCTGAACTCCA
	GK380D03rev	TGGCTTTGCTTCTCTGTTTCTGC
<i>kvag5-1</i>	GK498B04for	TTGCTTCTTCATCTTCTTCTCCGA
	GK498B04rev	TCAAGCTCAGGCAAATCCCAA
<i>ugt1-1</i>	GK229E08for	AGCCGAATCTCTTCTTCATGG
	GK229E08rev	CAGTCATGCCCTGACCACTAC

**Table 9.** Primers to amplify cDNA and promoter sequences.

The start codons for the cDNA fragments are underlined in the forward primers.

<b>Gene</b>	<b>Primer name</b>	<b>Primer sequence (5' – 3')</b>	<b>cDNA</b>
KVAG1	12500 for VI	CACCAA <u>ATG</u> GTTGAAGCTCAATCATGG	+1
	12500 rev VI	GTTTAGCAATTGGATCTCTTCC	+1077
KVAG2	pYES10290 for	CACCATA <u>ATG</u> TCGTCCCATGCTCGA	+1
	pYES10290 rev	TCTAAACCTGCGTTTAGTCTCTC	+1065
KVAG3	04160_GFP for 1	CACCA <u>TG</u> TCGTCTGCGAAGAAA	+1
	04160_GFP rev 1	TCTAAATCTGCGTTTTGTCTCTCC	+928
KVAG4	pYES05820for	CACCAAA <u>ATG</u> AAGATGGCGACGAATGGC	+1
	pYES05820rev	TCGTTTCTTGGCTTCGCTGTA	+918
KVAG5	pYES11320for	CACCAAA <u>ATG</u> AAGATAGCGGCCAATGG	+1
	pYES11320rev	TCGTTTCTTGGCTTCGCTGTAG	+1025
N <sub>161</sub> - KVAG2	pYES10290 for	CACCATA <u>ATG</u> TCGTCCCATGCTCGA	+1
	At3g10290_483rev	CGGCGTCGTAGCACCAAC	+483
UDP- GalT1	77610full for	CACCAA <u>ATG</u> GAGGAAGGAAGTATGTTTCAG ATCT	+1
	77610full rev	TTTGCCTTCGAGTTTATCATTATTAAC	+1005
prom KVAG1	12500prom:969 for	CACCCATGCATGATCAGTGGGAAAA	-1062
	12500exon2_3182 rev	ATCCGTCCTCGCTTTCTCG	+793
prom KVAG2	10290-1545 for	CCTAATCTGGGGGAAAAAGA	-1641
	10290-1844 rev	GAGGTGTACCAGAGAATGA	+203

## Acknowledgments

At this moment I want to acknowledge the help and support from the people that made possible this work and my own development along with it.

Prof. Dr. U.-I. Flügge who supported my work in his team and encouraged me all along in scientific discussions.

Prof. Dr. R. Krämer for his enthusiastic will of giving me a second opinion about the approaches and progress of the work.

The IMPRS at the MPIZ for providing my scholarship and the wonderful scientific and friendly atmosphere that allowed a trip around the world in the surroundings of a TATABAR.

Dr. Karsten Fischer, the leader of the PThomologous team, for bringing back to earth project ideas that were flying too high and for pushing others to rise up.

Dr. Silke Knappe who introduced me to many technical details of the work and her enormous patience with my German.

Diana Hille for the precious and laborious help especially evaluating mutants and preparing yeast membranes and keeping me updated with important social events within the group.

Inga Rollwitz “Inganita” for sharing unpublished information, hours of mutant pollinization and microscope observation, framed in a cherish mood with continuous exchange of cultural experiences.

Frau Lorbeer for making the paper work and logistics look so simple, and for having always 10 minutes (or more) to solve this kind of troubles.

Dr. Ralf Petri for being a wonderful trouble-solver and friend.

All the people of the greenhouses and the workshop at the Institute of Botany.

Siggi Werth for his expertise work by photographing plants.

Elena Galiana-Jaime and Rainer Sädler, colleagues and friends in all the up and low rides. Dr. Veronica Maurino for everlasting moments of life debate (in Spanish) accompanied by an energizing mate. Dr. Rainer Schwacke for a true friendship grown out from non-important things. Daniel Marquardt for strong and accurate “barks” at the right time (especially proofreading the manuscript) and a wonderful-unexpected friendship. Bettina (betinita) Berger for honest criticism and also for giving me shelter. All the members (present and past) of the AG Flügge for making possible my deepest wish in this period: to perform numerous cultural counter-exchanges.

And principally Enrique, for accompany me and enjoying along the adventure and being there looking for the spot where the sun shines through in my darkest days.

## Kurzzusammenfassung

Die Nukleotid-Zuckertransporter (NSTs) und die plastidären Phosphattranslokatoren (pPTs) weisen strukturelle und funktionelle Gemeinsamkeiten auf. Sie katalysieren den Transport von mit Phosphatresten oder Nukleotiden verknüpften Metaboliten über verschiedene Membranen, zum Beispiel Membranen der Plastiden, des Golgi Apparates oder des ER. In den letzten Jahren ist eine große Zahl dieser NST/pPT Proteine in *Arabidopsis* identifiziert worden, von denen aber erst eine kleine Zahl funktionell charakterisiert worden ist. Ein Teil dieser Proteine lässt sich in drei Unterfamilien unterteilen, die als KVAG, KT und KD Unterfamilien bezeichnet wurden. Zwei Mitglieder der KVAG Unterfamilie, KVAG1 und KVAG2, besitzen eine putative plastidäre Transitsequenz, was eine Funktion dieser Transporter in der plastidären Glykolipidsynthese vermuten ließ. In dieser Arbeit wurde die intrazelluläre Lokalisation und die physiologische Funktion dieser beiden Transporter untersucht. Fusionen der Proteine mit GFP wurden verwendet, um die subzelluläre Lokalisation zu ermitteln. Es konnte gezeigt werden, dass beide Proteine und ebenso weitere Proteine dieser Subfamilie im Golgi Apparat und nicht in Plastiden lokalisiert sind. Die Substratspezifitäten der Transporter sollten durch Expression in Hefe und anschließende Rekonstitution der Proteine in Liposomen ermittelt werden. Es konnte aber weder ein Transport von Nukleotidzuckern noch von CDP-Cholin oder CDP-Ethanolamin, beides Vorstufen der plastidären Lipidsynthese, nachgewiesen werden. Um die physiologische Funktion der Transporter der KVAG Unterfamilie zu bestimmen, wurden *Arabidopsis* Linien mit T-DNA Insertionen in den entsprechenden Genen identifiziert und analysiert. Alle Linien zeigten einen Phänotyp ähnlich dem der Wildtyp-Pflanzen.



## Abstract

The nucleotide sugar transporters (NST) and the plastidic phosphate transporters (pPT) proteins share structural and functional similarities. They mediate the transport of phosphorylated and nucleotide-coupled metabolites through the membranes of plastids, Golgi apparatus and endoplasmic reticulum (ER). Recently, a great number of proteins homologous to the NST/pPT proteins have been identified in *Arabidopsis* and only a few of them have been characterized. The majority of these homologous proteins cluster in three subfamilies, namely the KV/A/G, KT and KD subfamilies. Two members of the KV/A/G subfamily, KVAG1 and KVAG2, have a putative plastidic targeting signal. This made them interesting candidates as putative providers of nucleotide sugars for the synthesis of specific plastid lipids. In this study, the intracellular localization and *in planta* expression of these proteins was analyzed. cDNA fusions to GFP revealed the localization of both proteins in the Golgi apparatus and not in plastids. Transport experiments using liposomes and the proteins heterologously expressed in yeast were performed; however no significant transport of nucleotide sugars was detected. Homozygous knock-out T-DNA lines, *kvag1-1* and *kvag2-1*, presented general wild type phenotype and development, except for a small reduction in the phospholipid content in leaves. The transport of CDP-choline and CDP-ethanolamine, precursors of phospholipid biosynthesis, by KVAG2 was also evaluated; however the transport rates were not significantly higher than the controls. Additional evidence is presented for the Golgi localization of other members of the KV/A/G subfamily. T-DNA knock-out mutants for these genes were identified and they all showed a similar wild type phenotype.

**Erklärung:**

Ich versichere, dass ich die von mir vorgelegte Dissertation selbständig angefertigt habe, die benutzten Quellen und Hilfsmittel vollständig angegeben und die Stellen der Arbeit – einschließlich Tabellen, Karten und Abbildungen –, die anderen Werken im Wortlaut oder dem Sinn nach entnommen sind, in jedem Einzelfall als Entlehnung kenntlich gemacht habe; dass diese Dissertation noch keiner anderen Fakultät oder Universität zur Prüfung vorgelegen hat; dass sie abgesehen von unten angegebenen Teilpublikationen noch nicht veröffentlicht worden ist sowie, dass ich eine solche Veröffentlichung vor Abschluss des Promotionsverfahrens nicht vornehmen werde. Die Bestimmungen dieser Promotionsordnung sind mir bekannt. Die von mir vorgelegte Dissertation ist von Prof. Dr. U.-I. Flügge betreut worden.

**Teilpublikation:**

Characterization of a UDP-Galactose transporter from *Arabidopsis thaliana*.

Inga Rollwitz, Marcella Santaella, Diana Hille, Ulf-Ingo Flügge, and Karsten Fischer. In preparation.

**Beiträge in Mitteilungsbänden von Tagungen:**

Marcella Santaella, Nicole Walczyk, Ulf-Ingo Flügge and Karsten Fischer. Analysis of proteins homologous to plastidic phosphate translocators in *Arabidopsis thaliana*. 17<sup>th</sup> International Botanical Conference, 17-23 Juli, 2005, Austria Center Vienna, Wien, Österreich (Poster).

Marcella Santaella, Silke Knappe, Ulf-Ingo Flügge and Karsten Fischer. Analysis of proteins homologous to plastidic phosphate translocators in *Arabidopsis thaliana*. Botanikertagung 2004, 5-10 September, 2004, Technische Universität Carolo-Wilhelmina, Braunschweig.

Marcella Santaella, Silke Knappe, Ulf-Ingo Flügge and Karsten Fischer. Analysis of proteins homologous to plastidic phosphate translocators in *Arabidopsis thaliana*. 15<sup>th</sup> International Conference on *Arabidopsis* Research, 11-14 Juli, 2004, Berlin.

## Lebenslauf

### Persönliche Daten

Name	Marcela Santaella-Tenorio
Geburtsdatum, -ort	18.05.1974 in Bogotá, Kolumbien
Eltern	Ulises Santaella Liliana Tenorio
Familienstand	verheiratet mit Enrique A. Torres-Prieto
Staatsangehörigkeit	kolumbianisch

### Schulbildung

1981-1986	Grundschule Colegio del Sagrado Corazón
1986-1992	Gymnasium Colegio del Sagrado Corazón

### Studium

Sep. 1993	Immatrikulation an der Valle Universität für das Studienfach Biologie.
Aug. 1997- Jan. 1999	Diplomarbeit am Centro Internacional de Agricultura Tropical (CIAT), Dr. J. Tohme. Thema: "Towards isolation of resistance genes against <i>Pyricularia grisea</i> Sacc. in rice ( <i>Oryza sativa</i> )."
Sep. 2002 - Apr. 2004	Master Diploma am Botanischen Institut der Universität zu Köln, Prof. Dr. U.I. Flügge und Valle Universität, Dr. H. Cárdenas. Thema: "Study of the expression of two proteins homologous to plastid phosphate translocators in <i>Arabidopsis thaliana</i> through RT-PCR and promoter-reporter gene fusions."
Apr. 2004 – Mai 2006	Dissertation in der Arbeitsgruppe von Prof. Dr. U.I. Flügge im Hauptfach Botanik. Thema: "Characterization of proteins homologous to nucleotide sugar transporters and plastid phosphate translocators in <i>Arabidopsis thaliana</i> ."